

**Integrating crop growth simulation
and remote sensing
to improve resource use efficiency
in farming systems**

Promotoren:

Prof. dr. S. M. de Jong

Hoogleraar Geo-Informatiekunde en Remote Sensing, Wageningen Universiteit (-2001)

Hoogleraar Remote Sensing en Landdegradatie, Universiteit Utrecht (2001-)

Prof. dr. ir. H. van Keulen

Hoogleraar bij de Leerstoelgroep Plantaardige Productiesystemen, Wageningen Universiteit

Promotiecommissie:

Dr. F. Baret, l'Institut National de la Recherche Agronomique (INRA) Avignon, Frankrijk

Dr. ir. J. G. P. W. Clevers, Wageningen Universiteit

Prof. dr. ir. G. M. J. Mohren, Wageningen Universiteit

Prof. dr. ir. E. M. A. Smaling,

International Institute for Geo-Information Science and Earth Observation (ITC), Enschede

Dit onderzoek is uitgevoerd binnen de onderzoeksschool

'C. T. de Wit Production Ecology and Resource Conservation'

Integrating crop growth simulation and remote sensing to improve resource use efficiency in farming systems

R.E.E. Jongschaap

Proefschrift

ter verkrijging van de graad van doctor
op gezag van de rector magnificus
van Wageningen Universiteit,
Prof. dr. M. J. Kropff,
in het openbaar te verdedigen
op vrijdag 12 mei 2006
des namiddags te vier uur in de Aula.

R.E.E. Jongschaap, 2006.

Integrating crop growth simulation and remote sensing to improve resource use efficiency in farming systems.

Ph. D. Thesis, Wageningen University, Wageningen, the Netherlands, 130 pp.
- with summaries in English and Dutch -

ISBN 90-8504-426-x

Keywords: simulation; model; calibration; remote sensing; radar; optical; satellite; spatial; up-scaling; LAI; nitrogen; chlorophyll; fertilization; precision agriculture; maize; potato; wheat

“De schoonheid van de buitenkant, ontsierd door woorden”
(Frits Swart, 1976. Dichtbundel Bovenbouw Jenaplanschool OBS Midwolde)

“Outer beauty, disgraced by words”

Table of Contents

Chapter 1 - General introduction	1
1.1 Justification and needs to improve resource use efficiency in farming systems	1
1.2 Opportunities for integrating simulation modelling and remote sensing techniques	3
1.3 Objectives	6
1.4 Synopsis	7
1.5 References	7
Chapter 2 - Integrating crop growth simulation modelling and remote sensing for agriculture	9
2.1 Introduction	9
2.2 Crops	10
2.3 Crop growth simulation modelling	11
2.4 Remote sensing	16
2.5 Combinations of remote sensing and simulation modelling	26
2.6 Synopsis	27
2.7 References	27
Chapter 3 - Predicting wheat production at regional scale by integration of remote sensing data with a simulation model	35
3.1 Abstract	35
3.2 Introduction	36
3.3 Materials and methods	37
3.4 Results and discussion	45
3.5 Conclusions	48
3.6 Acknowledgements	48
3.7 References	49
Chapter 4 - Spectral measurements at different spatial scales in potato: relating leaf, plant and canopy nitrogen status	53
4.1 Abstract	53
4.2 Introduction	54
4.3 Material and methods	57
4.4 Results	62
4.5 Discussion and conclusions	68
4.6 Acknowledgements	70
4.7 References	70

Chapter 5 - Run-time calibration of simulation models by integrating remote sensing estimates of leaf area index and canopy nitrogen	73
5.1 Abstract	73
5.2 Introduction	74
5.3 Material and methods	75
5.4 Results and discussion	82
5.5 Discussion	86
5.6 Conclusions	87
5.7 Acknowledgements	87
5.8 References	87
Chapter 6 - The effect of LAI and N parameter variability used in run-time calibration of mechanistic and dynamic crop growth simulation models	91
6.1 Abstract	91
6.2 Introduction	92
6.3 Material and methods	93
6.4 Results and discussion	98
6.5 Conclusions	105
6.6 Acknowledgements	106
6.7 References	106
Chapter 7 - General discussion and conclusions	111
7.1 Gained insights and pursuing the objectives	111
7.2 Validation of the hypotheses	115
7.3 Future research and developments	116
7.4 References	118
Acronyms and symbols	119
Samenvatting	123
Curriculum vitae	127
Selected publications	128

Abstract

This study investigated the scope and constraints for integrated use of mechanistic crop growth simulation models and earth observation techniques. Integration of high-quality crop growth models and information derived from earth observations can contribute to improved use of resources, reduced crop production risks, reduced environmental degradation, and increased farm income. In the past, both, simulation modelling and remote sensing have been shown to be valuable tools in separate applications in agriculture. Crop growth simulation has made valuable contributions to yield forecasting, proto-typing crop varieties, generation of input-output coefficients for improved agricultural production technologies and to management decision support systems at field level. Likewise, remote sensing techniques have been successfully applied in classification of arable crops and in quantification of vegetation characteristics at different spatial and temporal scales. The starting point of this study was the hypothesis that integration of both techniques would lead to improvements in the dynamic simulation of the crop-soil system and thus contribute to improvements in management decision support systems for environmentally sound agricultural production.

Thus far, mutually beneficial linkages have been limited to land use classification via remote sensing (choice of adequate model) and quantification of crop growth and development curves using e.g. estimates of leaf area indices derived from remote sensing images for model calibration under (usually) favourable growth conditions. Only a few studies have considered the potentials of remote sensing for model initialization of growth and development characteristics of a specific crop. In this thesis these potentials have been extended to a more continuous approach, in which remote sensing information is not only used in model initialization, but also in model calibration in the course of the simulation run, so-called run-time calibration. During such a run-time calibration procedure, simulated values of e.g. leaf area index (LAI) and canopy nitrogen status (CNS) are replaced by values estimated from remote sensing images acquired at different stages in the course of the growing period. LAI and CNS are important controlling variables in models for arable crops such as wheat, potato and maize. This run-time calibration procedure has been performed for a full crop growth cycle, for optimal as well as sub-optimal growth conditions. This approach enables spatial differentiation in crop growth simulation, as variations in crop status, resulting from differences in growth conditions, lead to differences in remote sensing signals. The relationships between near and remote sensing observations at leaf, plant and canopy level have been investigated and the effects of variations in estimated values of LAI and CNS used in run-time calibration of dynamic crop growth simulation models on final model results (e.g. crop yield) have been analyzed.

Results from potato trials in the Netherlands show that leaf nitrogen contents derived from near sensing observations can be up-scaled to plant and canopy nitrogen status by taking into account the vertical nitrogen distribution in the crop. A vertical nitrogen extinction coefficient (k_N) of 0.41 resulted in an accuracy increase of the relation between leaf nitrogen (g N m^{-2} leaf) and SPAD readings (a near sensing technique at leaf level), with a correlation coefficient (r^2) of 0.91. Remote sensing observations

integrate nitrogen contents over canopy depth and do not require adjustment for vertical nitrogen gradients, if canopy nitrogen status is expressed in total nitrogen content per unit of soil surface. The red edge position (an index derived from remote sensing observations) could be related to canopy nitrogen content (g N m^{-2} soil) with a correlation coefficient (r^2) of 0.82. Leaf area indices of potato (Netherlands) and maize (Argentina, France, USA) crops, for use in run-time calibration, were also accurately derived from field, airborne and spaceborne remote sensing platforms. Introducing LAI values derived from RS in the simulation model and concurrently adjusting CNS by retaining leaf N-concentrations, led to more accurate simulation results for CNS than without such adjustment. The different crops, and the range in environmental conditions, soil fertility status and management practices that were examined in the different case-studies in this thesis, have demonstrated the broad applicability of mechanistic simulation models integrated with remote sensing information

Winter wheat fields, wheat phenological stages (emergence, flowering) and management operations (harvest) were successfully identified on the basis of information from optical and radar remote sensing data in a case-study in South-eastern France. Timing of these phenological stages and management operations is important in model calibration as they mark the length of the crop growth period and of the grain-filling period, which are co-determinants of grain yield. At flowering, C-band radar backscatter from the soil is maximally reduced by canopy moisture content. This characteristic was successfully used to estimate regional wheat flowering dates. Integration of RS data in the (point-based) crop growth simulation model allowed its spatial application for prediction of wheat production at regional scale. The estimated value was in agreement with regional yield statistics. This integration thus allows expansion of the application area of valuable research tools, as up-scaling has become feasible.

Introduction of remote sensing-based estimates of LAI and CNS in the course of the growing seasons into dynamic simulation of the growth of potato and maize resulted in improved simulation accuracy for aerial crop characteristics, as well as for variables that could not be directly observed by remote sensing, such as soil inorganic nitrogen contents. The degree of success and robustness of the integrated approach depends on the timing, accuracy and number of remote sensing observations available for re-setting the relevant state variables in the course of the simulation period. Simulation accuracy was positively correlated with the number of observation dates from remote sensing. Remote sensing observations around flowering had more impact on calculated final grain yield (FGY) for maize than earlier or later observations.

The investigations reported in this thesis have shown that the accuracy of predictions of dynamic and mechanistic crop growth simulation models significantly improves through integrating earth observation-derived information as input for the models and for their run-time calibration. Such integration not only yields more accurate estimates of crop bio-physical variables, such as leaf area index and canopy nitrogen status, but also contributes to improved prediction at regional scales. Such models, producing reliable, site-specific predictions of crop performance and crop requirements are thus effective tools in the development of environmentally-friendly production methods and in optimizing the use of our natural resources.

Further research should focus on the scope for estimating additional crop variables of interest for integration in simulation modelling through remote sensing. Management interventions may be triggered by various crop characteristics, such as: 1) canopy temperatures derived from thermal remote sensing systems as an indicator for water stress, 2) canopy discolouring derived from optical remote sensing systems as an indicator for nutrient shortages and 3) canopy architecture derived from radar remote sensing images as an indicator for water and nutrient supply. Remote sensing is also a valuable technique to identify spatial patterns of crop performance and crop status within arable fields. Moreover, remote sensing allows identification of patterns that may be related to specific diseases or special events, such as outbreaks of phytophthora in potato, or lodging in grain crops.

This study has demonstrated that a decision support system for crop and soil management based on the integration of crop growth simulation modelling and remotely sensed data is within reach. In addition, nitrogen uptake, its vertical distribution within the crop, and the inorganic nitrogen content of the soil can be simulated more accurately with such an integrated system. Such a decision support system can be used for fine-tuning of fertilizer regimes thus contributing to more environmentally sound and sustained agricultural production.

Preface

Little did I know about crop growth simulation modelling when I started my studies in 1987. I knew even less about remote sensing and the probable significance these techniques might have for addressing problems or evaluating opportunities in agricultural production systems. It took me almost 20 years to value the charms, opportunities, difficulties and pitfalls associated with these techniques. With time, my reluctance toward desk-study solutions for ‘real-life’ problems such as food insecurity, social inequity and environmental degradation gradually changed. Quantifying environmental processes by remote sensing and modelling techniques brought me closer to a better understanding and evaluation of agricultural production systems. Leaving my office, travelling around the world, performing field work, crossing borders and allowing different cultures and habits to penetrate my mind and soul naturally is an exciting part of my work. The integration of simulation modelling and remote sensing was a challenge that I primarily tackled behind my desk, but contrary to what I would have expected as a student, it was worthwhile. I recommend it to each and everyone!

Chronologically and in reverse order, I would like to express my sincere gratitude to the people who contributed to the realization of this thesis. You have all done this either full-consciously or unknowingly, but you can be sure that I appreciated every piece of your involvement. I’d like to thank Tom Dueck for reviewing my ‘Dunglish’ and suggesting improvements for the abstract, preface and my curriculum vitae. Thank you too, Rina Kleinjan-Meijering for your professional assistance and patience in formatting this booklet.

I especially value the supervision and guidance of my promoters Steven de Jong and Herman van Keulen, who took over after predecessors left, one after another. This of course, can be expected if one takes as long as I did to complete this work. I am extremely thankful that I could hold on to both of you. I quickly learned to appreciate your countless red marks and suggestions in my manuscripts. The two of you never failed to keep me going, and tempered my anger when the manuscripts were somehow ‘misinterpreted’ by referees. Furthermore, I could always rely on the assistance and faith of Prem Bindraban and the Agrosystems Innovations’ management team of Plant Research International, who provided the means (i.e. time and support) during the last stages of my thesis. It was not always easy to combine my projects at work with my Ph. D. research at home, where I also tried to be a ‘loving husband’, start a new life as a father, as a house owner, a reconstruction worker and in the meantime pursue an overestimated basketball career. I thank all of my colleagues in Agrosystems Innovations for their trust and continuous concern (...) about the progress of this work.

In the end I can say that I am truly grateful that Bas Bouman introduced me to the national and international remote sensing community and that I could occupy his position after he left our institute. Bas was responsible for keeping me from leaving for INRA in France for a Ph. D. research on the simulation of soil organic matter dynamics. I am happy that I could stay at the DLO Institute for Agrobiological Sciences and Soil Fertility Research (AB-DLO) and start a Ph. D. there. I have learnt a lot from my

roommates Daniel van Kraalingen, Jan Verhagen and Tom Schut and from my special colleague Rob Groot. My experiences with these four people will certainly not be exposed on these pages, but I want to thank you explicitly for the hilarious act on my wedding day. I am sorry that during my research period Remmie Booij passed away. He is the co-author of one of the articles in this thesis and was a unique colleague, not only for me.

I wish to thank Peter de Willigen and his family, who took me with them on holidays to Indonesia when I was 15 years old. These holidays provided the incentive for my study Tropical Crop Science in Wageningen. Crammed with guilt, Peter took his responsibility by realizing a position for me at the DLO Institute for Soil Fertility Research (IB-DLO) in Haren (Gr.) after my studies in 1993. It was a terrific start at an institute that provided a legendary environment with warm-hearted colleagues. Together with another 'freshman' Frank Jenniskens, we had many memorable moments, as we thoroughly enjoyed our new responsibilities in research, the freedom, (sporting) activities and other opportunities that were given to us. With warm feelings I recall the companionship of Gert Dijksterhuis and Els Verberne who guided me during the BuNaSols project in Burkina Faso at that time. I am proud to have been invited as a member of the Secret Haren Alliance, and I cherish the yearly mystical rituals in honour of the 'Pronkjewail in golden raand'. It may not come as a surprise that my two paranymphs Peter de Willigen and Bert Smit, both root specialists, symbolically stand for my ties with Groningen. Peter and Bert: thank you for keeping my roots with the north alive, and of course for your support at my defence.

Then some more informal thoughts about how all this came about. The students, supervisors and friends I met at the Atlantic Zone Programme in Costa Rica were a source of pure joy and passion during my studies and left an incredible impression that is still vividly alive. Muchas gracias Amos, Antje, Arthur, Björn, Celia, Donatus, Edzo, Eric, Fernando, Frank, Guillermo, Jetze, Johan, Jorg, Karin, Louise, Luis, Manuel, Margreet, Olga, Paul, Phillip, Robert, Roberto, Ronald, Sander, Wendoly and Wilhelmina! My experiences in Costa Rica explain my love for Latin America and my eagerness to spend another half year in Chile to work for Agraria in Coelemu. I want to thank César, Guáda, Jacqueline, Jorge, Léon, Maricela, Nolbert, Pedro, Ruth, Selva, Ximena and Yvonne for the joyful times we had! Speaking about joy during my studies, I also have to mention my basketball team mates at Sphinx and Pluto in Wageningen and Groene Uilen and Moestasj in Groningen. The practices and games always freed my mind from too complicating thoughts. We will see whether I will need man-to-man tactics at the defence of my thesis, or that I would benefit more from a fast-break offence. Don't worry though, both techniques are readily available.

Then I am indebted to my girlfriend and wife Heidi Lubberink. It was on the basketball court where we met and where we discovered that there was more than basketball that we shared or liked to share together. We lived through difficult moments when our close friend and dear colleague Wim Quak passed away much too young. Heidi, you have opened my eyes in many ways and I am still grateful for that. You did not hesitate to leave your home town and follow me to Wageningen and Heelsum. You have given me all the support and understanding I could wish for, both in my work and privately. You gave me the impression that I succeeded in combining

family life with my Ph. D. research, although you and our daughters Myrthe and Dagmar may have thought differently at times. You can tell me later. I certainly know that you covered for me when I was abroad for my work or when I slipped up on my parental duties, and I love you for that. In honour of you and your support, I am proud to display your last cover action (your impression of a false colour photograph of a wheat crop) as the wrapping for this thesis.

Last but not least I'd like to thank my parents Henk and Lidy who always supported me and my brother and sister for whatever direction in life we chose. You always pointed out how important it was to invest in yourself, preferably through education. From you I learned to stand up for my beliefs and feelings, no matter what others might say. I have learned from you never to give up, but always keep an eye on the things I value the most; a wise and warm lesson which has prevented me from losing track in life and which has brought me to where I am right now.

Once again, thank you all for your support!

Raymond Jongschaap

Heelsum, 2006

Chapter 1

General introduction

1.1 Justification and needs to improve resource use efficiency in farming systems

To improve the livelihoods for millions of people, the member states of the United Nations committed themselves in the year 2000 to eight quantifiable Millennium Development Goals (MDGs) that should be reached in 2015 (World Bank, 2000). With 70 percent of the MDGs' target group living in rural areas, most immediate gains in poor households' welfare may be achieved through agriculture. While the linkage with agriculture is especially strong for the first MDG (eradicating poverty and hunger), all MDGs have direct or indirect linkages with agriculture. As acknowledged in MDG7 (ensure environmental sustainability), agricultural practices can be both direct causes of, and important solutions to environmental degradation. Without doubt, this not only holds for poor rural areas in less developed countries, but also for agriculture in developed countries.

Resource use efficiency is of permanent concern to modern society. Governed by economic incentives and environmental awareness, scarce and thus expensive resources are used more and more efficiently. If resources are not limited however, danger of excessive use remains, leading to inefficiency, higher costs and possibly environmental pollution. Risk-avoidance strategies e.g., may lead to undesired side effects and degradation of the environment, such as pollution and soil fertility deterioration.

In the last decades it has been shown that modern agriculture with high-inputs is no exception to these economic rules. Arable and dairy farming may contribute to contamination of ground- and surface water (Langeveld *et al.*, 2005), and intensive animal husbandry faces problems of outbreaks of contagious diseases. The awareness of the negative side effects of agricultural practices on the environment has clearly grown over the years. In arable farming, solutions to the problems created by these side effects are sought in fine-tuning management practices, for instance through optimizing the match between crop nutrient demand and nutrient supply. Fine-tuning management practices on the basis of crop demands increases resource use efficiency and reduces risks of negative side-effects. To operationalize such principles, methodologies are needed to establish crop demand, for instance on the basis of crop-

soil status. New technologies, such as field sensors and remote sensors provide information that may have added value to conventional ways of crop-soil monitoring.

In agricultural research, eco-physiological processes in soils and crops are studied to unravel the complexities of underlying principles as a basis for identification of solutions to the negative side effects of mismanagement. The use of crop growth simulation models enables timely and quantitative prediction of the dynamics of crop requirements for a specific location (ten Berge *et al.*, 1997). Further improvements in fine-tuning management practices can be achieved by assessing the spatial variation in the crop growth environment as a basis for spatial fine-tuning of crop management. Applying this concept to a single field is known as precision agriculture (PA). The concept of PA illustrates that agricultural management is in need of geo-referenced information that can be generated through new techniques, such as remote sensing (RS) or through conventional measurement techniques in combination with a geographical positioning system (GPS) (van Alphen, 2002).

Availability of temporal and spatial information might provide detailed information for guiding management aimed at efficient use of inputs and prevention of environmental pollution or degradation. Remote sensing observations, acquired in the course of the growing season, can assist in assessing variability in crop performance and provide information of, and for, management interference. Technological developments, such as automated application equipment for fertilizers, irrigation and phyto-sanitary products make it possible to vary management within a field. Crop management could thus be improved on the basis of information generated through combining dynamic crop growth simulation with temporal remotely sensed information. In addition to applications in high-input farming, this method of linking crop growth simulation models to spatial remote sensing information has potential in low-input arable farming. Where resources are scarce or unavailable (e.g. in rainfed agriculture in West Africa or in the extensive rangelands in South America), this technique can contribute to early warning systems (EWS), or improve the results of risk analysis studies to assess food security.

Linking dynamic crop growth simulation models to spatial information provides a possibility to extend the use of an advanced and sophisticated research and advisory tool, originally developed for point-specific analyses, to larger areas.

Remote sensing information can be used to calibrate simulation models in data-scarce environments, and/or to increase simulation accuracy (e.g. for yield forecasting), by forcing observed values on the model in the course of the simulation period. This generates questions on how this can be technically achieved, what the requirements are for the spatial information (or what impact can be expected if these requirements are not met), and what the likely benefits would be.

1.2 Opportunities for integrating simulation modelling and remote sensing techniques

There is a need for methodology development with respect to the integration of soil and crop processes (as incorporated in simulation models), expert knowledge and observations from sensing techniques, to more adequately understand and respond to crop performance. Many new sensing techniques have been developed in recent years, to collect information on crop and soil systems (by remote sensing in various spectral bands, laser-induced fluorescence, radar, etc.). As the remotely or near sensed information is a representation of the actual soil-crop status, it is difficult to identify instantaneously which process(es) is (are) responsible for the observed crop and soil conditions. Identification of these processes is needed in order to select the most appropriate intervention through management. For such selection, one-time remote sensing observations are hard to interpret without additional information on crop and/or soil status. Multitemporal (or continuous) and multispectral measurements might improve the possibilities for identification of the relevant processes, if reliable methods are available for processing and interpretation of the observations. To maximize the possibilities for identification of appropriate management, the use of process simulation models is, where possible, linked to sensed information and the benefits of this integration are explored and discussed in this thesis.

Although remote sensing and crop growth simulation modelling each has proven its usefulness and applicability in various areas, such uses have in principle been separately, and not in combination. The challenge of showing synergy through generation of supplemental and more accurate information by integrating the two methodologies is taken up here. The methods of integrating remote sensing and simulation modelling are plentiful, however, as will become clear.

1. Remote sensing techniques can be used in calibration and validation procedures through supply of input data for spatial applications of crop growth simulation models. Important model state variables such as aboveground biomass, leaf area index and specific canopy characteristics, such as chlorophyll or nitrogen contents, can be estimated from remote sensing observations and can therefore be used for calibration and validation purposes.
2. Phenological events such as emergence, flowering and maturity (followed by crop harvest) are difficult to predict and in general are not accurately enough represented in simulation models (Porter *et al.*, 1993). Timing of these events has, however, a strong impact on crop performance and yield, both in reality and in simulation models. Remote sensing information allows identification of the timing of those events, which can be used to adjust simulation models.
3. Discrepancies between actual crop performance and simulation results may occur for various reasons: crop growth and soil processes can be wrongly interpreted or wrongly modelled or absent, and/or input data may be inaccurate or missing.

Unpredictable events that are not explicitly included in the simulation model, may lead to inaccurate simulation results. Natural catastrophes (i.e. hailstorms and flooding), or the occurrence of pests and diseases may significantly influence crop performance, but these events are hardly ever included in simulation models, as their occurrence is erratic. Furthermore, natural interference (such as grazing on pastures) may not be erratic, but will affect crop status. Remote sensing information of the crop-soil system allows identification of the occurrence of such events and their effects can be used to re-initialize and re-direct a model at various stages during run-time. Such a re-initialization will lead to more accurate simulation results, as will be shown in this study.

4. Remote sensing images also allows spatial differentiation of areas that, without such information, appear homogeneous (and are treated as such). The spatial and temporal differentiation in remote sensing information permits application of crop growth simulation models at smaller spatial scales, e.g. at sub-field level. Remote sensing images show spatial variability in reflection characteristics, due to variability in crop conditions, caused by heterogeneous environmental conditions. Application of crop growth simulation models at the level of sub-fields allows differentiating crop management at that scale. This may result in reduced waste of resources and/or reduced risk of environmental pollution.
5. Alternatively, a reverse pathway can be followed. Crop growth simulation models may provide information to support interpretation of remote sensing data. Interpretation of the results of complex, process-based simulation models may on the one hand benefit from remote sensing imagery, and on the other hand, where remote sensing images are missing, model-derived information on soil and crop temporal and spatial variability may prove useful to fill observation gaps. Estimates of the dynamics of soil characteristics such as soil moisture content and crop characteristics (i.e. biomass, leaf area index, canopy structure and chlorophyll contents) can be provided by simulation models. This feature has great potential in filling in missing remote sensing data due to unfavourable climatic conditions, such as clouds or due to technical problems. Remote sensing data can be emulated by constructing remote sensing signals from results of crop growth simulation models.

In the late 1980s, a method has been developed at the DLO Institute for Agrobiolgy and Soil Fertility Research (AB-DLO) in Wageningen, to integrate crop growth simulation models and remote sensing data for calculating production potentials of a number of crops in the Netherlands (Bouman, 1991). The method is based on estimating light interception and reflection characteristics of a green canopy, on the basis of simulated phenological development and biomass accumulation. Remotely sensed data are used to correct simulated values to improve yield forecasts. Van Leeuwen (1996) tested this method using airborne and satellite remote sensing data, and with emphasis on radar and optical measurements for sugar beet and winter wheat. He found that simple semi-empirical remote sensing models are more suitable for observations at canopy level than more complex models, especially for optimal growing conditions.

As this thesis aims at formulation of recommendations for improved crop management to increase resource use efficiency, the approach should be geared towards areas with sub-optimal growing conditions. Crop management based on a sophisticated decision support system could help to reduce negative side-effects of arable farming practices, as soil and crop processes may be sources of the observed variability in reflection characteristics.

Under sub-optimal growth conditions (i.e. imbalance in nutrient and water demand and supply), the interactions between soil and crop processes, that are unimportant under non-limiting growth conditions, play major roles in determining crop performance. Refining the method is the more relevant because of recent developments in designing decision support systems for precision agriculture. Therefore, remotely sensed and geo-referenced information needs to be interpreted appropriately to undertake necessary action. Booltink *et al.* (1996) already described a decision support system that incorporates simulation of crop growth and nutrient fluxes being fed by multisensor observations and weather generators. A new methodology would substantially extend and enhance such a decision support system, by introducing spatial variability patterns.

If a crop is suffering from e.g. moisture stress, canopy reflection will increase. Reflection signals in different spectral bands can be combined to calculate Vegetation Indices (VI) that can be directly related to vegetation characteristics. Jordan (1969) and Rouse *et al.* (1973) were the first to explore the application of VI for agricultural purposes. VI values change with crop development and when unfavourable conditions are causing stress. In this thesis, VI are mainly used for monitoring those crop and soil characteristics that are main drivers in dynamic crop growth simulation models, such as leaf area index (LAI), aboveground biomass, chlorophyll and/or nitrogen contents.

Nitrogen stress affects leaf colour and the vertical nitrogen profile in a crop and reduces light interception, and as a result crop production (Bindraban, 1999; Dreccer, 1999). Changes in leaf colour can be detected by sensor techniques, using optical remote sensing methods. Additional sensor methods to determine e.g. soil moisture and soil organic matter contents may be derived at the same moment to extend the information on the crop and soil system. Testing and application of this methodology could provide important information in process simulation models for crop and soil dynamics.

Application of the principles explained above, aims at the development of an integrated model for application at regional and field level, for purposes such as crop growth monitoring (CGM), management decision support (MDS) (e.g. precision agriculture) and yield forecasting.

To integrate multisensor, multitemporal measurements and crop growth simulation models in moisture- and nutrient-limiting situations, technical specifications should be implemented in a software application. This application should enable execution of a simulation model in a 2-dimensional grid, with possibilities to reset the model with values retrieved from remote sensing. A sophisticated simulation model should be used because of the high level of detail in soil and crop process simulation. For the simulation model to benefit from the sensor data, it is essential that the model sufficiently accurately simulates those crop and soil variables with the largest influence

on the remote sensing signal. As the recorded sensor signal is associated with differences in specific crop and soil characteristics, in this context, leaf area index, leaf chlorophyll contents and leaf water contents are the most important crop features. Leaf area index and leaf chlorophyll contents are the main drivers in a large number of simulation models that are applied at field level, as they determine radiation interception capacity and radiation use efficiency. In addition to the model variables that are linked directly to the sensor information, additional variables should be simulated that are associated with risk assessment and environmental pollution, associated with water and nutrient flows. Methodologies to explore the options for integrated approaches are investigated and analyzed in order to contribute to the realization of the objectives.

In conclusion, integration of remote sensing information and crop growth simulation modelling shows great potential in contributing to the general objectives of increased resource use efficiency, risk avoidance, the prevention of environmental degradation and improved farming practices. A number of integration configurations are explored and examined to reveal the accuracy, trade-off and costs of the configurations.

1.3 Objectives

Integrating remote sensing and simulation modelling in this thesis has the following objectives:

- To derive values of important crop state variables from various remote sensing data and link these with field measurements
- To technically integrate important crop state variables derived from remote sensing time-series in dynamic simulation models in order to increase simulation accuracy
- To define the requirements for successful implementation and identify situations where this new integrated technique shows promising results, and to illustrate the effect of timing and accuracies of the remote sensing observations
- To apply point-based simulation models at a spatial scale, based on remote sensing observations
- Eventually improve resource use efficiency, avoid production risks and prevent environmental degradation by arable farming practices

The methodology and backgrounds described above lead to compilation of the following hypotheses, which will be examined in various case studies at spatial scales ranging from a sub-field to a region:

1. Under sub-optimal production conditions, soil and crop processes that cause the production limitations can be identified through the integration of multi-sensor and multi-temporal measurements and simulation models.
2. Using numerical, spatially and temporarily distributed values of selected variables obtained through remote sensing techniques improves the dynamic simulation of the crop-soil system. The required complexity of the variable integration methods

depends on the crop production level: simple for potential growth conditions to more complex for sub-optimal growth conditions.

3. Multi-sensor and multi-temporal observations linked to dynamic modelling improve management decision support systems for environmentally sound agricultural production.

1.4 Synopsis

Chapter 1 contains the justification for the current study and describes its societal significance. Chapter 2 presents the background and state-of-the-art of remote sensing and dynamic crop growth simulation applications in agriculture. Chapter 3 deals with the application of a point-based simulation model for regional yield estimates via the use of remote sensing images. Chapter 4 presents and discusses derivation of biophysical variables from near and remote sensing observations, with emphasis on the relation between leaf, plant and canopy nitrogen status. In Chapter 5, the practical integration and run-time calibration of remotely sensed information into a dynamic simulation model and the consequences for simulation accuracy are presented and discussed. In Chapter 6, the effect of variability in leaf area index (LAI) and crop nitrogen status (CNS) used in run-time calibration of a mechanistic and dynamic crop growth simulation model is analyzed. In Chapter 7 follows the general discussion and summary of the results.

1.5 References

- Alphen, B.J. van, 2002.
Soil processes as a guiding principle in precision agriculture. Ph. D. Thesis, Wageningen University, Wageningen, the Netherlands, 113 pp.
- Berge, H.F.M. ten, T.M. Thiyagarajan, Q. Shi, M.C.S. Wopereis, H. Drenth, 1997.
Numerical optimization of nitrogen application to rice. Part I. Description of *MANAGE-N*. *Field Crops Res.* 51, 29-42.
- Bindraban, P.S., 1999.
Impact of canopy nitrogen profile in wheat on growth. *Field Crops Res.* 63, 63-77.
- Booltink, H.W.G., J. Verhagen, J. Bouma, P.K. Thornton, 1996.
Application of simulation models and weather generators to optimize farm management strategies. In: Proc. of the 3rd International Conference on Precision Agriculture. 23-26 June 1996, Minneapolis, USA, pp. 343-360.
- Bouman, B.A.M., 1991.
Linking X-band radar backscattering and optical reflectance with crop growth models. Ph. D. Thesis, Wageningen Agricultural University, Wageningen, the Netherlands, 167 pp.

- Dreccer, M.F., 1999.
Radiation and nitrogen use in wheat and oilseed rape crops. Ph. D. Thesis, Wageningen Agricultural University, Wageningen, the Netherlands, 135 pp.
- Jordan, C.F., 1969.
Derivation of leaf area index from quality of light on the forest floor. *Ecol.* 50, 663-666.
- Langeveld, J.W.A., H. van Keulen, J.J. de Haan, B.M.A. Kroonen-Backbier, J. Oenema, 2005.
The nucleus and pilot farm research approach: experiences from the Netherlands. *Agric. Syst.* 84, 227–252.
- Leeuwen, H.C.J. van, 1996.
Methodology for combining optical and microwave remote sensing in agricultural crop monitoring: The sugar beet crop as special case. Ph. D. Thesis, Wageningen Agricultural University, Wageningen, the Netherlands, 233 pp.
- Porter, J.R., P.D. Jamieson, D.R. Wilson, 1993.
Comparison of the wheat simulation models *AFRCWHEAT2*, *CERES-Wheat* and *SWHEAT* for non-limiting conditions of crop growth. *Field Crops Res.* 33, 131-157.
- Rouse, J.W., R.H. Haas, J.A. Schell, D.W. Deering, 1973.
Monitoring vegetation systems in the Great Plains with ERTS. 3rd ERTS Symposium, NASA, SP-351, pp. 309-317.
- World Bank, 2000.
Agriculture and achieving the Millenium Development Goals. World Bank/International Food Policy Research Institute, Report 32729-GLB, Washington, USA, 80 pp. + appendices.

Chapter 2

Integrating crop growth simulation modelling and remote sensing for agriculture

2.1 Introduction

Information technologies, such as simulation modelling and remote sensing, have, from their inception, played important roles in agricultural research and in agricultural production systems. Since that moment, substantial technical progress has been made in both, simulation modelling and remote sensing, which still continues, due to the increasing possibilities in computer hard- and software and technological progress, combined with greater knowledge on modelled and observed systems.

Originally in isolation, crop growth simulation and remote sensing methodologies have played significant, but different roles in agricultural applications. For crop growth simulation modelling, the interest has predominantly been in yield forecasting of different cropping systems and the use of resources for crop growth, such as radiation, water and nutrients (van Ittersum *et al.*, 2003a). For remote sensing, applications in agriculture have focused traditionally on classification themes, but quantification of yields and biophysical crop properties has become more and more important.

There are similarities between crop growth simulation modelling and remote sensing as well: since their introduction, both techniques have always been advocated because of their large potentials, but a relatively small fraction of these potentials has led to actual applications. Although the number of actual applications is still quite impressive, there are numerous unused potential applications for both methodologies. The reasons for the limited applications are at the same time the reasons for their success: the rapid technological progress makes applications rapidly outdated, as new chances and opportunities appear at the horizon, even before the potentials of an application have been fully realized. The ability to rapidly adapt to changing demands, induced either through technological developments or through socio-economic developments, increases the possibilities for sustainable application of crop growth modelling and remote sensing.

It is hypothesized in this study that added value is generated through combining crop growth modelling and remote sensing. Acquired benefits are important if they contribute to improved resource use efficiency, reduced production risks and reduced environmental impact of agricultural activities. To successfully realize this integration, both methodologies will have to be merged seamlessly. The needs, conditions and

requirements for such a successful integration, will be analyzed and presented in the following chapters.

The crops considered, the two technologies, their development and applications in agriculture and agricultural research are treated first, followed by a description of some examples of successful combinations of simulation modelling and remote sensing in research and in applications. Subsequently, the approaches are identified having priority in integration for study objectives, as well as the necessary steps to successfully attain the integration. As the potential number of applications in simulation modelling and remote sensing is large, a well-founded choice is made to focus on those types of simulation models and remote sensing applications that are expected to contribute the most to study objectives.

2.2 Crops

The arable crops addressed in this thesis are potato (*Solanum tuberosum* L.), wheat (*Triticum aestivum* L.) and maize (*Zea mays* L.). These crops are of interest because they are grown world-wide and have been intensively studied. Food security for many people depends on these crops, and silage maize is an important component in the ration of large numbers of farm animals. The global extent of cultivation of these crops implies a large variation in environmental and social settings, including sub-optimal agro-ecological conditions and/or situations prone to environmental degradation due to mismanagement. Crop improvements and specific crop management are based on decades of agricultural research aiming at optimization of crop production and associated goals. The use of dynamic crop growth simulation modelling has played a substantial role in prototyping crop varieties and optimizing management practices in different environmental and social settings.

Potato, wheat and maize have well-pronounced characteristics that are of interest for remote sensing applications. Their growing period is characterized by a distinct pattern of phenological development (i.e. the order and rate of appearance of vegetative and reproductive organs), starting from emergence, i.e. the appearance of the growing point above the soil surface, followed by gradual coverage of the soil by canopy biomass, and ending at harvest with an abrupt change from canopy cover to bare soil. Crop growth is characterized by an increase in biomass, of which the aboveground part can be observed through optical remote sensing, especially through infrared channels. The quantity of water contained in the aerial biomass increases with increasing aboveground crop biomass, until ripening sets in (wheat, maize) or until the leaves start senescing or are removed (potato). The spatial arrangement of water (as reflected in canopy structure) of the aboveground crop organs can be observed through radar remote sensing at an appropriate wavelength. Differences in canopy structure, characterized by leaf angle distribution and leaf sizes, shapes, allow spectrally differentiating among crops. The grains (wheat, maize) are characterized by long erect stems and ears with grains (for wheat in the top layer of the canopy) and erectophile small (wheat) or large (maize) leaves. Potato is characterized by a well-pronounced

structure at the beginning of the growth cycle, but loses that structure in the course of the growth cycle, when stems collapse under the weight of the canopy. In wheat, stems may collapse due to nitrogen overdressing (lodging). Canopy structure can be decisively influenced by extreme weather, such as (hail) storms and frost. Total uptake of nutrients, specifically nitrogen, in potato, wheat and maize affects canopy colour, as nitrogen is part of the (green) chlorophyll that is responsible for the photosynthesis process. Higher concentrations of chlorophyll lead to increased 'greenness' of crop tissue; the chlorophyll concentration in the crop is characterized by a vertical gradient, reflecting the light intensity distribution in the crop. The seasonal patterns of chlorophyll concentration in potato, wheat and maize allow the use of optical remote sensing equipment for quantification of canopy nitrogen status that may be included in decision support systems for crop management. A number of these features will be explored in the following chapters of this thesis. The crops considered in this study show a strong differentiation in biomass, nutrient uptake and leaf area index development, resulting from differences in physiological processes and temporal development. If the integration of simulation modelling and remote sensing can be successfully demonstrated for the 3 crops, it is to be expected that the methodology can be extrapolated to other crops as well.

2.3 Crop growth simulation modelling

Crop growth simulation modelling may serve many purposes and can be performed to attain a broad range of objectives. A range of models (varying in structure, mathematical formulation and degree of detail) may aim at achieving one single objective, each claiming to provide the solution for a specific problem.

Simulation modelling comprises consistent quantitative integration of knowledge with respect to complex (bio) systems. The basis for simulation modelling in the systems approach is the mathematical description of system processes that are linked through physical, physiological and biochemical laws. Insight in individual system processes and their interactions is needed to understand system functioning. Therefore, simulation models are developed to organize and quantitatively describe these processes and relations in a systematic way. Models contain mathematical descriptions of physical, physiological and biochemical basic processes, either empirical or explanatory, but the aggregated result is a model that is a quantitative explanatory representation of the system under study. As such, all assumptions, inputs and results are made explicit and quantified, which allows to make them subject of discussion (Metselaar, 1999).

The increase in process knowledge and the concurrent improvements in computer technology have led to the development of increasingly complicated models of complex systems, such as the crop-soil system. Increased insight in individual processes allows more accurate quantitative descriptions that gain value in a systems approach where they are integrated to provide quantitative descriptions (models) of the functioning of the system as a whole. Such models allow explanation of observed phenomena from insight in the underlying processes. A systems approach enables

analysis of effects at higher integration levels, caused by influences at process levels. This feature is exploited in dynamic crop growth simulation models by analyzing, predicting and exploring the dynamics of crop growth as affected by environmental conditions. Such crop growth simulation models can thus be applied to analyze the effects of crop and soil management with or without climate change or extreme events on crop performance as the basis for the design of sustainable crop production systems, necessary to guarantee food security and sustained use of our resources for the next generations.

2.3.1 History

As one of the first, de Wit (1965) used a ‘computer model’ for explaining crop performance, which was followed in the late 1960s by the initiation of formal crop growth simulation (Brennan *et al.*, 1970; de Wit *et al.*, 1970). In the years that followed, the ‘School of De Wit’ developed increasingly complex dynamic simulation models, such as *ELCROS* and *BACROS*, evolving to a simple and universal model (*SUCROS*), of which the basic approaches are still valued to this day (Bouman *et al.*, 1996a; van Laar *et al.*, 1997; van Ittersum *et al.*, 2003b). One of the important developments associated with modelling of crop growth was encouragement of multidisciplinary research through system approaches, as interdisciplinary communication between different biophysical disciplines was an absolute necessity to develop these models. In that sense, simulation models still play an important role in knowledge transfer, training, education and decision-support systems (Donatelli *et al.*, 2002a).

Different problems at different scales call for different levels of model complexity. If potential biomass production is a key issue, for example, it is not necessary to use complex simulation models with details on photosynthesis processes or management interactions with soil characteristics and soil organic matter dynamics. It then suffices to convert intercepted radiation via potential radiation use efficiency into biomass production. If more detail is needed on stomatal behaviour and heat transfer of a specific crop variety under different management scenarios in order to understand remote sensing signals, much more complex models are needed.

Greater model complexity and greater degree of detail in model processes require more, more detailed and more accurate input data, which by definition are more difficult to obtain. Greater model complexity however, is not a guarantee for good and accurate model performance. On the one hand, chances of introducing uncertainty increase with the use of more complex mathematical functions and with the increase in number of input parameters, as each estimated or measured parameter value will comprise a certain error. On the other hand, systematic bias increases when (over) simplified models represent more complex situations. Passioura (1996) has discussed the effect of error development for situations where system structures are well understood (Figure 2.1a) and where systems are wrongly interpreted (Figure 2.1b).

Additionally, measuring large numbers of input parameters contributes to making

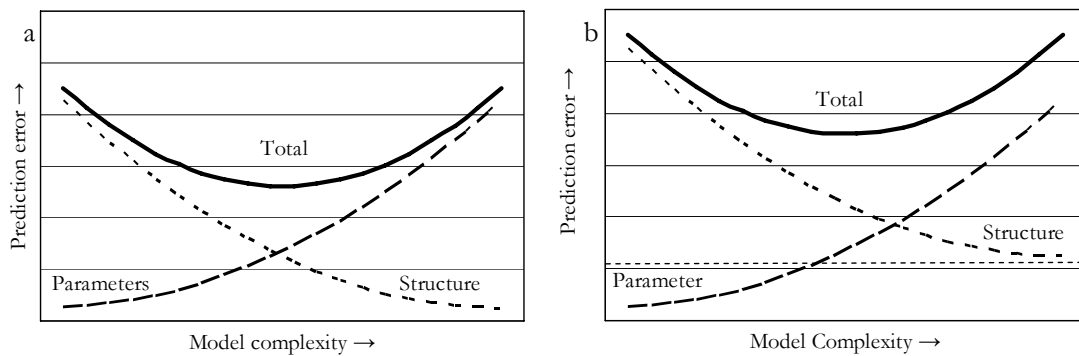


Figure 2.1 Components of prediction error in models of increasing complexity: a) when the structure of the system is well understood; b) when the structure is wrong, with irreducible structural error represented by the dashed asymptote. (After: Reynolds and Acock, 1985).

models more site-specific, limiting their applicability to local situations, and hampering their portability to other (environmental) conditions. At the same time, spatial variability of (especially soil) input parameters is disregarded if results are to be applied to whole plots. The uncertainty propagation of errors introduced in input parameters should not be neglected, but is often underestimated. Awareness of these aspects of simulation of ecosystems has led to the development of simple so-called summary models that are applied successfully (e.g. Penning de Vries, 1982; Spitters, 1990).

Global, regional and landscape modelling benefit from the general nature of process models with the precision and predictive power of empirical models (Korzukhin *et al.*, 1996). The aspect of selecting the appropriate complexity level for a specific problem should be recognized at all stages in the systems approach and will be discussed extensively.

In addition to a large number of well-known and published crop growth simulation models (cf. Donatelli *et al.*, 2002b), an even larger number of half-products, clones and replicas exists. Far too often such models are used only once, for local definition of input parameters to control the biotic and abiotic feedback systems. The majority of simulation models is poorly documented and has little value for re-use and verification, violating an important base rule of reliable science. Models are regularly applied in settings for which they were not developed, without the necessary and documented calibration and validation procedures. Hence, the limitations specified during their development are ignored. Operation of simulation models requires expert knowledge and specific interpretative skills, which make sharing and re-use of simulation models and modules a tough challenge. The development of modelling frameworks, in which models and modules are linked, even if originating from various sources and written in different programming languages, increases the re-usability of research results, while the model components retain their original structure. Such modelling frameworks generally incorporate tools for easy interpretation and visualisation of simulation results (e.g. Acock *et al.*, 1999; Hillyer *et al.*, 2003). These developments have to be encouraged, as they serve the scientific community by open-source approaches and standard requirements for model use.

2.3.2 Model types

Crop growth simulation models can be grouped in various ways. A popular classification is that in descriptive, statistical and mechanistic models. Descriptive and statistical models mimic growth patterns, using statistics or fitted curves of observed values to reproduce growth patterns under similar circumstances. These types of models are not of interest here, although the mechanistic simulation models advocated here, do take advantage of growth statistics and growth descriptions by using empirical relations to simulate basic processes.

For all dynamic simulation models it should be decided what integration time-step is best (or optimal). Optimal time-step size depends on base process rates in the simulation model (Leffelaar, 1993), and process reaction time to environmental change (which is scale-dependent). As a leading rule, reaction time to system interference should be taken as a time-step. System interference can be of natural nature (such as weather characteristics) and human nature (such as by management practices).

In mechanistic crop models an environmental system is initialized, after which the simulated pools are depleted and/or replenished at rates calculated according to the laws of physics and biochemistry under the influence of environmental forces. Well-defined, mechanistic models are based on insights in the underlying processes and are therefore more appropriate for system approach analyses and research.

Most common mechanistic crop growth simulation models are canopy functioning models. In such dynamic simulation models, a crop emerges in dependence of environmental conditions following sowing or planting and starts to intercept incoming radiation by its developing green area. The fraction absorbed photosynthetically active radiation (f_{APAR} , -) determines the proportion of incident photosynthetically active radiation (PAR, MJ m⁻²) available for conversion into biomass. Net primary production (NPP, g m⁻²) can be calculated by multiplying absorbed radiation (MJ m⁻²) by radiation use efficiency (RUE_n, g MJ⁻¹). Gross primary production (GPP, g m⁻²), the net result of carboxylation and photorespiration is more related to light absorption than NPP, as NPP also includes autotrophic respiration terms and C₃ and C₄ biochemical pathways differ in this aspect (Goetz and Prince, 1999). Monteith (1972) suggested that RUE is stable across species and Field (1991) demonstrated the convergence of net RUE across vegetation types, but later studies have shown significant variation in net RUE among crops. Thus, net RUE varies among crops and crop varieties, but is more stable with location and/or crop management. Crop location determines available growth resources, such as incoming radiation, temperature and precipitation. Soil characteristics modified by management co-determine the availability of these resources for crop growth.

Simple and more complex mechanistic models exist, ranging from RUE-based models (with a single parameter for the conversion of intercepted radiation into biomass (cf. *DSSAT* (Porter and Jones, 1998)), to comprehensive models that include detailed descriptions of photosynthesis processes, such as introduced by Farquhar *et al.* (1980). In the latter type, photosynthesis, maintenance and growth respiration processes are simulated explicitly (such as in the models *SUCROS* (van Laar *et al.*, 1997), *WOFOST* (Supit *et al.*, 1994), and some crop modules in *APSIM* (McCown *et al.*, 1996). There is a clear distinction in modelling approach between canopy functioning models and so-

called SVAT-models (soil-vegetation-atmospheric-transfer). SVAT-models are based on functions quantitatively describing transfers over crop and soil boundaries and over crop internal boundary layers. Time-steps are typically less than a day (minutes or seconds), as reaction times of incorporated processes are of that order of magnitude. Simulation pools should therefore be integrated with the calculated process rates (Leffelaar, 1993). In both model types, moisture and nutrient stress may hamper crop growth and development, but they use different methodological approaches to account for these effects. The reason for the interest in using SVAT-models, in combination with remote sensing is that SVAT-models use energy balances and are therefore easily integrated with remote sensing information. In general, input requirements for SVAT-models are higher, and they are more difficult to upscale from plant to canopy, and larger scales.

Usually, mechanistic crop growth simulation models are executed with a time-step of 1 day, but weekly, ten-day, monthly and annual time-steps are also applied. Ultimately, the simulation time-step is determined by the process rates that are important for the study objectives. For example, if accurate estimation of nitrogen leaching is important, all processes that affect nitrogen leaching should be considered: precipitation, mineralization and nitrogen uptake. In that situation, time-steps of 1 day (or less) are required.

In general, simulation scale is highly correlated with time-step: small time-steps for the simulation of small areas, such as points and (sub) plots, to larger time-steps for larger scales, such as landscape, region or continent. Some input parameters are easily established at small scales, while at larger scales they can not be established at all (Wopereis, 1993). Moving up to larger spatial scales requires generalisation of simulation models, at higher levels of integration, different types of inputs and larger time-steps.

As crop growth interacts with its environment, (simple or complex) soil water and nutrient modules are added to the crop growth module. A soil water module comprises the water fluxes, such as precipitation, irrigation, evaporation, transpiration, and vertical or lateral drainage. A soil nutrient module describes nutrient fluxes, such as organic and inorganic fertilizer application, wet and dry deposition of nutrients, build-up and decomposition of organic matter pools, nutrient uptake and leaching. From applications in scientific research, where environmental conditions are either fully controlled or continuously monitored, and their main aim was contributing to increased insight in crop functioning, crop growth simulation modelling has moved towards applications in crop management. Management modules may be part of simulation models to describe management interactions with the crop-soil system, in order to contribute to development of decision support systems.

Crop functioning models find their applications for a range of objectives, such as prediction of the onset of the growing season, prediction of crop emergence, prediction of crop nitrogen demand, yield forecasting and assessing the impact of climatic change. The here advertised system approach integrates important processes and enables to identify where to interact with the system if necessary.

Functional modelling and good modelling practice imply focusing only on those soil and crop processes considered relevant in solving of a well-defined problem. Identification of 'relevant processes' is not only guided by crop and soil requirements, but also by socio-economic circumstances. In this study, identification of the relevant

processes was guided by the requirement to incorporate those processes that easily interact with remote sensing observations. The main objectives for model use and applications are related to generation of support for crop-, soil- and site-specific crop management. The simulation models *PlantSys* and *Rotask 1.5*, both based on *Rotask 1.0* (Jongschaap, 1996) and built upon the approaches of the ‘School of De Wit’ simulation models (van Ittersum *et al.*, 2003b) have been selected for use in dynamic integration with remote sensing information.

2.3.3 Model applications in agriculture

From model applications in agriculture, a limited number of them are geared towards yield prediction based on the farmers’ environment (crops, soils and climate) and possible management interactions. Such simulation models are used as components in Decision Support Systems (DSS) to guide crop management, such as for nitrogen fertilizer recommendations (Acock *et al.*, 1999; Booij and Meurs, 2002; van Delden *et al.*, 2002; Flowers *et al.*, 2003) or irrigation (Bergez *et al.*, 2001). Keating and McCown (2001) concluded that the real challenges of model applications in agriculture lay in the interface of ‘hard’ scientific approaches to the analysis of biophysical systems and ‘soft’ approaches to intervention in social management systems, both for commercial farming and for small subsistence farming systems.

The Crop Growth Monitoring System (CGMS) developed in the project Monitoring of Agriculture with Remote Sensing (MARS) that started in 1988, provides the European Commission (DG Agriculture) with objective, timely and quantitative yield forecasts at regional and national scale. CGMS predicts crop development, growth and yield in Europe, driven by meteorological conditions modified by soil characteristics and crop parameters. This mechanistic approach describes crop phenological development and dry matter accumulation, partitioned into the various organs (roots, leaves, stems and storage organs) from sowing to maturity with a daily time-step. The main characteristic of CGMS is its spatial component, integrating interpolated meteorological data, whereas soil and crop parameters are obtained through elementary mapping units for simulation in the crop model. The core of the system is based on the crop growth model *WOFOST* (Supit *et al.*, 1994) and the grass growth model *LINGRA* (Bouman *et al.*, 1996b). GIS tools are used to prepare input data and to produce output maps. Input and output are stored in a Relational Data Base Management System (RDBMS). Statistical procedures are used to forecast crop yields.

2.4 Remote sensing

The chronological development or history of the use of remote sensing from platforms that fly or orbit above the Earth’s surface is shortly introduced based on the Remote Sensing Tutorial (NASA, 2004) and Remote Sensing in History (NASA, 1995-1998).

Different remote sensing observation methods and successful applications in agriculture will be highlighted.

2.4.1 History

Remote sensing as a technology started with the first aerial photographs taken from a balloon over Paris in the middle of the 19th century. Photography has served as a prime remote sensor for more than 150 years. It found major military applications in World War I. From then on, until the early 1960s, aerial photography remained the single standard tool for depicting the surface of the earth from a vertical perspective (Figure 2.2).

In the 1930s radar (Radio Detection And Ranging) technologies were developed in Germany. In World War II, a range of imaging systems, such as near-infrared photography, thermal sensing and radar were explored. Near-infrared photography and thermal-infrared observations appeared valuable in distinguishing real vegetation from camouflage.

In the 1950s, remote sensing systems continued to evolve from the systems developed for the war effort. Colour Infrared Photography (CIR) was found to be very useful in the plant sciences. In 1956, experiments were conducted on the use of CIR for recognition and classification of vegetation types and for detection of diseased and damaged or stressed vegetation. Also in the 1950s, significant progress was made in radar technology, with the development of two new radar types, side-looking airborne radar (SLAR) and Synthetic Aperture Radar (SAR). Both developments aimed at acquisition of images at the highest possible resolution.

Remote sensing above the atmosphere started early in the space age with the launch of Sputnik I by the Soviet Union in 1957, the start of the space race between the USA and



Figure 2.2 From left to right: Caricature of Gaspard Felix Tournachon in 'Le Boulevard' (1860), early aerial photography: Boston photographed from a balloon (James Wallace Black in 1859), mounting pigeons with cameras (1903) and oblique photographs taken out of an aeroplane 44 (1909 and today). Source: NASA (1995-1998).

the USSR. The Sputnik launch led directly to the creation of the National Aeronautics and Space Administration (NASA) in 1958, and further explorations from space followed. Russian missile deployments, such as those of the Cuba crisis and monitoring of new missile sites have been successfully performed by remote sensing. In the 1960s, as man entered space, cosmonauts and astronauts in space capsules took photos from the window. In the course of the 1960s, the first sophisticated imaging sensors were incorporated in orbiting satellites. At first, these sensors were basic television cameras that imaged crude, low-resolution black and white pictures of clouds and the earth's surface (TIROS: Television Infrared Observation Satellite). Subsequently, other types of sensors were developed that took images using the electromagnetic (EM) spectrum beyond the visible, into the near and thermal infrared regions. The field of view (FOV) was broad, usually hundreds of kilometres to one side. Such synoptic areas of regional coverage were of great value to meteorologists, collecting information on clouds, air temperatures, wind patterns, etc. A significant advance in sensor technology was the subdivision of spectral ranges of radiation into bands (intervals of continuous wavelengths), allowing sensors in several bands to form multispectral images.

The first multispectral photographs came from the manned Apollo 9 mission in 1968. Various specialists, particularly geologists, hydrologists, agronomists, forestry specialists and scientists dealing with environmental monitoring and land use/cover assessment rapidly recognized the value of multispectral photography. In 1970, the TIROS programme was renamed into NOAA (National Oceanic and Atmospheric Administration), financed by the US Administration. Until today, the NOAA Advanced Very High Resolution Radiometer (AVHRR) is orbiting the globe and collecting information on weather patterns in visible, near-infrared and thermal wavelengths.

In 1972, the first civilian satellite remote sensor was launched, ERTS1 (Earth Resources Technology Satellite, later in 1975 renamed into Landsat-1). This satellite has played an important role in increasing our understanding of many of the earth's features. The French followed the American efforts in 1986 with the launch of SPOT-1, followed by India with IRS-1a in 1988, and Japan with JERS1 and JERS2 in 1990. The European Space Agency launched ERS-1 in 1991. In the meantime, successors to Landsat, SPOT and ERS satellites have been launched.

In the same period, Imaging Spectroscopy (IS) went through a revolutionary phase and became available for remote sensing applications (van der Meer and de Jong, 2001). Imaging Spectroscopy provides a continuum of many narrow spectral bands in the visible, near infrared and mid infrared which reveal individual absorption bands of biochemical components and water in vegetation and soil. The development of IS enabled to look more specifically at vegetation (composition) and the possibility for 'finger printing' soil and vegetation by their specific hyperspectral signatures (Goetz *et al.*, 1985). Examples of such systems are the Digital Airborne Imaging Spectrometer (DAIS) and Airborne Visible Infrared Imaging Spectrometer (AVIRIS).

The first of a new generation of commercial high-resolution remote sensing satellites became operational when Space Imaging launched its Ikonos satellite in 1999. With 1-meter panchromatic and 4-meter multispectral sensors and the capacity to be tasked at specific optimal times, Ikonos provides options for a variety of applications. With

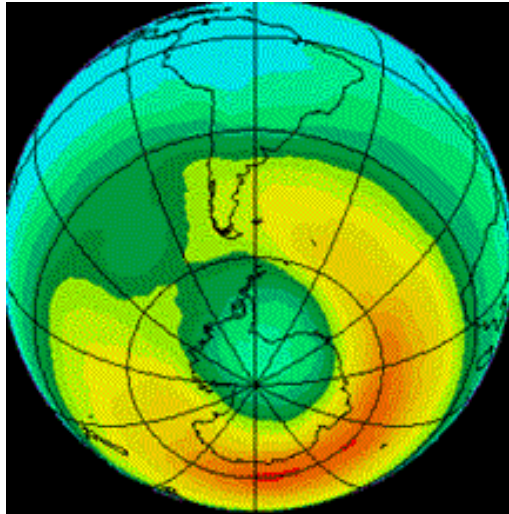


Figure 2.3 Depiction of ozone gas concentrations projected on the Earth's surface, with the low ozone concentrations around the south pole. Source: NASA (1995-1998).

Ikonos and similar systems, such as Quickbird, spaceborn remote sensing approaches the quality of airborne photography.

In 2002, the European Space Agency launched Envisat, an advanced polar-orbiting Earth observation satellite that provides images of the atmosphere, ocean, land, and ice, ensuring the continuity of ERS satellite measurements.

Chronologically, some of the interesting records of mayor events 'observed' by remote sensing are presented, such as the discovery of the hole in the ozone layer (Figure 2.3): data derived from satellite information led to the internationally agreed 50 % reduction in the use of chlorofluorocarbons (CFCs). In 1986, satellite remote sensing monitored the radioactive effects of the world's largest nuclear disaster in Chernobyl, Russia. Now, remote sensing is considered an important component in emergency detection, not only for natural disasters, such as volcano eruptions, forest fires and hurricanes, but also for human-induced catastrophes, such as deforestation and environmental pollution.

In Europe, an important and succesful development in remote sensing was supported by the European Commission, who, as a control mechanism for agriculture subsidies in the European Union, applied RS at large scale in their member states. As a result of the monitoring system that covered Europe, ineligible subsidy claims could be recovered and potential new fraud could be reduced (Boogaard *et al.*, 2002).

2.4.2 Remote sensing types

Observations from remote sensors can be classified in several ways. Two methods of classification are presented here, to answer the question: what exactly are we looking at? The type of information that can be retrieved from remote sensing information and the degree to which it can be quantified are important issues in the current study. The

first classification is based on the electromagnetic spectrum, as the electromagnetic range of the sensor determines the type of information that can be retrieved from recorded signals. The second classification is based on the sensor's operational platform, in other words: how and from where can the sensor be operated? The use of a specific platform is determined by other factors than technical factors alone, but has specific consequences for the information that is retrieved.

Spectra

Looking at the electromagnetic spectrum (Figure 2.4), a classical and logical method to categorise remote sensors presents itself. Each part of the electromagnetic spectrum is absorbed, transmitted and reflected differentially by materials of different origin and/or different texture. This feature forms the physical basis for remote sensing observations and is pertinent for the present study.

Optical remote sensors are the sensors operating between $0.3 \mu\text{m}$ and $15 \mu\text{m}$ and cover the wavelengths that can be reflected and refracted with lenses and mirrors. The visible domain is located between the ultraviolet (ending at $\approx 400 \text{ nm}$) and the infrared (starting at $\approx 800 \text{ nm}$), and consists by definition of the registration domain of the human eye. Atmospheric effects on signal transmittance can be substantial in particular wavelength (Figure 2.5). Unless the atmosphere itself is studied, using these absorption features of the atmosphere should be avoided when studying the earth's surface. This should be realized by selecting the appropriate bandwidths for observations.

At some wavelengths, radiation energy is absorbed and thus 'blocked' for remote sensing, but there are clear windows through which electromagnetic waves can penetrate more easily in the atmosphere. The absorption peaks (or transmittance minima) can be assigned to specific components of the atmosphere, such as water absorption at 1.4 and $1.9 \mu\text{m}$. A longer pathway through the atmosphere results in lower radiation energy at the receiving end, restricting the possibilities to record strong

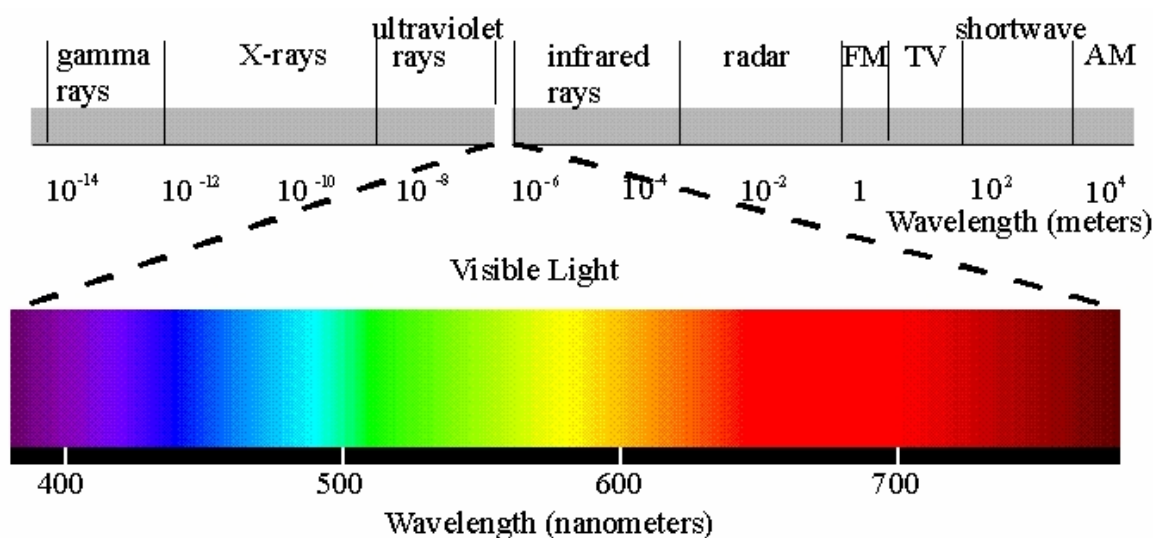


Figure 2.4 Electromagnetic spectrum (source: Kaiser, 2005).

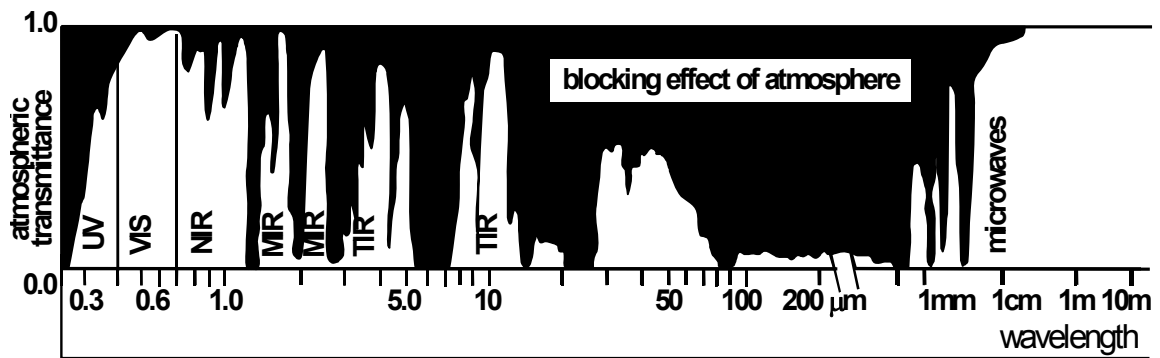


Figure 2.5 Relative transmittance of electromagnetic energy through the atmosphere (cf. Lillesand and Kiefer, 2000). The white area is the solar spectrum (as received at the Earth's surface) and the black area is the blocking effect (absorption) by the atmosphere. UV=ultraviolet, VIS=Visible, NIR=Near InfraRed, MIR=Middle InfraRed, TIR=Thermal InfraRed.

signals. Note that atmospheric absorption is nearly absent in the microwave domain (Figure 2.5). Due to longer wavelengths, radar beams are not absorbed in the atmosphere and thus retain their energy status. This feature enables radar beams to penetrate through clouds at longer wavelengths and penetrate more deeply into vegetation and soil. The selected radar wavelength controls the penetration depth and thus the size of objects that can be detected (Table 2.1).

Radar remote sensors can be sub-divided into passive and active radar systems. Active radar systems have their own transmitter: radar beams emitted first are received after interfering with objects. The change in intensity between the emitted and the received signal enables identification and quantification of the objects interfering with the radar beams. Passive radar sensors pick up energy signals transmitted naturally by objects.

Platforms

Remote sensors may operate on diverse platforms (or stages), i.e. spaceborne, airborne or field-based. It is useful to make this specific distinction among sensors, because it is

Table 2.1 Radar bands: names and wavelengths (Source: Evans, 1995).

Band	Wavelength (cm)		
Ka	0.75	-	1.13
K	1.13	-	1.67
Ku	1.67	-	2.40
X	2.40	-	3.75
C	3.75	-	7.50
S	7.50	-	15.00
L	15.00	-	30.00
P	30.00	-	100.00

a factor in determining their success in agricultural applications. Although sensor resolution may be part of its specifications, the platform (or distance from the earth's surface) on which it is operated also influences the resolution of the observed objects (observation scale). This observation scale determines the possible degree of interference with the observed objects.

Furthermore, sensor platform selection affects the image pre-processing procedures (and time). The further the platform is from the earth's surface, the more procedures are necessary to correct the signals geographically and atmospherically. Radiometric corrections are needed as well, but these are not platform-dependent. With the use of microcomputers, the cost of image processing has greatly decreased, while the quality of the output is superior to that of older methods.

Geographical corrections include corrections for skew: the effect due to rotation of the earth, and hence the ground target that continuously moves below the advancing sensor. The space (or air) craft also moves, and various corrections may be needed for observations deviating from the vertical direction. If pixel images are off-nadir (oblique), they are elongated, the degree depending on the observation angle, which should be corrected. Recording platform movements is a pre-requisite for airborne and spaceborne sensors. Once the various corrections have been implemented, the result is usually a shift in position of any given pixel in its new framework.

Atmospheric corrections can be necessary due to a variety of natural causes. For example, the presence of water vapour influences radiation transmission. Measured intensity values for a specific target thus vary with different climatic conditions, for which remote sensing observations can be corrected.

Radiometric corrections may be needed for variations in detector response and electronic perturbations. Most common are systematic differences in sensors, such as random noise (speckling). 'Standardized' computer-based procedures are available to implement all these corrections, improving overall image quality. Instrumental correction is generally done onboard, as it is a relatively easy process compared to geographical and atmospheric corrections that are performed mostly on the ground.

The three stages considered in this study are:

- a) **Ground-based** stages (e.g. hand-held sensors, sensors mounted on static platforms or on mobile ones),
- b) **Airborne** platforms (e.g. unmanned or manned aeroplanes, balloons, zeppelins, etc.), and
- c) **Spaceborne** platforms (satellites).

Ground-based stages are relatively cheap and can record signals at high spectral resolution, high geographical resolution and high temporal resolution (to the user's needs), but generate point measurements. With the aid of a Geographical Positioning System (GPS) and spatial statistics such as Kriging, spatial distributions can be obtained from these point measurements. Airborne applications are relatively more expensive (flight costs), but may be performed at high geographical resolution (varying altitude). An advantage of airborne and spaceborne sensors is that they can cover larger

spatial scales. A disadvantage of spaceborne stages is that their multispectral sensors are often broad-banded (and not always in the appropriate electromagnetic domain), and hyperspectral sensors are not common (yet). Moreover, their temporal resolution (observation frequency) is problematic, as the satellite orbit rate, which especially for multispectral and hyperspectral sensors is relatively low, determines observation frequency. Additionally, climatic conditions (in the optical domain) may hamper observations at the right time, which may result in lack of information in support of management decisions on the ground. Pre-processing times of airborne and satellite images are relatively long due to geographical, atmospheric and radiometric corrections.

2.4.3 Remote sensing applications in agriculture

It has been shown that remote sensing can provide important information on agricultural environments. At the scale of leaves, plants, sub-fields, fields, regions, and at global scales, efforts have been made to retrieve useful information in support of a variety of activities. These activities comprise retrieving leaf and plant biochemical composition, plant (health) status, crop (health) status, regional and global estimates of vegetation cover (including arable crops) in order to improve farm management and to support local, regional or higher scale policy makers. Table 2.2 summarizes successful studies (with references) at different scales, including information on sensor techniques and application scale.

The majority of vegetation characteristics that can be retrieved from remote sensing and that are useful in agriculture settings is derived from so-called vegetation indices (VI). Vegetation indices are derived from combinations of measurements in those electromagnetic bands that correlate with specific vegetation features. Observations from a number of electromagnetic bands are combined, often as ratios, to increase the discriminative power of remote measurements. For example, biomass strongly reflects in the infrared part of the spectrum, while reflection is high in the green part of the spectrum, and absorption is high in the red part of the spectrum. Combining observations in those electromagnetic wavelengths enhances the possibilities for biomass detection and increases the possibility to discriminate other objects, such as water bodies.

Further important reasons for using VI are reducing or removing background effects, such as the influence of the soil (e.g. SAVI (Huete, 1988) and WDVI (Clevers, 1989)). The benefit of soil correction is a more linear relation between biomass and VI and greater responsiveness of VI to biophysical plant characteristics. Such soil background correction is highly beneficial in vegetation studies, because it minimises saturation problems at high vegetation cover. Table 2.3 presents important VI and detection themes of successful studies.

Being able to retrieve biophysical information from remote sensing observations opens the way to applications in agricultural settings. In the following sections we deal with the most important ones with the greatest success.

Table 2.2 Vegetation indices (VI) with formulas, parameters and references.

Abbreviation	Full name	Formula	Parameters	Reference
ATSAVI	Adjusted transformed soil adjusted vegetation index			Baret and Guyot (1991)
CACI	Chlorophyll absorption continuum index			Broge and Leblanc (2000)
CARI	Chlorophyll absorption in reflection index			Kim <i>et al.</i> (1994)
DVI	Difference vegetation index	$R_{nir} - R_{red}$		Jordan (1969)
EVI	Enhanced vegetation index	$a*(R_{nir} - R_{670}) / (b + R_{nir} + c*R_{670} - d*460)$	$a=2.5, b=1, c=6, d=7.5$	Justice <i>et al.</i> (1998)
F735/F700	Chlorophyll fluorescence ratio	R_{735} / R_{700}		
fWBI	Floating water band index	$R_{900} / (\min(R_{930} - R_{980}))$		Strachan <i>et al.</i> (2002)
GEMI	Global environment monitoring index	$(nir - br - a) / (R_{red} + z)$		Pinty and Verstraete (1992)
GESAVI	Generalized soil adjusted vegetation index	$(R_{nir} - R_{green}) / (R_{nir} + R_{green})$		Gilbert <i>et al.</i> (2002)
GNDVI	Green normalized difference vegetation index	$(R_{700} - R_{670}) - 0.2 * (R_{700} - R_{550}) * (R_{700} / R_{670})$		Gitelson <i>et al.</i> (1996)
MCARI	Modified chlorophyll absorption in reflection index	$(2 * (R_{nir} + 1) - SQR(2 * (R_{nir} + 1)^2 - 8 * (R_{nir} - R_{red}))) / 2$		Daughtry <i>et al.</i> (2000)
MSAVI	Modified soil adjusted vegetation index	$(2 * (R_{nir} + 1) - SQR(2 * (R_{nir} + 1)^2 - 8 * (R_{nir} - R_{red}))) / 2$		Qi <i>et al.</i> (1994)
MSAVI2	Modified soil adjusted vegetation index, No.2	$(R_{nir} - R_{vis}) / (R_{nir} + R_{vis})$		Qi <i>et al.</i> (1994)
NDVI	Normalized difference vegetation index	$(R_{570} - R_{531}) / (R_{570} + R_{531})$		Rouse <i>et al.</i> (1974)
OSAVI	Optimized soil adjusted vegetation index	(R_{800} / R_{680})		Rondeux <i>et al.</i> (1996)
PRI	Photochemical reflectance index	(R_{800} / R_{635})		Gamon <i>et al.</i> (1992)
PSSRa	Pigment specific simple ratio (Chl a)	(R_{800} / R_{470})		Blackburn (1998)
PSSRb	Pigment specific simple ratio (Chl b)	$(R_{nir} - b * R_{red} - a) / (SQR(1 + b^2))$		Blackburn (1998)
PSSRc	Pigment specific simple ratio (Carotenoids)	$(R_{675} / R_{700}) / (R_{675} / R_{700})$		Blackburn (1998)
PVI	Perpendicular vegetation index	$(R_{675} / R_{650} * R_{700}) * (R_{675} / R_{650} * R_{700})$	$a = \text{interec}, b = \text{gradient nir/red soil line}$	Richardson and Wiegand (1977)
RARSa	Ratio analysis of reflection spectra (Chl a)	$(R_{760} / R_{500}) / (R_{760} / R_{500})$	$r = \text{reflectance of well developed species}$	Chapelle <i>et al.</i> (1992)
RARSb	Ratio analysis of reflection spectra (Chl b)	$SQR(NDVI * DVI)$	$r = \text{reflectance of well developed species}$	Chapelle <i>et al.</i> (1992)
RARSc	Ratio analysis of reflection spectra (Carotenoids)	point of maximum slope between vis and nir	$r = \text{reflectance of well developed species}$	Chapelle <i>et al.</i> (1992)
RdVI	Renormalized difference vegetation index	$(VI_{pix} - VI_{min_pix}) / (VI_{max_pix} - VI_{min_pix}) * 100$		Roujean and Breon (1995)
REP	Red edge position	R_{nir} / R_{red}		Miller <i>et al.</i> (1990)
RGI	Relative greenness index	R_{nir} / R_{red}		Burgan <i>et al.</i> (1998)
RVi	Ratio vegetation index	R_{nir} / R_{red}		Jordan (1969)
SAVI	Soil adjusted vegetation index	$R_{nir} / (R_{red} + b/a)$	$a = \text{interec}, b = \text{gradient nir/red soil line}$	Huete (1988)
SAVI2	Soil adjusted vegetation index, No.2	$(R_{800} - R_{445}) / (R_{800} - R_{680})$		Baret and Guyot (1991)
SIPI	Structure independent pigment index	R_{nir} / R_{red}		Peñuelas <i>et al.</i> (1995)
SR	Simple ratio	$a * (R_{nir} - (a8R_{red}) - b) / (R_{red} + (a * R_{nir}) - (a * b))$	$a = \text{slope}, b = \text{gradient of Red/nir plot}$	Jordan (1969)
TSAVI	Transformed soil adjusted vegetation index	R_{900} / R_{970}		Baret <i>et al.</i> (1989)
TVI	Triangular vegetation index	$R_{nir} - a * R_{red}$		Broge and Leblanc (2000)
WBI	Water band index			Peñuelas <i>et al.</i> (1994)
WDVI	Weighted difference vegetation index		$a = \text{ratio } R_{vis} / R_{nir} (\text{soil})$	Clevers (1989)

Classification of Agricultural Land Use

Biophysical parameters can be related to specific vegetation features, such as architecture, colour and composition. These features are vegetation type-specific and significantly influence reflection and absorption characteristics. As these characteristics can be established under varying conditions, successful classification of vegetation types is possible and has widely been performed (e.g. Jago *et al.*, 1999; Turner *et al.*, 2002). Classification is used for identification and for mapping purposes, e.g. at the request of the European Union at large scales, or by order of local authorities at small scales to map actual land use and areas.

Quantification of Biophysical Variables in Agriculture

As has been shown, various characteristics of the earth's surface can be identified and classified, using appropriate remote sensing specifications (i.e. resolution, spectral domain). For agricultural objectives, quantification of several of these characteristics is relevant, as they may give an indication of vegetation status or crop (growth) performance. In some cases, management interactions can be invoked, if quantitative information can be retrieved with appropriate accuracy and timing.

Successful investigations to relate dry matter yield or biomass to remote sensing signals are quite common (e.g. Aparicio *et al.* (2000) for durum wheat at field scale). Such relations with fresh weight have also been established (Thenkabail *et al.*, 2000). Quantification of leaf area index is very important as it determines a crop's capacity to intercept incoming radiation and thereby crop production potential. Leaf area index quantification has been the subject of various studies, such as Turner *et al.* (1999) and Broge and Leblanc (2000). Successful determination of evapotranspiration rates for irrigated farming and water resource management has been demonstrated by Bastiaanssen *et al.* (2000). Water supply is important for crop growth, as photosynthesis is accompanied by unavoidable water loss, and crop water supply is therefore linearly related to crop production. Estimation of evapotranspiration is therefore an important indicator for crop growth reduction. As vegetation growth is driven by photosynthesis which occurs in chlorophyll, located in vegetation canopies, quantification of chlorophyll contents by remote sensing techniques has been studied by various authors, with varying degrees of success. Quantification of chlorophyll content has been quite successful at leaf level, based on hyperspectral and high resolution measurements with fluorescence techniques (e.g. Zarco-Tejada *et al.*, 2003). Up-scaling chlorophyll quantification from leaf to canopy level introduces confounding effects of leaf area index and background that can be partially eliminated by combining different vegetation indices as shown by Daughtry *et al.* (2000). Successful mapping of chlorophyll spatial patterns, derived from field and airborne spectra have been demonstrated by Jago *et al.* (1999), with a root mean square error (RMSE, a measure of goodness of fit) of 0.42 mg g^{-1} ($\pm 13 \%$ of the mean) for grassland and 2.09 mg g^{-1} ($\pm 16 \%$ of the mean) for winter wheat. Some Decision Support Systems (DSS) have been based on crop light reflection to monitor crop nitrogen status, such as for barley (Booltink and Verhagen, 1997) and potato (Booij *et al.*, 2001; Jongschaap and Booij,

2004). Studies on detection of the phosphorus status of vegetation canopies have not been very successful. Osborne *et al.* (2002) have shown that hyperspectral data can be used to estimate nitrogen and phosphorus concentrations under nutrient stress. Phosphorus is most accurately estimated at early growth stages.

For more complex structures and spatially heterogeneous vegetation canopies, with varying background properties, previously found relations between spectral features and the pigment and biophysical properties of vegetation (Table 2.2) do not necessarily hold (Blackburn and Steele, 1999). Other agriculturally interesting properties that have been subject to quantification through remote sensing observations include crop establishment, defoliation fraction, disease infestation, fraction intercepted radiation, plant height, radiation use efficiency and crop temperature.

2.5 Combinations of remote sensing and simulation modelling

Combinations of remote sensing and simulation modelling can be synergistic in various ways. The first area of interest here is the input of remotely-sensed data into simulation models. Two approaches are possible:

- a) Estimates of intrinsic values to set the crop simulation environment (e.g. crop classification, emergence, flowering and harvest dates, etc.), and
- b) The use of estimates of values of biophysical variables that can be used to drive the simulation model during run-time ('run-time calibration').

For the second area of interest, the spatial aspect of remote sensing images can be integrated, i.e. the synoptic overview that earth observation imagery provides. Two application fields are important:

- a) Using sub-field or sub-region variability to differentiate within an area, originally considered homogeneous.
- b) Using the spatial aspect of remote sensing images to upscale simulation results, to obtain field, or regional results.

2.5.1 Estimating the simulation environment

Most of the combined use of remote sensing and simulation modelling is based on classification of the earth's surface by remote sensing, in order to use appropriate crop growth simulation models. Large areas (160.000 km²) of natural grasslands in the highlands of Peru and Bolivia could be classified (using ERS and NOAAH satellite data) as specific pasture types to predict biomass production and biomass quality in the region (Jongschaap and Quiroz, 2000). Crop growth simulation models were used to estimate soil properties, starting from a set of soil parameters quantified through expert knowledge and simulating 30 years of climatic influences on the prevailing pasture

types. The same approach was used in Australia: Landsat TM satellite images were used to set pasture type, pasture condition and fertility status (Hill *et al.*, 1999).

2.5.2 Estimating crop-soil system development

Time-series of estimates of biophysical characteristics retrieved from remote sensing can be used for model calibrations and this combination is therefore useful. Clevers *et al.* (2002) used SPOT data to calibrate a wheat growth model under Mediterranean conditions, by estimating leaf area indices and introducing these as calibration sets. Jongschaap and Schouten (2005) successfully applied model calibration by estimating regional sowing, emergence, flowering and harvest dates of wheat. More often, simulation models are validated by remote sensing estimates of biophysical variables, e.g. on a regional scale for biomass production (Sparrow *et al.*, 1997). There is a growing tendency in the direction of continuous monitoring in highly developed agriculture, such as precision agriculture in the USA and in Western Europe.

2.6 Synopsis

In this chapter, I provided an overview of the most important properties of the crops studied in this thesis, of the range of crop growth simulation models and their historic development and of the various remote sensing observation methods and their developments over time. Additionally, I highlighted the application so far of these techniques in agriculture. The next chapters of my thesis present methods to integrate crop growth simulation models with remote sensing information. New and advanced methods are discussed and their possibilities and constraints are considered.

2.7 References

- Acock, B., Y.A. Pachepsky, E.V. Mironenko, F.D. Whisler, V.R. Reddy, 1999.
GUICS: A generic user interface for on-farm crop simulations. *Agron. J.* 91, 657-665.
- Aparicio, N., D. Villegas, C. Royo, 2000.
Spectral vegetation indices as non-destructive tools for determining durum wheat yield. *Agron. J.* 92, 83-91.
- Baret, F., G. Guyot, 1991.
Potentials and limitations of vegetation indices for LAI and APAR assessment. *Rem. Sens. Environ.* 35, 161-173.
- Baret, F., G. Guyot, D. Major, 1989.
TSAVI: A vegetation index which minimizes soil brightness effects on LAI and

- APAR estimation. In: Proc. 12th Canadian symposium on remote sensing and IGARSS '89, Vol. 3. 10-14 July 1989, Sydney, BC, Australia, pp. 1355-1359.
- Bastiaanssen, W.G.M., D.J. Molden, I.W. Makin, 2000.
Remote sensing for irrigated agriculture: examples from research and possible applications. *Agric. Water Mngmnt.* 46, 137-155.
- Bergez, J.E., P. Debaeke, J.M. Deumier, B. Lacroix, D. Leenhardt, P. Leroy, D. Wallach, 2001.
MODERATO: an object-oriented decision tool for designing maize irrigation schedules. *Ecol. Mod.* 137, 43-60.
- Blackburn, G.A., 1998.
Spectral indices for estimating photosynthetic pigment concentrations: a test using senescent tree leaves. *Int. J. Rem. Sens.* 19, 657-675.
- Blackburn, G.A., C.M. Steele, 1999.
Towards the remote sensing of Matorral vegetation physiology: relationships between spectral reflectance, pigment, and biophysical characteristics of semi-arid bushland canopies. *Rem. Sens. Environ.* 70, 278-292.
- Boogaard, H.L., H. Eerens, I. Supit, C.A. van Diepen, I. Piccard, P. Kempeneers, 2002.
Description of the MARS crop yield forecasting system (MCYFS). METAMP report 1/3, Alterra, Wageningen, the Netherlands/VITO, Mol, Belgium/Supit Consultancy, Houten, the Netherlands.
- Booij, R., B. Meurs, 2002.
Supplementary nitrogen application in leeks, based on determination of crop nitrogen status. *Acta Hort.* 571, 155-161.
- Booij, R., D. Uenk, C. Lokhorst, C. Sonneveld, 2001.
Monitoring crop nitrogen status in potatoes, using crop light reflection. In: G. Grenier, S. Blackmore, J. Steffe (Eds.). Proc. 3rd European Conference on Precision Agriculture. 18-20 June 2001, Montpellier, France, Montpellier, Agro Montpellier, Ecole Nationale Supérieure Agronomique, pp. 893-897.
- Booltink, H.W.G., J. Verhagen, 1997.
Using decision support systems to optimize barley management on spatially variable soil. In: M.J. Kropff, P.S. Teng, P.K. Aggarwal, J. Bouma, B.A.M. Bouman, J.W. Jones, H.H. van Laar (Eds.). Applications of systems approaches at the field level. *Systems Approaches for Sustainable Agricultural Development 6*, Kluwer Academic Publ., Dordrecht, the Netherlands, pp. 219-233.
- Bouman, B.A.M., H. van Keulen, H.H. van Laar, R. Rabbinge, 1996a.
The 'School of the Wit' crop growth simulation models: a pedigree and historical overview. *Agric. Syst.* 51, 171-198.
- Bouman, B.A.M., A.H.C.M. Schapendonk, W. Stol, D.W.G. van Kraalingen, 1996b.
Description of the growth model *LINGRA* as implemented in CGMS. Graduate School for Production Ecology (PE) and DLO Institute for Agrobiological and Soil Fertility Research (AB-DLO), Wageningen University and Research centre (WUR), Quantitative Approaches in Systems Analysis 7, Wageningen, the Netherlands, pp. 11-22.

- Brennan, R.D., C.T. de Wit, W.A. Williams, E.V. Quattrin, 1970.
The utility of a digital simulation language for ecological modeling. *Oecol. (Berl.)* 4, 113-132.
- Broge, N.H., E. Leblanc, 2000.
Comparing prediction power and stability of broadband and hyperspectral vegetation indices for estimation of green leaf area index and canopy chlorophyll density. *Rem. Sens. Environ.* 76, 156-172.
- Burgan, R.E., R.W. Klaver, J.M. Klaver, 1998. Fuel models and fire potential from satellite and surface observations. *Int. J. Wildland Fire* 8, 159-170.
- Chapelle, E.W., M.S. Kim, J.E. McMurtrey, 1992.
Ratio analysis of reflectance spectra (RARS): an algorithm for the remote estimation of the concentrations of chlorophyll a, chlorophyll b and the carotenoids in soybean leaves. *Rem. Sens. Environ.* 39, 239-247.
- Clevers, J.G.P.W., 1989.
The application of a weighted infrared-red vegetation index for estimating Leaf Area Index by correcting for soil moisture. *Rem. Sens. Environ.* 29, 25-37.
- Clevers, J.G.P.W., O.W. Vonder, R.E.E. Jongschaap, J.F. Desprats, C. King, L. Prévot, N. Bruguier, 2002.
Using SPOT data for calibrating a wheat growth model under Mediterranean conditions. *Agronomie* 22, 687-694.
- Daughtry, C.S.T., C.L. Walthall, M.S. Kim, E. Brown de Colstoun, J.E. McMurtrey III, 2000.
Estimating corn leaf chlorophyll concentration from leaf and canopy reflectance. *Rem. Sens. Environ.* 74, 229-239.
- Delden, A. van, J.J. Schröder, M.J. Kropff, C. Grashoff, R. Booij, 2002.
Simulated potato yield and crop and soil nitrogen dynamics under different organic nitrogen management strategies in the Netherlands. *Agric. Ecosyst. Environ.* 96, 77-95.
- Donatelli, M., M.K. van Ittersum, M. Bindi, J.R. Porter, 2002a.
Modelling cropping systems - highlights of the symposium and preface to the special issues. *Eur. J. Agron.* 18, 1-11.
- Donatelli, M., M. Bindi, J.R. Porter, M.K. van Ittersum (Eds.), 2002b.
Process simulation and application of cropping system models: first special issue with selected papers from the 2nd international symposium on modelling cropping systems. 16-18 July 2001, Florence, Italy. *Eur. J. Agron.* 18, 1-185.
- Evans, D.L. (Ed.), 1995.
Spaceborne synthetic aperture radar: current status and future directions, a report to the committee on Earth Sciences Space Studies Board, National Research Council. NASA, Tech. memo. 4679.
- Farquhar, G.D., S. von Caemmerer, J.A. Berry, 1980.
A biochemical model of photosynthetic CO₂ assimilation in leaves of C₃ species. *Planta* 149, 78-90.
- Field, C.B., 1991.
Ecological scaling of carbon gain to stress and resource gain. In: A. Mooney,

- W.E. Winner (Eds.). Response of plants to multiple stresses. Academic Press, San Diego, CA, USA, pp. 35-65.
- Flowers, M., R. Weisz, R. Heiniger, B. Tarleton, A. Meijer, 2003.
Remote sensing. Field validation of a remote sensing technique for early nitrogen application decisions in wheat. *Agron. J.* 95, 167-176.
- Gamon, J.A., J. Peñuelas, C.B. Field, 1992.
A narrow-waveband spectral index that tracks diurnal changes in photosynthetic efficiency. *Rem. Sens. Environ.* 41, 35-44.
- Gilbert, M.A., J. González-Piqueras, F.J. García-Haro, J. Meliá, 2002.
A generalized soil-adjusted vegetation index. *Rem. Sens. Environ.* 82, 303-310.
- Gitelson, A.A., Y.J. Kaufman, M.N. Merzlyak, 1996.
Use of green channel in remote sensing of global vegetation from EOS-MODIS. *Rem. Sens. Environ.* 58, 289-298.
- Goetz, S.J., S.D. Prince, 1999.
Modelling terrestrial carbon exchange and storage: evidence and implications of functional convergence in light use efficiency. *Adv. Ecol. Res.* 28, 57-92.
- Goetz, A.F.H., G. Vane, J.E. Solomon, B.N. Rock, 1985.
Imaging spectrometry for earth remote sensing. *Sci.* 228, 1147-1153.
- Hill, M.J., G.E. Donald, P.J. Vickery, A.D. Moore, J.R. Donnelly, 1999.
Combining satellite data with a simulation model to describe spatial variability in pasture growth at a farm scale. *Austr. J. Exp. Agric.* 39, 285-300.
- Hillyer, C.C., J. Bolte, F.K. van Evert, E.J.J. Lamaker, 2003.
The *ModCom* modular simulation system. *Eur. J. Agron.* 18, 333-343.
- Huete, A.R., 1988.
A soil-adjusted vegetation index. *Rem. Sens. Environ.* 25, 295-309.
- Ittersum, M.K. van, P.A. Leffelaar, H. van Keulen, M.J. Kropff, L. Bastiaans, J. Goudriaan, 2003a.
Developments in modelling crop growth, cropping systems and production systems in the Wageningen School. *Neth. J. Agric. Sci.* 50, 239-247.
- Ittersum, M.K. van, P. A. Leffelaar, H. van Keulen, M. J. Kropff, L. Bastiaans, J. Goudriaan, 2003b.
On approaches and applications of the Wageningen crop models. *Eur. J. Agron.* 18, 201-234.
- Jago, R.A., M.E.J. Cutler, P.J. Curran, 1999.
Estimating canopy chlorophyll concentration from field and airborne spectra. *Rem. Sens. Environ.* 68, 217-224.
- Jongschaap, R.E.E., 1996.
Rotaské 1.0 - A dynamic simulation model for continuous cropping systems. Reference manual. DLO Institute for Agrobiology and Soil Fertility Research (AB-DLO), Report 70, Haren/Wageningen, the Netherlands, 40 pp. + annexes.
- Jongschaap, R.E.E., R.A. Quiroz, 2000.
Integrating remote sensing with process-based simulation models to assess primary production capacity for grazing lands in The Andes. In: Proc. 5th seminar on GIS and developing countries: GISDECO 2000 (CD-ROM). 2-3 November 2000, Los Baños, Philippines.

- Jongschaap, R.E.E., R. Booij, 2004.
Spectral measurements at different spatial scales in potato: relating leaf, plant and canopy nitrogen status. *Int. J. Appl. Earth Obs. Geoinf.* 5, 205-218.
- Jongschaap, R.E.E., L.S.M. Schouten, 2005.
Predicting wheat production at regional scale by integration of remote sensing data with a simulation model. *Agron. Sust. Dev.* 25, 481-489.
- Jordan, C.F., 1969.
Derivation of leaf area index from quality of light on the forest floor. *Ecol.* 50, 663-666.
- Justice, C.O., E. Vermote, J.R.G. Townshend, R. Defries, D.P. Roy, D.K. Hall, V.V. Salomonson, J.L. Privette, G. Riggs, A. Strahler, W. Lucht, R.B. Myneni, Y. Knyazikhin, S.W. Running, R.R. Nemani, Z. Wan, A.R. Huete, W. van Leeuwen, R.E. Wolfe, L. Giglio, J.P. Muller, P. Lewis, M.J. Barnsley, 1998.
The Moderate Resolution Imaging Spectroradiometer (MODIS): land remote sensing for global change research, *IEEE Trans. Geosci. Rem. Sens.* 36, 1228-1249.
- Kaiser, P.K., 2005.
The joy of visual perception: a web book. www.yorku.ca/eye/. Consulted in January 2005.
- Keating, B.A., R.L. McCown, 2001.
Advances in farming systems analysis and intervention. *Agric. Syst.* 70, 555-579.
- Kim, M.S., C.S.T. Daughtry, E.W. Chappelle, J.E. McMurtrey III, C.L. Walthall, 1994.
The use of high spectral resolution bands for estimating absorbed photosynthetically active radiation. 6th Symp. on Physical Measurements and Signatures in Remote Sensing. 17-21 January 1994, Val d'Isere, France, pp. 299-306.
- Korzukhin, M.D., M.T. Ter-Mikaelian, R.G. Wagner, 1996.
Process versus empirical models: which approach for forest ecosystem management? *Can. J. Forest Res.* 26, 879-887.
- Laar, H.H. van, J. Goudriaan, H. van Keulen, 1997.
SUCROS97: Simulation of crop growth for potential and water-limited production situations as applied to spring wheat. DLO Institute for Agrobiological and Soil Fertility Research (AB-DLO)/C.T. de Wit Graduate School for Production Ecology (PE), Quantitative Approaches in Systems Analysis 14, Wageningen, the Netherlands, 52 pp.
- Leffelaar, P.A. (Ed.), 1993.
On system analysis and simulation of ecological processes, with examples in CSMP and FORTRAN. *Curr. Issues in Prod. Ecol.* 1., Kluwer Academic Publ., Dordrecht, the Netherlands, 294 pp.
- Lillesand, T.M., R.W. Kiefer, 2000.
Remote Sensing and Image Interpretation. 4th edition. John Wiley and Sons Inc., New York, USA, 724 pp.
- McCown, R.L., G.L. Hammer, J.N.G. Hargreaves, D. Holzworth, D.M. Freebairn, 1996.
APSIM: A novel software system for model development, model testing, and simulation in agricultural systems research. *Agric. Syst.* 50, 255-271.

- Meer, F.D. van der, S.M. de Jong (Eds.), 2001.
Imaging spectrometry: basic principles and prospective applications. Kluwer Academic Publ., Dordrecht, the Netherlands, 451 pp.
- Metselaar, K., 1999.
Auditing predictive models: a case study in crop growth. Ph. D. Thesis, Wageningen Agricultural University, Wageningen, the Netherlands, 265 pp.
- Miller, J.R., E.W. Hare, J. Wu, 1990.
Quantitative characterisation of the vegetation red edge reflectance. I. An inverted-Gaussian reflectance model. *Int. J. Rem. Sens.* 11, 1755-1773.
- Monteith, J.L., 1972.
Solar radiation and production in tropical ecosystems. *J. Appl. Ecol.* 9, 747-766.
- NASA, 1995-1998.
Remote sensing in history. National Aeronautics and Space Administration (NASA). NASA's Observatorium, USA. Consulted in January 2005.
observe.arc.nasa.gov/nasa/exhibits/history/history_0.html.
- NASA, 2004.
Remote Sensing Tutorial (RST) by N. Short (Ed.). National Aeronautics and Space Administration (NASA), USA. Updated March 1st, 2004. Consulted in January 2006. rst.gsfc.nasa.gov.
- Osborne, S.L., J.S. Schepers, D.D. Francis, M.R. Schlemmer, 2002.
Detection of phosphorus and nitrogen deficiencies in corn using spectral radiance measurements. *Agron. J.* 94, 1215-1221.
- Passioura, J.B., 1996.
Simulation models: science, snake oil, education or engineering? *Agron. J.* 88, 690-694.
- Penning de Vries, F.W.T., 1982.
Systems analysis and models of crop growth. In: F.W.T. Penning de Vries, H.H. van Laar (Eds.). *Simulation of plant growth and crop production*, Simulation Monographs, Pudoc, Wageningen, the Netherlands, pp. 9-25.
- Peñuelas, J., J.A. Gamon, A.L. Fredeen, J. Merino, C.B. Field, 1994.
Reflectance indices associated with physiological changes in nitrogen- and water-limited sunflower leaves. *Rem. Sens. Environ.* 48, 135-146.
- Peñuelas, J., F. Baret, I. Filella, 1995.
Semi-empirical indices to assess carotenoids/chlorophyll a ratio from leaf spectral reflectance. *Photosynthetica* 31, 221-230.
- Pinty, B., M.M. Verstraete, 1992.
GEMI: a non-linear index to monitor global vegetation from satellites. *Vegetation* 101, 15-20.
- Porter C.H., J.W. Jones, 1998.
Modular structure in *DSSAT*. Documentation and source code listing. Agricultural and Biological Engineering Department, Report 98-601, University of Florida, Gainesville, USA.
- Qi, J., A. Chehbouni, A.R. Huete, Y.H. Kerr, 1994.
Modified Soil Adjusted Vegetation Index (MSAVI). *Rem. Sens. Environ.* 48, 119-126.

- Reynolds, J. F., B. Acock, 1985.
Predicting the response of plants to increasing carbon dioxide: a critique of plant growth models. *Ecol. Mod.* 29, 107-129.
- Richardson, A.J., C.L. Wiegand, 1977.
Distinguishing vegetation from soil background information. *Photogram. Engineer. Rem. Sens.* 43, 1541-1552.
- Rondeaux, G., M. Steven, F. Baret, 1996.
Optimization of soil-adjusted vegetation indices. *Rem. Sens. Environ.* 55, 95-107.
- Roujean, J.L., F.M. Breon, 1995.
Estimating PAR absorbed by vegetation from bidirectional reflectance measurements. *Rem. Sens. Environ.* 51, 375-384.
- Rouse, J.W., R.W. Haas, J.A. Schell, D.W. Deering, J.C. Harlan, 1974.
Monitoring the vernal advancement and retrogradation (Greenwave effect) of natural vegetation. NASA/GSFCT Type III Final report, Greenbelt, MD, USA.
- Sparrow, A.D., M.H. Friedel, D.M. Stafford Smith, 1997.
A landscape model of shrub and herbage dynamics in Central Australia, validated by satellite data. *Ecol. Mod.* 97, 197-216.
- Spitters, C.J.T., 1990.
Crop growth models, their usefulness and limitations. *Acta Hort.* 267, 349-368.
- Strachan, I.B., E. Pattey, J.B. Boisvert, 2002.
Impact of nitrogen and environmental conditions on corn as detected by hyperspectral reflectance. *Rem. Sens. Environ.* 80, 213-224.
- Supit, I., A.A. Hooijer, C.A. van Diepen (Eds.), 1994.
System description of the *WOFOST* 6.0 crop simulation model implemented in CGMS. Volume 1: Theory and Algorithms. Office for Official Publications of the European Communities, Luxembourg. Catno: CL-NA-15956-EN-C, 146 pp.
- Thenkabail, P.S., R.B. Smith, E. de Pauw, 2000.
Hyperspectral vegetation indices and their relationship with agricultural crop characteristics. *Rem. Sens. Environ.* 71, 158-182.
- Turner, D.P., W.P. Cohen, R.E. Kennedy, K.S. Fassnacht, J.M. Briggs, 1999.
Relationships between leaf area index and Landsat TM spectral vegetation indices across three temperate zone sites. *Rem. Sens. Environ.* 70, 52-68.
- Turner, D.P., S.T. Gower, W.B. Cohen, M. Gregory, T.K. Maiersperger, 2002.
Effects of spatial variability in light use efficiency on satellite-based NPP monitoring. *Rem. Sens. Environ.* 80, 397-405.
- Wit, C.T. de, 1965.
Photosynthesis of leaf canopies. Agricultural Research Report 663, Pudoc, Wageningen, the Netherlands, 88 pp.
- Wit, C.T. de, R. Brouwer, F.W.T. Penning de Vries, 1970.
The simulation of photosynthetic systems. In: Prediction and measurement of photosynthetic productivity. Proc. IBP/PP Techn. Meeting. 14-21 September 1969, Trebon, Czechoslovakia. Pudoc, Wageningen, the Netherlands, pp. 47-70.
- Wopereis, M.C.S., 1993.
Quantifying the impact of soil and climate variability on rainfed production. Ph. D. Thesis, Wageningen Agricultural University, Wageningen, the Netherlands, 188 pp.

Zarco-Tejada, P.J., J.C. Pushnik, S. Dobrowski, S.L. Ustin, 2003.

Steady-state chlorophyll a fluorescence detection from canopy derivative reflection and double-peak red-edge effects. *Rem. Sens. Environ.* 84, 283-294.

Chapter 3

Predicting wheat production at regional scale by integration of remote sensing data with a simulation model

Raymond E.E. Jongschaap¹⁾, Léon S.M. Schouten²⁾

- ¹⁾ *Wageningen University and Research centre, Plant Sciences Group, Plant Research International, P.O. Box 16, NL-6700AA Wageningen, the Netherlands. Tel.: +31-317-475953; Fax: +31-317-423110; E-mail: raymond.jongschaap@wur.nl*
- ²⁾ *Vexcel, P.O. Box 117, NL-6700AC Wageningen, the Netherlands*

© 2005 *Agron. Sust. Dev.* 25, 481-489. Reprinted with permission from EDP Sciences.

3.1 Abstract

Optical remote sensing satellite data (SPOT HRV XS, Landsat 5 TM) were used to estimate winter wheat area in a pilot area of 5 x 5 km in the Southeast of France. The approach was scaled up to a larger area of 45 x 50 km and finally to the regional level covering several departments. Microwave remote sensing data (ERS SAR C-band) were used to estimate regional wheat flowering dates to calibrate a wheat growth simulation model used to calculate wheat yields, subsequently used to estimate regional wheat production. Soil maps were used to spatially vary model input parameters for the region. Wheat area could be estimated with >80 % users' accuracy and model-based estimates of regional wheat production were in agreement with agricultural statistics. These results demonstrate that results from point-based simulation models can be applied at spatially higher levels with the aid of remote sensing data.

Keywords: Landsat, SPOT, ERS SAR C-band, classification, simulation model, calibration, point to region scaling, wheat, flowering date

3.2 Introduction

Timely and accurate information on crop and soil status is critical for management decision-making in arable farming to optimize crop production and to reduce environmental pollution. Normally, field observations are performed repeatedly, at specific crop stages, to enable timely intervention with appropriate management measures. Availability of up-to-date and accurate information on the crop-soil status at the (sub-) plot or farm scale will benefit farmers, whereas local and regional policy makers or food processing industries will be more interested in regional crop production estimates. So far, both, remote sensing applications and dynamic simulation models have played significant, but different (and mostly separate) roles in generation of such information (Jones *et al.*, 2001). Combining remote sensing applications and dynamic simulation models has been explored in several studies (Bouman, 1991; van Leeuwen, 1996; Clevers *et al.*, 2002; Prévot *et al.*, 2003), but these approaches aimed at quantitative biomass, leaf area index and canopy nitrogen estimates from remote sensing data to reconstruct crop growth curves used for calibrating dynamic simulation models at field scale. Another more direct technique to integrate remote sensing observations in crop growth simulation models has been demonstrated by others (Boegh *et al.*, 2004; Jongschaap, 2006). Jongschaap (2006) used remote sensing observations of model variables (leaf area index and canopy nitrogen) for ‘run-time calibration’; i.e. resetting the simulated value with the value estimated from remote sensing data. This approach resulted in more accurate predictions of the dynamics of characteristics of the crop-soil system, including variables that were not directly adjusted. A more innovative and useful combination of both remote sensing and simulation modelling integrates knowledge of lower-scale processes in the crop and soil systems, captured in simulation models, with the possibility to analyze effects at higher (spatial) scales. Therefore the aim of this study was to find a method that allows integrating simulation results at point or field scales and use remotely sensed data to estimate grain production at higher (regional) scales. To reach this objective, optical remote sensing data is used for the classification of winter wheat fields and radar remote sensing data are used to establish a regional estimate for flowering date of winter wheat.

Remote sensing applications originally dealt with classification themes, such as identification and mapping of (originally military) objects. Classification is still of major importance in civil remote sensing applications (Lloyd *et al.*, 2004; de Wit and Clevers, 2004), but quantification of object variables from remotely sensed information has become increasingly important (Moreau and Le Toan, 2003). To transform remote sensing signals into useful information, spectral ‘Vegetation Indices’ (VI) are computed, e.g. by combining visible and near infrared bands. VI are significantly related to important crop characteristics, such as leaf area index (LAI), biomass and chlorophyll content (Guyot *et al.*, 1988; Jago *et al.*, 1999; Thenkabail *et al.*, 2000; Jongschaap and Booij, 2004). One of the VI that is well related with (green) biomass is the Normalized Difference Vegetation Index (NDVI; Rouse *et al.*, 1974) that can be used to distinguish bare soil from vegetation, and to filter grasslands from winter crops if the timing of the image is well chosen. As a consequence of using (broad band)

satellite sensors, operating at lower spatial resolutions than spectral field-based sensors, relations between VI and crop-soil characteristics are less accurate. Another disadvantage of airborne and satellite remote sensing is the spatially distributed atmospheric distortion, which is practically absent in field-based or airborne remote sensing observations. Furthermore, sensors that operate in the visible domain may be hampered by cloud cover, which may be a problem for the calculation of VI at important crop development stages. It is assumed that spectral and spatial resolution of SPOT HRV XS (multispectral) and Landsat 5 TM provide enough detail, and that cloudless images can be selected from appropriate time windows. At the appropriate wavelengths, radar data are not hampered by cloud cover. Target objects in size exceeding the radar wavelengths result in radar backscattering, whereas smaller objects attenuate the radar signal (Hamacher, 2000; Macelloni *et al.*, 2002). The ERS SAR C-band radar data that are used have wavelengths of about 5.6 cm, so the radar signal is expected to attenuate more strongly with increasing (wet) biomass, but will show an increase with wheat ear layer development and drying of the crop canopy towards maturity.

In this study, spaceborne remote sensing observations (SPOT HRV XS, Landsat 5 TM and ERS SAR radar data C-band) are used and combined with crop growth simulation modelling to estimate regional production volumes, in this case for winter wheat (*Triticum aestivum* L.) that is grown in the Southeast of France. The advantage in this methodology is that regional grain production estimates can be provided at an early stage, even before harvest.

3.3 Materials and methods

The approach for integration of remote sensing imagery and crop growth simulation to arrive at regional estimates of wheat production comprises the following steps:

1. Optical remote sensing data (SPOT HRV XS and Landsat 5 TM) are used to locate winter wheat crops in the region;
2. Radar remote sensing data (ERS-SAR C-band) are used to determine wheat flowering dates for the region;
3. Field observations from pilot areas are used to calibrate a wheat growth model to local conditions;
4. Flowering dates as found in steps 2 and 3, in combination with regional soil data, are used to extrapolate the simulation model from a point-based to a regional application;
5. Potential and sub-optimal conditions for wheat growth are assumed to determine the yield gap, defined as the difference between (simulated) potential production and (simulated and observed) actual production (van Ittersum and Rabbinge, 1997);
6. Actual production statistics from the production region are used to evaluate simulation results.

3.3.1 Test sites

The calibration and validation test sites were situated in the Southeast of France near Avignon, in the department *Bouches-du-Rhône*. Model calibration (step 3) was performed on data from a pilot site of 5 x 5 km: *Alpilles* –named after the small mountain chain that borders the area in the south. A larger area in the same region (45 x 50 km) was used to extrapolate model simulations (step 4). This area is further referred to as *Arles* –named after the town that is situated in this region. The approach was further validated (step 6) at the department level (regional scale) in the regions *Midi-Pyrénées* (*MP*) and *Provence-Alpes-Côte d’Azur* (*PAC*).

Alpilles is a very flat area with altitudes around 10 meters above sea level. Main crops are wheat, maize, sunflower and grassland. Some minor crops are tomatoes, artichoke and alfalfa. Fields at the test sites have an average size of ca. 200 x 200 m, which is large enough to extract pure pixels from high spatial resolution satellites such as SPOT HRV XS, Landsat 5 TM and ERS-SAR. *Alpilles* is representative for the *Arles* region and for *MP* and *PAC* with regard to cropping patterns and crop management.

3.3.2 Classification of wheat fields using optical imagery

The growth patterns of winter crops form the basis for winter wheat classification in the *Alpilles* pilot area and in the larger *Arles* region by using the sequential information of three optical satellite images acquired during the growing season. The optical images that were required are a Landsat 5 TM image and two SPOT HRV XS images (Table 3.1). Atmospheric correction using the 6S software (Vermote *et al.*, 1997) was applied before the geometrical correction. The aerosol model was based on actual atmospheric optical thickness measurements during satellite overpass, using a sun photometer installed at the *Alpilles* test site.

In wintertime, arable fields are normally not covered by significant amounts of crop biomass, unless pastures or winter crops are grown. At the end of the summer growing season (October/November in Europe) winter crops may be sown, that can accumulate a substantial amount of green biomass before crop growth and development cease due to decreasing temperatures and reduced solar radiation. In early spring (March/April in Europe), when temperatures are rising and incoming solar radiation increases, these winter crops benefit from their advanced development: the green canopy is able to capture early incoming radiation and a partially developed root system can take up water and nutrients from the soil.

Table 3.1 Specification of the optical remote sensing data.

Satellite and sensor	Scene coordinates	Date
SPOT1 HRV XS	K 49 - J 261	February 1 st , 1997
Landsat 5 TM	path 196 row 30	April 13 th , 1997
SPOT2 HRV XS	K 49 - J 261	July 7 th , 1997

The Normalised Difference Vegetation Index or NDVI (Rouse *et al.*, 1974) identifies green biomass and is calculated from the visible and near infrared bands provided in SPOT HRV XS and Landsat 5 TM images. Green plots, with high NDVI values, comprising green winter wheat fields and green pastures, were identified from the Landsat 5 TM image and the February SPOT1 image by unsupervised classification (iso-data clustering with 50 classes that were identified and clustered by field observations in the *Alpilles* pilot area). These fields were sampled again in the July 1997 SPOT2 image, taken after winter wheat harvest, so that winter wheat fields show up as bare soil in the remote sensing image. By looking at the difference between summer images and winter images, winter wheat fields were identified as the only winter crop grown in this region. The classification result was majority-filtered (box size 3 x 3) to assign values of neighbouring pixels to isolated pixels if these were situated within an identified wheat field. Field observations and ancillary data were used to calculate the users' accuracy of the above method in the *Arles* region, i.e. dividing the number of correctly classified samples by the total number of samples that were classified as belonging to that category (Story and Congalton, 1986).

3.3.3 Radar detection of flowering in wheat

Flowering is a very important and a distinctive phenological event in wheat production that marks the start of grain growth in ears at the top of the canopy. Ear biomass per unit area increases over time through the increase in the number of flowering plants, through grain growth from current photosynthesis products, and through translocation of carbohydrates from temporary storage organs (mainly stems) to the developing grains. Growing ears significantly affect radar backscatter signals, as their presence and increasing biomass at the top of the canopy modify crop geometry and crop moisture distribution and hence, attenuation of the radar signal (Hamacher, 2000; Macelloni *et al.*, 2002).

With the Cloud-model (Equation 3.1), radar backscatter and attenuation of a vegetation-soil system can be simulated (Attema and Ulaby, 1978). In the model, vegetation and soil are represented as clouds of water drops, and radar backscatter (γ) depends on the radar beam incidence angle (θ) and on the moisture content and its distribution in vegetation (C-term) and soil (G-term). High values for W (canopy water content per unit soil surface) mask the influence of the soil term.

$$\gamma = C_{\theta} \cdot \left(1 - e^{\left(\frac{-D \cdot W}{\cos(\theta)} \right)} \right) + G_{\theta} \cdot e^{\left(\frac{m \cdot K \cdot -D \cdot W}{\cos(\theta)} \right)} \quad (\text{Equation 3.1})$$

With γ = radar backscatter per unit projected area ($\text{m}^2 \text{ m}^{-2}$), C = backscatter of an optically dense vegetation cover ($\text{m}^2 \text{ m}^{-2}$), θ = incidence angle ($^{\circ}$), D = crop moisture extinction coefficient (m^{-1}), W = canopy water content per unit soil surface (kg m^{-2}), G = backscatter of dry soil ($\text{m}^2 \text{ m}^{-2}$), m = volumetric soil moisture content ($\text{cm}^3 \text{ water cm}^{-3} \text{ soil}$), K = top soil moisture extinction coefficient (m^{-1}).

ERS time-series (Table 3.2) were selected as wheat signatures are reported to behave consistently in C-band VV (even under varying soil moisture conditions), contrary to those of crops with more planophile oriented leaves such as sugar beet, potato and maize (van Leeuwen, 1996).

ERS radar beams in the C-band (at a frequency ≈ 5.3 GHz and with a wavelength ≈ 5.6 cm) acquire radar backscatter from objects larger than ≈ 5.6 cm. Broad leaves (such as sunflower leaves, sugar beet leaves and maize leaves) will produce C-band backscatter, in contrast to small-sized leaves (such as those of wheat and grasses). Instead, radar signals will attenuate in the vegetation biomass (Macelloni *et al.*, 2002). The use of ERS time-series of winter wheat fields to identify crop phenological stages is legitimate, if values for crop moisture extinction coefficients (D) are relatively stable in time. Dry soil backscatter (G) is different for different soil types and may vary among studies. The relative contributions of crop water content (D) and soil moisture content (G) to radar backscatter signals (D:G) may vary between 83-96 % (Table 3.3). D and G parameter values were established for the *Alpilles* pilot area by fitting the Cloud-model to field observations.

As D-values appeared to be stable (Table 3.3), a method was developed to detect flowering dates in wheat crops, based on the associated change in crop moisture distribution and crop geometry, with the flowering stage marking the point where aboveground water contents start to decrease and minimum radar backscatter can be expected (Hamacher, 2000). In the pre-flowering growth phase, canopy water content per unit soil surface area (W) increases with increasing biomass and the radar signal will be decreased due to attenuation by the canopy. After the onset of flowering, an optically dense vegetation cover of ear biomass starts to develop that prevents radar beams from penetrating deeply into the wheat canopy, thereby reducing the radar signal maximally. Fully developed ears may produce backscatter, and as soon as grains start to ripen, the moisture content of the crop decreases resulting in increased radar backscatter as the influence of the soil is no longer masked. The absolute minimum in

Table 3.2 Specification of the radar (ERS1 SAR) remote sensing data.

Date	Mode ^{a)}	Orbit	Frame
December 19 th , 1996	D	8707	2727
January 23 rd , 1997	D	9208	2727
January 26 th , 1997	A	9259	873
February 27 th , 1997	D	9710	2727
April 6 th , 1997	A	10261	873
May 8 th , 1997	D	10712	2727
June 12 th , 1997	D	11213	2727
July 17 th , 1997	D	11714	2727
August 21 st , 1997	D	12215	2727
September 25 th , 1997	D	12716	2727

^{a)} A=Ascending, D= Descending

the radar signal (i.e. at maximum attenuation) therefore denotes the maximum water content per unit surface area and hence flowering.

Regional dynamics of these phenological events can be detected by ERS (radar) remote sensing. Success rate increases if more comparable (wheat) fields are included in the detection procedure. Based on this approach, regional flowering dates have been estimated for simulation model calibrations with time-series of ERS (radar) data (taken in the period November 1996 - May 1997). For the *Alpilles* area, 10 ERS radar images were available of which 7 coincided with the wheat growth period. The 8 descending ERS-SAR images were co-registered (linear transformation to the file coordinates of one reference scene) and the 2 ascending images also. Subsequently all images were speckle-filtered (Gamma Maximum A Posteriori filter (GMAP); Lopez *et al.*, 1991) that best retains edge and line features, with a window of 7 x 7 pixels that is appropriate for the medium-sized wheat fields. Remote sensing time-series were transformed to the Lambert III projection, the standard map projection for this part of France. All ERS-images were re-sampled (nearest neighbour) to pixels representing 25 m². Classified SPOT images were overlaid with ERS images to generate mean backscatter (DN values) for winter wheat fields only.

3.3.4 Wheat growth simulation model

Winter wheat simulations were performed with the mechanistic crop growth model *Rotask* (Jongschaap, 1996), that uses (simple) algorithms based on knowledge of the underlying physical, physiological and biochemical processes. The model quantifies water fluxes (precipitation, irrigation, run-off, soil evaporation, transpiration and drainage), nitrogen fluxes (mineralization/immobilization during soil organic matter decomposition, mineralization from dead plant material, (in-) organic fertilization, wet deposition, leaching and root nitrogen uptake by mass flow and diffusion), for fallow or field crop rotation systems. Light interception and heat accumulation govern crop growth and development, respectively. Crop nitrogen contents may vary as a result of variations in nitrogen availability. Management decisions accounted for in the model refer to ploughing (date, depth), incorporation of organic fertilizer (date, rate, type), and application of inorganic fertilizer (date, rate, type), sowing (rate, depth), irrigation (date, rate) and harvest (date, method). Crops currently included in the model are wheat, sugar beet, potato, barley, rape-seed and maize. For this study, simulations were performed for winter wheat only. The model has been calibrated for winter wheat and for the soil conditions of the *Alpilles* pilot area, using 1996, 1997 and 1998 field data (Jongschaap, 2000; ReSeDA, 2000).

3.3.5 Up-scaling from point to regional level

Two methods were applied to scale-up point-based simulations to the regional scale. Firstly, sowing dates were varied over the month of November in 1996 to introduce variation in the model variable 'sowing date', to mimic the observed variable sowing

dates of winter wheat in the area. Temperature sums calibrated for the *Alpilles* pilot area were applied for the periods sowing to flowering and flowering to maturity.

Secondly, the spatial variability in soil characteristics was derived from the FAO/UNESCO 1:5,000,000 Soil Map of the World (FAO, 1995). Higher resolution soil maps of the region are available from different sources, but in our approach we wanted to use broad-scale soil information to be applied at regional level. The soil map resolution of 5 arc minutes results in a grid of 10 x 10 km at the latitude of the *MP* and *PAC* region. On the soil map, 3 legend units were identified in the region: 3086 (17 %), 3139 (80 %) and 6498 (3 %). The remote sensing data showed that only unit 3139 contained wheat fields. Derivation of the relevant soil characteristics for the simulation model, available water content and slope (Table 3.4), resulted in 10 % of its area having a water storage capacity of 190 mm m⁻¹ and a slope exceeding 8 %, while the remainder had a water storage capacity of 200 mm m⁻¹ and a slope below 8 %.

The simulation model was executed for 3 production situations with significantly different grain yields (van Ittersum and Rabbinge, 1997), because of production constraints that were included in the model:

1. **Potential production;** wheat growth and development are governed only by crop characteristics, intercepted radiation and average daily temperatures.
2. **Water-limited production;** as 1, but accounting for inadequate soil moisture supply during crop growth: daily assimilation rates are reduced proportionally to daily relative crop transpiration deficits.
3. **Nitrogen- and water-limited production;** as 2, but accounting for the effect of inadequate soil nitrogen supply during crop growth, which may cause canopy nitrogen contents to reach critical values, resulting in reduced assimilation rates.

When water and nitrogen supply from natural sources do not meet crop requirements, production situation 1 results in higher yields than production situation 2 (yield gap for production situation 2), which in turn gives higher yields than production situation 3 (yield gap for production situation 3). The production situations were implemented without irrigation water supply (situations 2 and 3) and without nitrogen fertilizer application (situation 3). Irrigation and fertilizer application data were available for the calibration data set, but not for extrapolation to the regional scale.

Hence, the simulation experiment was set up as follows (Figure 3.1): the region was first filtered for winter wheat fields, and subsequently the simulations were performed for the 3 production situations. The two soil types were used in production situations 2 and 3 only, as for production situation 1 soil characteristics are not taken into account. Sowing dates were varied over the month of November 1996 (Date of Experiment (DoE): 304-334), leading to grain yields P (t ha⁻¹). After calibration of the temperature sums between sowing and flowering to DoE 467 (estimated from ERS data), grain yields were P' (t ha⁻¹). Multiplication by the estimated area resulted in regional estimates of winter wheat grain production (t).

Simulation results per soil type are given as Final Grain Yield (FGY, Dry Matter (air-dry) in t ha⁻¹), with a standard deviation resulting from the simulated variation in sowing date. Multiplication of FGY with the wheat area identified through optical remote sensing resulted in regional grain yield estimates for the 1997 season.

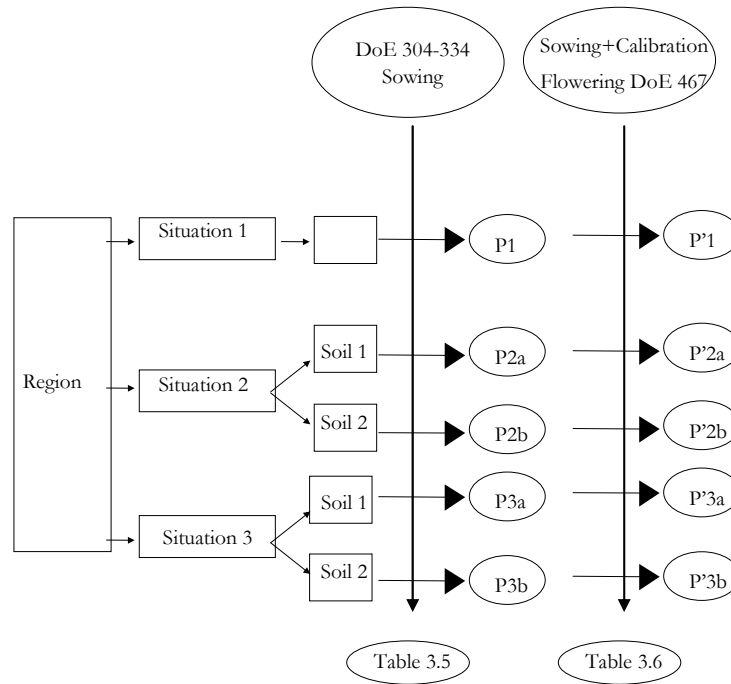


Figure 3.1 Simulation scheme for estimation of regional grain production P and P' after determination of wheat area and soil types and estimation of regional flowering date.

Table 3.3 Cloud model parameters K , D and G (See Equation 3.1) from various experiments.

K	D	G	Study area	Reference
0.035	0.4800	0.0863	Alpilles (France)	Prévot <i>et al.</i> (1998)
0.058	0.4501	0.0384	Alpilles (France)	Synoptics (1996)
0.078	0.4330	0.0186	Flevoland (Netherlands)	Bouman <i>et al.</i> (1999)
0.130	0.4338	0.0028	Alpilles (France)	Synoptics (1996)

Table 3.4 FAO/UNESCO legend unit 3139, its constituent soil codes and the interpretation for simulation purposes in Rotask v1.5.

Soil (code)	Texture (class)	Slope (class)	Area ^{a)} (%)	Soil depth (cm)	Available water content (mm m ⁻¹)
Calcaric Fluvisols (Jc)	1	1	25	130	200
Gleysols (G)	2	1	20	130	200
Eutric Fluvisols (Je)	2	1	20	130	200
Cambisols (B)	2	2	10	130	190
Calcaric Fluvisols (Jc)	3	1	25	130	200

^{a)} Percentage of the soil legend unit area that is covered by the soil code.

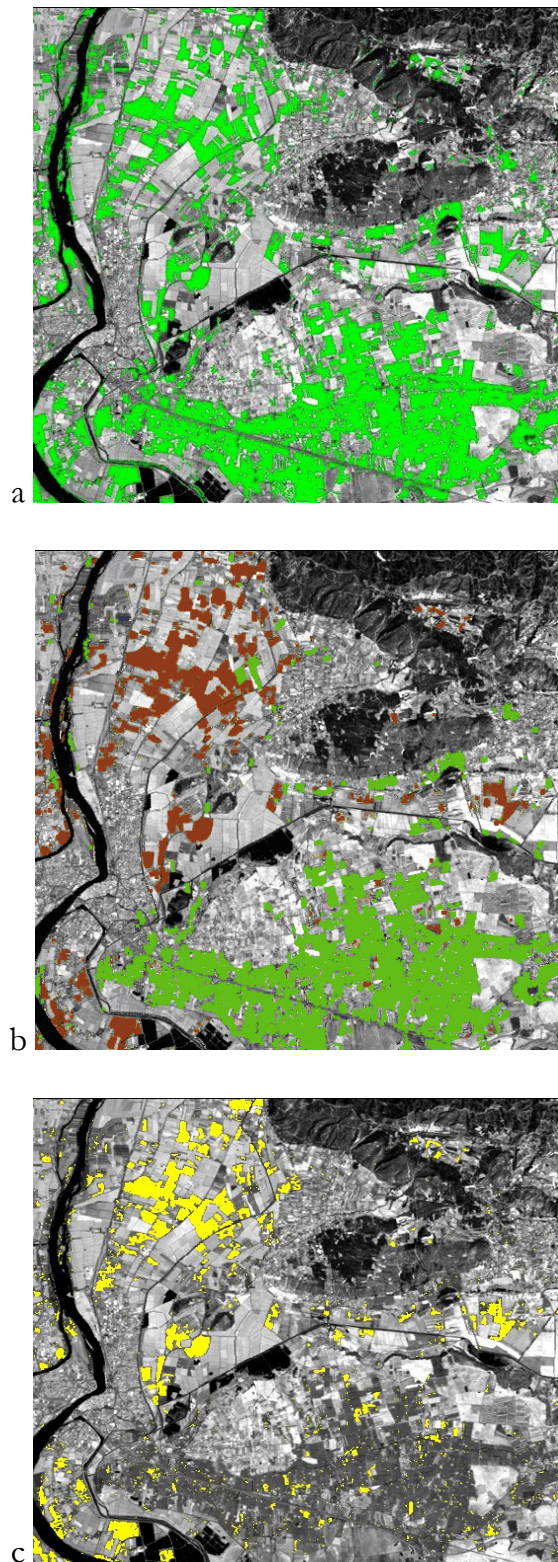


Figure 3.2 Classification results for the Alpilles test site (45×50 km): a) Green biomass detection (in light-green) by combining February SPOT1 image and April Landsat 5 TM image, b) fallow fields (in brown) and fields with biomass (in dark-green) on July SPOT2 image, and c) resulting wheat fields (in yellow) after majority box (3×3) filtering.

3.4 Results and discussion

3.4.1 Remote sensing estimates of wheat area and flowering date

About 145 ha of wheat fields in the *Alpilles* pilot area were used to validate the remotely sensed unsupervised classification process, which resulted in a users' accuracy >80 % (Story and Congalton, 1986). In the *Arles* region of 45 x 50 km, about 3000 ha of winter wheat fields were identified, i.e. 1.4 % of the 211,800 ha of wheat reported for the *MP* and *PAC* region (Figure 3.2).

The crop moisture extinction coefficient (D) of the Cloud-model (Attema and Ulaby, 1978) was stable over time and its value agreed with those from other studies (Table 3.3), although reported standard errors are relatively large. Nonetheless, ERS (radar) time-series are useful for estimation of wheat flowering dates in the region, as average backscatter behaviour of radar time-series of winter wheat fields is consistent (ESA, 1998; Hamacher, 2000). A 5th order polynomial function fitted best through the 10 points representing backscatter values of winter wheat fields (Figure 3.3). Theoretically, the 5th order agrees with the number of local maximum and minimum values that can be expected for the studied time period. Starting with a local maximum for soil backscattering (only), to a local minimum when the soil backscatter is fully masked at flowering, continuing to a local maximum at maturity with backscatter of the ear layer, towards a local minimum after all the fields have been harvested and a dry soil is exposed at the end of summer. As the harvest starts and progresses in June/July, the curve is increasingly influenced by soil characteristics and less by the crop. Flowering date of the wheat crop was set at the 1st local minimum of the fitted polynomial function, which was closest to April 12th 1997 or Julian day 102, and in agreement with the calibrated *Rotask* simulation model and field observations (Julian day 105-107).

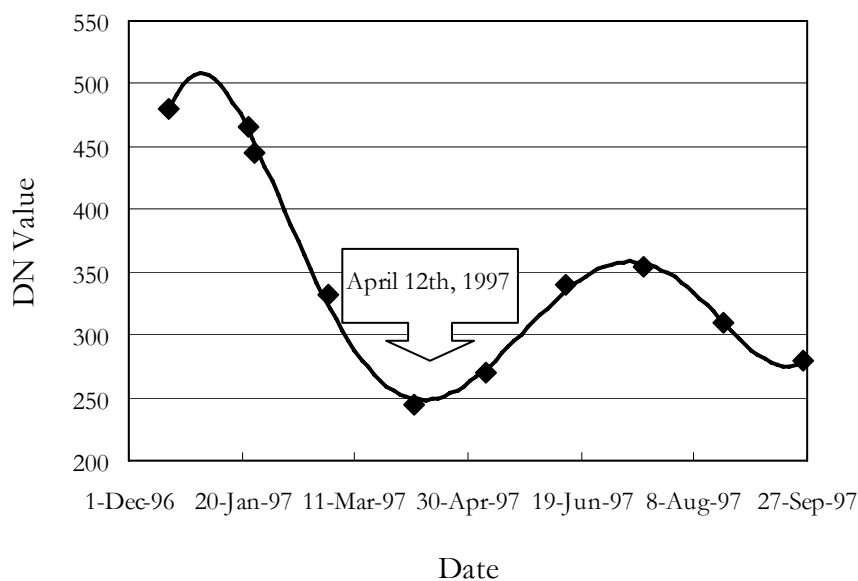


Figure 3.3 Identification of the date of flowering from the 1996-1997 ERS-SAR time-series.

3.4.2 Crop growth simulation results

Calibration of *Rotask* resulted in temperature sums between sowing-emergence of 420 degree-days (base temperature of $-10\text{ }^{\circ}\text{C}$), emergence-flowering of 1050 degree-days (base temperature of $0\text{ }^{\circ}\text{C}$) and flowering-maturity of 850 degree-days (base temperature of $0\text{ }^{\circ}\text{C}$). On the basis of the flowering date for the region derived from radar remote sensing (April 12th 1997), the simulated variation in temperature sum between emergence and flowering was 930-1180 degree-days, depending on sowing date in November 1996. This variation was applied to run the model for the 3 production situations.

The simulation results and regional yield estimates (Table 3.5 and 3.6) illustrate the yield-limiting effects of insufficient water and nutrient supply in the absence of irrigation and fertilizer application. Hence, appropriate management (irrigation and fertilizer application) leads to appreciably higher production levels, in the absence of pests and diseases.

From Tables 3.5 and 3.6 can be concluded that using field observations or remote sensing estimates of a flowering date give comparable results for yield simulations and that differences can be related to differences in crop management (sowing date and cultivar). This supports the assumption that this method can be used to regionally

Table 3.5 *Calculated regional grain production P (without calibration on observed flowering date in pilot area Alpilles) for the 3 production situations. Values in parentheses are standard deviations from the mean.*

Scenario	Soil type	Area (ha)	Yield (t ha ⁻¹)	Production (P) (t)	Regional production (t)
1 Potential	-	3000	11.35 (1.02)	34050	34050
2 Water-limited	1	2700	6.08 (0.51)	16416	17997
	2	300	5.27 (0.39)	1581	
3 Water- and nitrogen-limited	1	2700	4.70 (0.28)	12690	13947
	2	300	4.19 (0.21)	1257	

Table 3.6 *Calculated regional grain production P' (with calibration on remote sensing estimate on regional flowering date) for the 3 production situations. Values in parentheses are standard deviations from the mean.*

Scenario	Soil type	Area (ha)	Yield (t ha ⁻¹)	Production (P') (t)	Regional production (t)
1 Potential	-	3000	11.45 (0.19)	34350	34350
2 Water-limited	1	2700	5.84 (0.15)	15768	17274
	2	300	5.02 (0.16)	1506	
3 Water- and nitrogen-limited	1	2700	4.53 (0.08)	12231	13446
	2	300	4.05 (0.08)	1215	

calibrate the model on phenological characteristics. The decrease in standard deviation for the remote sensing approach (Table 3.6) is caused by the fact that the start of the reproductive (grain filling) phase was fixed at the flowering date estimated from remote sensing (causing a variable temperature sum between emergence and flowering). The use of remote sensing data integrates the effects of varying wheat crop management over the region into one representative value for flowering date. In the original approach (Table 3.5), the temperature sum between emergence and flowering was calibrated on field-data in the *Alpilles* pilot area and then applied with a variable sowing date, which consequently resulted in a variable flowering date.

3.4.3 Validation

Actual wheat production data of the departments in the *MP* and *PAC* region obtained from Arvalis (Table 3.7; Arvalis, 2003) included total wheat production (t), wheat area (ha) and average grain yield (t ha⁻¹). The simulated values of 5-6 t ha⁻¹ agree well with observed values that are remarkably low ($\approx 50\%$ of their potential). According to Arvalis (op. cit.), average nitrogen application in 1997 was about 100 kg ha⁻¹ in the *MP* and *PAC* region, which is about 55% of total crop requirements for realization of the potential yield of 11.5 t ha⁻¹.

Inadequate water supply may have been limiting yield (if additional irrigation was not applied, especially since 1997 was an extremely dry year), while yield reductions may have resulted from non-controlled pests and diseases. In the simulation model, inadequate water and nitrogen supply was taken into account (production situations 2 and 3), but the regional distribution of crop management practices could not be simulated. Fertilizer application rates of 100 kg N ha⁻¹ could be simulated, but information on irrigation rates and dates were not available for the region.

Introducing the effects of local management can be simulated in point-based simulation models, but retrieving the necessary (regional) data is very difficult and requires extensive field work. However, remote sensing data may be used to spatially estimate crop status (e.g. biomass, nitrogen content and moisture status) that may be integrated in the simulation process for run-time calibration (Jongschaap, 2006), but that is beyond the scope of this paper.

Table 3.7 Wheat production (1997) in departments 82 and 83, area and average yield (Arvalis, 2003).

Department	Region	Total Production	Area	Yield
		(t)	(ha)	(t ha ⁻¹)
82	<i>Midi-Pyrénées (MP)</i>	540600	104400	5.18
83	<i>Provence Alpes-Côte d'Azur (PAC)</i>	518500	98100	5.29

3.5 Conclusions

In this paper we present a method to estimate regional, quantitative production volumes of winter wheat on the basis of spaceborne remote sensing observation in combination with a dynamic crop growth simulation model. The most important conclusions are:

- For purposes of regional winter wheat yield estimations, an approach combining optical and radar remote sensing data with point-based crop growth modelling yields satisfactory results that are in agreement with regional yield statistics. Regional wheat production can be estimated at an early stage, even before harvest.
- Flowering dates for wheat crops can be estimated from time-series of C-band radar data, as radar signals are attenuated maximally at the flowering stage. This requires that radar signals from wheat fields can be isolated from those from other fields, which appeared feasible with an accuracy >80 % by combining optical remote sensing data from early winter and late summer.
- Flowering dates for wheat crops that are estimated from time-series of C-band radar data may replace phenological field observations for the use of model calibration and give comparable simulation results. This enables scaling up point models to regional applications without an increase in (phenological) field observations on the ground.
- Use of field-specific flowering dates for simulations within a region would result in more accurate estimates of regional grain production, than the use of one single value for the whole region. This does require however sufficiently large wheat fields. Wheat fields in the *Alpilles* area were medium-sized on average, and therefore it is not certain that an individual field approach would have increased simulation accuracy.
- As the differences between simulated and observed production levels are presumably associated with management practices, such as irrigation and fertilizer application, the use of a remote sensing run-time calibration method for dynamic simulation models (Jongschaap, 2006) may result in increased simulation accuracy.

3.6 Acknowledgements

The Alpilles-ReSeDA project was funded by the European Commission (EU-DG XII, contract ENV4-CT96-0326 - PL952071), the French 'Program National de Télédétection Spatiale', 'Programme de Recherches en Hydrologie' and by the Dutch Ministry of Agriculture, Nature Management and Fisheries through their programmes on precision agriculture. Philippe Desvignes (Arvalis - Institut du Végétal, France) provided the regional wheat data and fertilizer data. We are grateful to Prof. Dr. Steven M. de Jong and Prof. Dr. Herman van Keulen and two anonymous reviewers for useful comments on the manuscript.

3.7 References

- Arvalis, 2003.
Institut du Végétal, France, www.arvalisinstitutduvegetal.fr
- Attema, E.P.W., F.T. Ulaby, 1978.
Vegetation modelled as a water cloud. *Radio Sci.* 13, 357-364.
- Boegh, E., M. Thorsen, M.B. Butts, S. Hansen, J.S. Christiansen, P. Abrahamsen, C.B. Hasager, N.O. Jensen, P. van der Keur, J.C. Refsgaard, K. Schelde, H. Soegaard, A. Thomsen, 2004.
Incorporating remote sensing data in physically based distributed agro-hydrological modelling. *J. Hydrol.* 287, 279-299.
- Bouman, B.A.M., 1991.
Linking X-band radar backscattering and optical reflectance with crop growth models. Ph. D. Thesis, Wageningen Agricultural University, Wageningen, the Netherlands, 167 pp.
- Bouman, B.A.M., D.W.G. van Kraalingen, W. Stol, H.J.C. van Leeuwen, 1999.
An agroecological modelling approach to explain ERS SAR radar backscatter of agricultural crops. *Rem. Sens. Environ.* 67, 137-146.
- Clevers, J.G.P.W., O.W. Vonder, R.E.E. Jongschaap, J.F. Desprats, C. King, L. Prévot, N. Brugier, 2002.
Using SPOT data for calibrating a wheat growth model under mediterranean conditions. *Agronomie* 22, 687-694.
- ESA, 1998.
Vegetation retrieval by combining microwave and optical remote sensing. Final Report ESA/ESTEC, Contract 11154/94/NL/NB(SC), Synoptics, AB-DLO, TNO-FEL, Wageningen, the Netherlands, 113 pp.
- FAO, 1995.
Digitized Soil Map of the World and derived Soil Properties (version 3.5). CD-ROM, FAO, Rome, Italy.
- Guyot, G., F. Baret, D.J. Major, 1988.
High spectral resolution: Determination of spectral shifts between the red and the near infrared. *Int. Arch. Photogram. Rem. Sens.* 11, 750-760.
- Hamacher, M., 2000.
Zustandserfassung von Wintergetreide und Zuckerrüben während des Wachstums mit Hilfe des C-Band Radars der ERS-1 und ERS-2 Satelliten. Ph. D. Thesis, Rhine Friedrich Wilhelms University, Bonn, Germany, 114 pp.
- Hill, M.J., G.E. Donald, P.J. Vickery, A.D. Moore, J.R. Donnelly, 1999.
Combining satellite data with a simulation model to describe spatial variability in pasture growth at a farm scale. *Aust. J. of Exp. Agr.* 39, 285-300.
- Ittersum, M.K. van, R. Rabbinge, 1997.
Concepts in production ecology for analysis and quantification of agricultural input-output combinations. *Field Crops Res.* 52, 197-208.
- Jago, R.A., M.E.J. Cutler, P.J. Curran, 1999.
Estimating canopy chlorophyll concentration from field and airborne spectra. *Rem. Sens. Environ.* 68, 217-224.

- Jones, J.W., B.A. Keating, C.H. Porter, 2001.
Approaches to modular model development. *Agric. Syst.* 70, 421-443.
- Jongschaap, R.E.E., 1996.
Rotaské 1.0 - a simulation model for continuous cropping and tillage systems.
Reference manual. DLO Institute for Agrobiological and Soil Fertility Research (AB-DLO), Report 70, Haren/Wageningen, the Netherlands, 40 pp. + annexes.
- Jongschaap, R.E.E., 2000.
Calibration and validation of *Rotaské* v1.5 simulation model on field data of the ReSeDA project in Southern France, with special reference to winter wheat. In: Final report ReSeDA, EU-DG XII, ENV4-CT96-0326 - PL952071. France: BRGM, CESBIO, CETP, INRA (coordinator); Italy: IROE; the Netherlands: WAU, AB-DLO, Synoptics; United Kingdom: UC; Spain: UV.
- Jongschaap, R.E.E., 2006.
Run-time calibration of simulation models by integrating remote sensing estimates of leaf area index and canopy nitrogen. *Eur. J. Agron.* 24, 328-336.
- Jongschaap, R.E.E., R.A. Quiroz, 2000. Integrating remote sensing with process-based simulation models to assess primary production capacity for grazing lands in The Andes. 5th seminar on GIS and developing countries: GISDECO 2000, 2-3 November 2000, Los Baños, Philippines.
- Jongschaap, R.E.E., R. Booij, 2004.
Spectral measurements at different spatial scales in potato: relating leaf, plant and canopy nitrogen status. *Int. J. Appl. Earth Obs. Geoinform.* 5, 205-218.
- Leeuwen, H.J.C. van, 1996.
Methodology for combining optical and microwave remote sensing in agricultural crop monitoring: The sugar beet as special case. Ph. D. Thesis, Wageningen Agricultural University, Wageningen, the Netherlands, 233 pp.
- Lloyd, C.D., S. Berberoglu, P.J. Curran, P.M. Atkinson, 2004.
A comparison of texture measures for the per-field classification of Mediterranean land cover. *Int. J. Rem. Sens.* 25, 3943-3965.
- Lopez, A., E. Nezry, R. Touzi, H. Laur, 1993.
Structure detection and statistical adaptive speckle filtering in SAR images. *Int. J. Rem. Sens.* 14, 1735-1758.
- Macelloni, G., S. Paloscia, P. Pampaloni, R. Ruisia, M. Dechambre, R. Valentin, A. Chanzy, L. Prévot, N. Bruguier, 2002.
Modelling radar backscatter from crops during the growth cycle. *Agronomie* 22, 575-579.
- Moreau, S., T. Le Toan, 2003.
Biomass quantification of Andean wetland forages using ERS satellite data for optimizing livestock management. *Rem. Sens. Environ.* 84, 477-492.
- Prévot, L., F. Baret, A. Oliso, B.A.M. Bouman, J.G.P.W. Clevers, R.E.E. Jongschaap, H.J.C. van Leeuwen, L.S.M. Schouten, O.W. Vonder (*et al.*), 1998.
Assimilation of multi-temporal remote sensing data to monitor vegetation and soil: the Alpilles-ReSeDA project. In: Proc. IGARSS '98 Symposium, Vol. 5. 6-10 July 1998, Seattle, WA, USA, pp. 2399-2401.

- Prévo, L., H. Chauki, D. Troufleau, M. Weiss, F. Baret, N. Brisson, 2003.
Assimilating optical and radar data into the STICS crop model for wheat.
Agronomie 23, 297-303.
- ReSeDA, 2000.
Assimilation of multisensor and multitemporal remote sensing data to monitor vegetation and soil functioning. Final report. EU-DG XII, ENV4-CT96-0326 - PL952071. France: BRGM, CESBIO, CETP, INRA (coordinator); Italy: IROE; the Netherlands: WAU, AB-DLO, Synoptics; United Kingdom: UC; Spain: UV.
- Rouse, J.W., R.H. Haas, D.W. Deering, J.A. Schell, J.C. Harlan, 1974.
Monitoring the vernal advancement and retrogradation (Greenwave effect) of natural vegetation. NASA/GSFC Type III Final Report, Greenbelt, MD, USA.
- Shupe, S.M., S.E. Marsh, 2004.
Cover- and density-based vegetation classifications of the Sonoran Desert using Landsat TM and ERS-1 SAR imagery. *Rem. Sens. Environ.* 93, 131-149.
- Story, M., R.G. Congalton, 1986.
Accuracy assessment: a user's perspective. *Photogr. Engin. Rem. Sens.* 52, 397-399.
- Susan Moran, M., D.C. Hymer, J. Qi, Y. Kerr, 2002.
Comparison of ERS-2 SAR and Landsat TM imagery for monitoring agricultural crop and soil conditions. *Rem. Sens. Environ.* 79, 243-252.
- Synoptics, 1996.
Integrated Remote Sensing & GIS application. Vegetation retrieval by combining microwave and optical remote sensing. DLO Institute for Agrobiolgy and Soil Fertility Research (AB-DLO), TNO Physics and Electronics laboratory, Wageningen Agricultural University (WAU), ESTEC Contract 11154/94/NL/NB (SC), the Netherlands.
- Thenkabail, P.S., R.B. Smith, E. de Pauw, 2000.
Hyperspectral vegetation indices and their relationship with agricultural crop characteristics. *Rem. Sens. Environ.* 71, 158-182.
- Vermote, E.F., D. Tanré, J.L. Deuzé, M. Herman, J.J. Morcrette, 1997.
Second simulation of the satellite signal in the solar spectrum, 6S: An overview. *IEEE Trans. Geosci. Rem. Sens.* 35, 675-686.
- Wit, A.J.W. de, J.G.P.W. Clevers, 2004.
Efficiency and accuracy of per-field classification for operational crop mapping. *Int. J. Rem. Sens.* 25, 4091-4112.

Chapter 4

Spectral measurements at different spatial scales in potato: relating leaf, plant and canopy nitrogen status

Raymond E. E. Jongschaap, Rennie Booi†

Plant Research International, P.O. Box 16, NL-6700AA Wageningen, the Netherlands.

© 2004 *Int. J. Appl. Earth Obs. Geoinform.* 5, 205-218. Reprinted with permission from Elsevier.

4.1 Abstract

Chlorophyll contents in vegetation depend on soil nitrogen availability and on crop nitrogen uptake, which are important management factors in arable farming. Crop nitrogen uptake is important, as nitrogen is needed for chlorophyll formation, which is important for photosynthesis, i.e. the conversion of absorbed radiance into plant biomass. The objective of this study was to estimate leaf and canopy nitrogen contents by near and remote sensing observations and to link observations at leaf, plant and canopy level. A theoretical base is presented for scaling-up leaf optical properties to whole plants and crops, by linking different optical recording techniques at leaf, plant and canopy levels through the integration of vertical nitrogen distribution. Field data come from potato experiments in the Netherlands in 1997 and 1998, comprising 2 potato varieties: *Eersteling* and *Bintje*, receiving similar nitrogen treatments (0, 100, 200 and 300 kg N ha⁻¹) in varying application schemes to create differences in canopy nitrogen status during the growing season. Ten standard destructive field samplings were performed to follow leaf area index and crop dry weight evolution. Samples were analyzed for inorganic nitrogen and total nitrogen contents. At sampling dates, spectral measurements were taken both at leaf level and at canopy level.

† Rennie Booi passed away in December 2003

At leaf level, an exponential relation between SPAD-502 readings and leaf organic nitrogen contents with a high correlation factor of 0.91 was found. At canopy level, an exponential relation between canopy organic nitrogen contents and red edge position (λ_{rep} , nm) derived from reflectance measurements was found with a good correlation of 0.82. Spectral measurements (SPAD-502) at leaf level of a few square mm were related to canopy reflectance measurements (CropScan™) of approximately 0.44 m². Statistical regression techniques were used to optimize theoretical vertical nitrogen profiles that allowed scaling-up leaf chlorophyll measurements to canopy nitrogen values. A nitrogen attenuation coefficient (k_N) of 0.41 g N m⁻² soil resulted in highest correlation coefficients for scaling-up nitrogen contents from leaf to canopy values. Remote sensing of canopy nitrogen (g N m⁻² soil) did not require considering vertical nitrogen profiles, as canopy reflectance measurements were able to integrate organic nitrogen over total canopy depth. The integration of near sensing techniques, theories on the interpretation of reflectance signatures and vertical crop nitrogen distribution allowed scaling between leaf chlorophyll measurements and canopy nitrogen values. This results in more accurate quantification of the nitrogen status of a potato crop, which is important information in potato crop management.

Keywords: chlorophyll, nitrogen, SPAD-502, red edge position, leaf-to-canopy scaling, potato, remote sensing, near sensing

4.2 Introduction

Timely and accurate information on crop and soil status is important for management actions in arable farming to optimize crop production and to avoid environmental pollution. Field observations are normally performed repeatedly throughout the field, at specific crop stages to allow timely intervention with appropriate measures. Extension services, fertilizer producers and phyto-sanitary companies support management decisions by monitoring field crops and recommending their products to the farmers. Crop and soil status, advice from third parties and farmers' experience together may trigger management actions that are aimed at improved crop performance, reduced environmental impact through pollution, such as nutrient leaching, and/or mitigation of the effects of pests and diseases.

Continuous monitoring of crops and soils is laborious and tedious (or may be impossible), if aimed at monitoring every square meter of a field at regular time intervals. Higher observation frequencies at higher spatial resolution are needed to assess within-field variability of crop growth conditions. Conventional crop chlorophyll and nitrogen monitoring methods alone are not suitable for providing this information, as they are time-consuming, expensive or destructive. New monitoring techniques, such as remote and near sensing, that can easily be applied at field scale, have become available at affordable costs. However, scientific proof is needed of the suitability of these new monitoring techniques aiming at observing crops at leaf, plant and canopy

levels before they can replace or complement conventional monitoring methods. In this paper, their application potential is investigated.

Crop optical properties recorded by passive, optical and active microwave sensors in different spectral bands and at different spectral resolutions, provide information on various crop characteristics at different spatial scales. Significant relationships have been established between leaf area index, ground cover and crop reflectance characteristics (e.g. Bouman, 1992; Bouman *et al.*, 1992a and 1992b; Thenkabail *et al.*, 2000). Crop canopy colour ('greenness') e.g., is closely linked to crop characteristics determining light use efficiency, such as chlorophyll content and nitrogen status.

Optical reflectance measurements at leaf level do not necessarily provide detailed information on plant and crop performance, as that is co-determined by vertical nitrogen distribution, canopy structure and biomass allocation. Yet, the spatial and temporal variation in canopy nitrogen status that can be observed by remote sensing is of interest in farming practice. Spectral mixing of reflectance patterns over a whole plot however, may mask the spatial variability within the plot that forms the basis for application of innovative techniques in agriculture, such as precision farming.

At leaf level, chlorophyll contents can be derived non-destructively from special optical techniques with hand-held devices such as the SPAD-502 (Minolta, 2003). Linear relations have been described between SPAD-502 readings on one hand and leaf chlorophyll content (mg g^{-1}), leaf nitrogen content (mg g^{-1}) and nitrate content (mg l^{-1}) in potato petiole sap on the other (Vos and Bom, 1993). If measurements are taken on first full-grown leaves, the normal practice in field observations, transformation of leaf chlorophyll readings into leaf nitrogen status and plant nitrogen status requires assumptions on nitrogen distribution within the plant.

Nitrogen may be taken up by the roots as nitrate and ammonia, and enters into a soluble nitrogen pool. From this pool, nitrogen is used for formation of stable components, such as chlorophyll and Rubisco, and inert structural components in cell tissue. Inert and structural nitrogen contents increase as the crop develops and may comprise up to 30 per cent of total nitrogen at harvest.

The vertical distribution of nitrogen in the crop is not homogeneous but follows a gradient, which may present a problem in nitrogen observations by remote sensing, if only the top layers are 'seen'. In a mathematical approach, Goudriaan (1995) showed that to achieve maximum canopy assimilation rates, the vertical nitrogen distribution within a canopy should follow the light profile. Self-shading of lower leaves accelerates leaf senescence, which enables nitrogen translocation to younger (upper) leaves, exposed to higher radiation intensities (Vos and van der Putten, 2001). In this process, part of the Rubisco disintegrates and is transported to growing plant parts that are exposed to higher radiation intensities, where it is assembled into chlorophyll for the photosynthesis process (Ono *et al.*, 1996). Older leaves at the bottom of the canopy retain a residual non-transportable fraction of nitrogen. This inert fraction is significantly higher for crops well-supplied with nitrogen in juvenile growth stages (Groot, 1988).

Nitrogen profiles in crops tend to the optimal distribution, but with a lag, because of high crop growth rates or nitrogen shortage. The requirement for similarity of vertical nitrogen patterns and vertical light patterns to optimize crop assimilation has been

widely reported (e.g. Mooney and Gulmon, 1979; Anten *et al.*, 1995), but this only holds if the relation between leaf nitrogen content and maximum leaf assimilation rate is linear. For non-linear relations, as described by Bindraban (1999) and Evans (1983), maximum crop assimilation may be attained with incongruent vertical light and nitrogen distribution patterns. Canopy photosynthesis is strongly determined by photosynthetic efficiency at low radiation intensities, which depends on nitrogen content (Dreccer *et al.*, 2000). Vertical light profiles can be described by an exponential function of leaf area index (Monsi and Saeki, 1953), with the light extinction coefficient (k_L), expressing light attenuation per unit leaf area (Equation 4.1). Similarly, the vertical nitrogen profile can be described with the nitrogen extinction coefficient (k_N), expressing attenuation of light per unit leaf nitrogen (Equation 4.2).

$$k_L = -\left(\frac{\ln(T)}{LAI}\right) \quad (\text{Equation 4.1})$$

With:

k_L = light extinction coefficient ($\text{m}^2 \text{ soil m}^{-2} \text{ leaf}$)

T = transmittance fraction of incoming radiation (-)

LAI = leaf area index ($\text{m}^2 \text{ leaf m}^{-2} \text{ soil}$)

$$k_N = -\left(\frac{\ln(T)}{\text{LeafN}}\right) \quad (\text{Equation 4.2})$$

With:

k_N = nitrogen extinction coefficient ($\text{m}^2 \text{ soil g}^{-1} \text{ N}$)

LeafN = leaf nitrogen content ($\text{g N m}^{-2} \text{ soil}$)

Potato canopies are expected to show lower nitrogen extinction coefficients (k_N) than light extinction coefficients (k_L) as LeafN ($\text{g N m}^{-2} \text{ soil}$) is always larger than LAI ($\text{m}^2 \text{ leaf m}^{-2} \text{ soil}$), especially in the measurement domain ($LAI > 0.5 \text{ m}^2 \text{ m}^{-2}$; $\text{LeafN} > 1.5 \text{ g N m}^{-2}$). An example will clarify this: at emergence, potato specific leaf weight has a value of about 33 g m^{-2} , which increases with crop development to about 66 g m^{-2} . Leaf nitrogen content is high at emergence (up to $0.10 \text{ g N g}^{-1} \text{ leaf}$) and declines as crop development proceeds (to values below $0.02 \text{ g N g}^{-1} \text{ leaf}$). In the example of $0.10 \text{ g N g}^{-1} \text{ leaf}$ at emergence at a $LAI = 0.1 \text{ m}^2 \text{ m}^{-2}$, the value for LeafN is $0.33 \text{ g N m}^{-2} \text{ soil}$. This value increases at $LAI = 0.5$ to $1.65 \text{ g N m}^{-2} \text{ soil}$, and the difference between values for LAI and LeafN continues to increase as development proceeds, as increasing LAI coincides with decreasing leaf nitrogen contents expressed per unit leaf area and with increasing specific leaf weight.

Values for k_N range between $0.1\text{-}0.8 \text{ m}^2 \text{ soil g}^{-1}$, depending on crop (architecture), nitrogen status and light distribution (Dreccer, 1999). Light extinction coefficients (k_L) in potato canopies range between $0.3\text{-}0.8 \text{ m}^2 \text{ soil m}^{-2} \text{ leaf}$. Both, k_L and k_N may vary

among crops and varieties and over years, and they may change in the course of the growing season, depending on environmental conditions and crop management, which determine crop nutritional and health status and crop architecture. From a crop management point of view, for potatoes a canopy nitrogen status $>6 \text{ g N m}^{-2}$ soil is considered non-limiting for crop growth, even at low leaf area indices.

The objectives of this study are three-fold:

- 1) To investigate whether nitrogen status of potato canopies can be derived accurately from both SPAD-502 leaf measurements and canopy reflectance measurements, thereby opening ways for remote sensing applications at larger distances from the field such as by airborne and spaceborn sensor systems.
- 2) To investigate whether we can improve the correlation between SPAD-502 leaf measurements (taken at top leaves, with high nitrogen contents) and CropScan™ canopy reflectance measurements. In other words, to investigate whether SPAD-502 measurements can be related to canopy nitrogen status instead of leaf nitrogen status.
- 3) To investigate whether we can improve the correlation between remote sensing estimates of canopy nitrogen contents and laboratory nitrogen analyses of leaves randomly taken throughout the canopy by correcting these values on the basis of theoretical considerations with respect to vertical nitrogen distribution.

4.3 Material and methods

4.3.1 Field experiments

In 1997 a potato (*Solanum tuberosum* L.) field experiment was conducted at *Plant Research International* in the Netherlands ($51^{\circ} 58' \text{ N}$ and $5^{\circ} 40' \text{ E}$). Tubers of 35-45 mm of two potato varieties (early variety *Eersteling* and late variety *Bintje*) were planted at an approximate density of 44,444 plants ha^{-1} (0.75 m between rows and 0.30 m within rows). A base fertilizer application of 115 kg P ha^{-1} (Triple Super Phosphate) and 120 kg K ha^{-1} (Kali) was followed by nitrogen applications ranging from 0 to 300 kg ha^{-1} , in various application schemes (including split-dressings), to create different crop nitrogen levels in the course of the growing season. ‘Split-dressings’ refers to techniques where fertilizer doses are split in various portions that are applied to the crop-soil system at different moments. Each treatment had 3 replicates that were assigned randomly to plots of ca. 25 m^2 . The experimental design was repeated in trials in 1998, which included potato variety *Bintje* only.

4.3.2 Crop analysis

In both 1997 and 1998, 10 periodic harvests were carried out, consisting of 12 plants per plot (30 plants at final harvest), removed from inner rows to avoid disturbing

effects from adjacent plots. Samples were taken at predetermined soil cover stages (5-10 %, 25 %, 50 %, 75 % and 100 %) and at fixed time-intervals after the 100 % cover date (at 2, 4 and 6 weeks after 100 % cover). The last sampling date was at crop harvest. Leaf area of young and full-grown fresh leaves was measured by LI-COR 3100, providing at its highest resolution standard deviations for leaf area between 0.5-1.0 % (LI-COR, 2001). Fresh weight of (young and full-grown) leaves, stems, tubers and roots was measured, as well as their dry weight after 24 hours in an oven at 105 °C. Sub-samples of leaves, stems, tubers and roots were chemically analyzed for total nitrogen and nitrate. Total nitrogen was determined by the Dumas method on Vario-EL equipment (Hereaus, the Netherlands), nitrate on a Bran and Luebbe Traacs 800 continuous flow system (Maarssen, the Netherlands) (Meurs and Kreuzer, 1995). Leaf organic nitrogen contents (g N m⁻² soil) were calculated as the difference between total nitrogen and nitrate contents.

4.3.3 Spectral measurements

In both 1997 and 1998, incoming photosynthetically active radiation intensity (PAR, 400-700 nm) at the top of the canopy was measured¹, while in 1997 PAR intensity was also measured at the bottom of the potato canopy to calculate transmittance and light extinction coefficient k_L (Equation 4.1). In 1997, PAR intensity was sampled 25 times: at each destructive sampling date (10) and 15 times between these dates.

At each sampling date, ten SPAD-502 leaf chlorophyll readings per plot were taken by clamping the instrument on randomly selected first full-grown leaves from the top. Values were averaged per plot. SPAD-502 records leaf transmittance of induced light beams in two wavelengths, i.e. 650 and 750 or 920 nm (Minolta, 2003). Chlorophyll strongly absorbs radiation at 650 nm, and hardly at the other wavelengths (750 or 920 nm). By comparing the transmittance at these two wavelengths, a characteristic is calculated that is linearly related to chlorophyll content (Vos and Bom, 1993; Minolta, 2003). Actual chlorophyll contents (µmol m⁻² leaf) are derived from a calibration curve obtained from solvent extraction of leaf pigments. In this study, SPAD-502 readings have been calibrated on organic nitrogen contents of potato leaves and stems, as organic nitrogen is the mayor component of chlorophyll.

At each sampling date, 3 canopy reflectance readings (percentage of incoming solar radiation in each wavelength band) per plot were taken with CropScan™ equipment (CropScan™, 1993), equipped with 8 spectral bands, each approximately 20 nm width, centred at 460, 510, 560, 610, 660, 710, 760 and 810 nm. The 3 measurements per plot were averaged. CropScan™ equipment was positioned horizontally at about 1.5 m above the potato canopy. The viewing angle of ± 28 degrees results in an area of view of ± 0.44 m². Reflectance measurements of bare soil were taken at each sampling date to enable calculation of specific spectral vegetation indices, such as the Weighted Difference Vegetation Index (WDVI) as introduced by Clevers (1989). These spectral vegetation indices are correlated to important biophysical parameters, such as leaf area index (LAI) used in k_L calculations.

¹ PAR interception meter (TFDL, Wageningen, the Netherlands; Meurs and Kreuzer, 1995).

CropScan™ reflectance signatures of the continuous electromagnetic spectrum were computed by fitting data from the 8 bands to Boltzmann sigmoidal curves (Equation 4.3). The main inflexion point in the red-infrared slope (λ_{rep}) of this curve is correlated to chlorophyll and nitrogen status at leaf level (Guyot and Baret, 1988; Clevers and B ker, 1991; B ker and Clevers, 1992; Clevers and Jongschaap, 2001) and its validity at canopy level should be proven. Lower chlorophyll contents result in a reduction in the value of λ_{rep} , i.e. a shift towards blue wavelengths and therefore referred to as blue shift.

$$R_{\lambda} = R_{min} + \left(\frac{R_{max} - R_{min}}{1 + e^{\left(\frac{\lambda_{rep} - \lambda}{s} \right)}} \right) \quad (\text{Equation 4.3})$$

With:

R_{λ} = reflectance at wavelength λ (%),

R_{min} = minimum reflectance value (%),

R_{max} = maximum reflectance value (%),

λ_{rep} = red edge position (nm),

λ = wavelength (nm),

S = inflexion point: first derivative zero value for R_{λ} at λ_{rep} (nm)

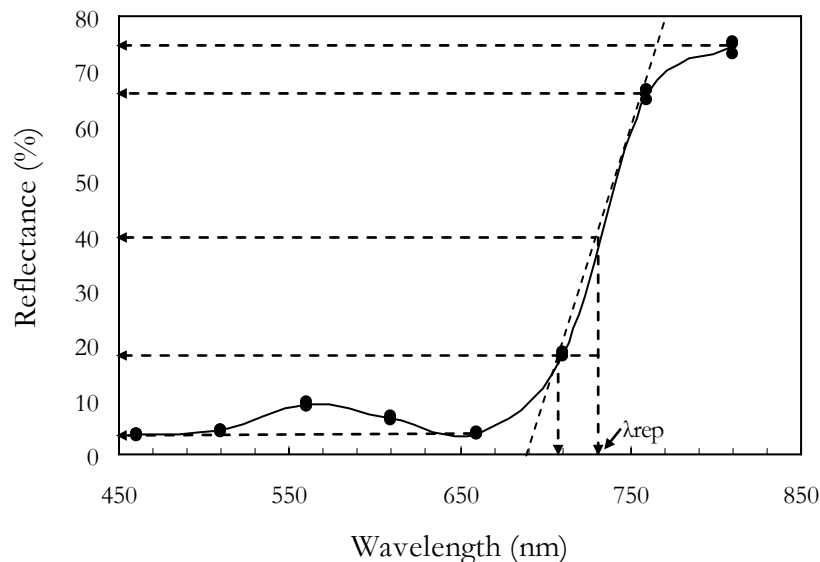


Figure 4.1 Example of CropScan™ reflectance values of a potato canopy (variety Bintje) at maximum leaf area index ($LAI=5.34$) on 24th June 1997 for N3-treatment (200 kg N ha^{-1}) with a red edge position (λ_{rep}) of 731.9 nm. Solid line is eye-fitted curve that smoothly connects the average of 3 replicates (•) to emulate a continuous spectrum. Dashed lines and arrows indicate how red edge position is retrieved (Equation 4.4).

Instead of fitting Boltzmann sigmoidal curves to CropScan™ measurements and computing the first derivative zero-value for R_λ at λ_{rep} (nm), a simpler method with fewer wavebands that is computationally simple and straightforward, was used for calculating λ_{rep} (Equation 4.4; Guyot and Baret, 1988). The accuracy of this method is similar to that of the original curve fitting method with a Coefficient of Variance (CV) of about 0.05 (Clevers and B ker, 1991; B ker and Clevers, 1992). The simple method uses 4 reflectance bands around λ_{rep} (660, 710, 760 and 810 nm) for the calculation of the red edge position (λ_{rep}) (Figure 4.1).

$$\lambda_{rep} = 710 + 50 \cdot \left(\frac{\left(\frac{1}{2} \cdot (R_{810} + R_{660}) - R_{710} \right)}{(R_{760} - R_{710})} \right) \quad (\text{Equation 4.4})$$

With:

660, 710 = CropScan™ bands, wavelengths below λ_{rep} (nm),

760, 810 = CropScan™ bands, wavelengths above λ_{rep} (nm),

50 = difference between 710 and 760 (nm),

R_λ = reflectance (%) at wavelength λ (nm)

4.3.4 Spectral and nitrogen relations at leaf, plant and canopy level

SPAD-502 readings for potato leaves and red edge position for potato canopies were evaluated against leaf organic nitrogen contents of the total canopy. Leaf organic nitrogen per unit soil area ($\text{LeafN}_{s_{org}}$, g N m⁻² soil) was calculated as the difference between leaf total nitrogen content ($\text{LeafN}_{s_{tot}}$, g N m⁻² soil) and leaf nitrate content ($\text{LeafN}_{s_{NO_3^-}}$, g N m⁻² soil). Leaf organic nitrogen per unit leaf area ($\text{LeafN}_{l_{org}}$; g N m⁻² leaf) was calculated as $\text{LeafN}_{s_{org}}$ divided by leaf area index (LAI, m² leaf m⁻² soil), determined in field measurements.

A vertical gradient in nitrogen content within the crop was assumed, following an exponential extinction with increasing depth (expressed in terms of leaf area) in the canopy. The vertical profiles were calculated on the basis of total canopy nitrogen values obtained by chemical analyses and by integrating the nitrogen extinction coefficient k_N (Equation 4.2). Nitrogen contents in the top leaves ($\text{LeafN}_{l_{org, top}}$, g N m⁻² leaf) were recalculated from laboratory results with average values for the whole canopy. Top leaf nitrogen contents resulted from assumptions on exponential attenuation of leaf organic nitrogen (k_N) and values for leaf area index (LAI) (Equation 4.5; Yin *et al.*, 2000). Statistical regression techniques were used to determine the most accurate value for k_N , i.e. giving the highest correlation coefficient with optical measurements. Five different values for k_N were tested for different reasons:

1. $k_N 41$ = 0.41 m² g⁻¹ N, the calculated mean (Equation 4.2) for 1997 experimental data,
2. $k_N 55$ = 0.55 m² g⁻¹ N, as reported by Yin *et al.* (2001),
3. $k_N 70$ = 0.70 m² g⁻¹ N, the calculated mean (Equation 4.1) for k_L (theoretical optimum distribution),
4. $k_N -ncalc$ = k_N m² g⁻¹ N, calculated for each observation date (Equation 4.2)
5. $k_N -lcalc$ = k_L m² g⁻¹ N, calculated for each observation date (Equation 4.1), following the theoretical optimum distribution.

$$LeafN_{L_{org,top}} = \frac{LeafN_{S_{org}} \cdot k_N}{(1 - e^{-k_N \cdot LAI})} \quad (\text{Equation 4.5})$$

With:

LeafN_{L_{org,top}} = organic nitrogen content of top leaves (g N m⁻² leaf),

LeafN_{S_{org}} = total organic nitrogen content of leaves (g N m⁻² soil),

k_N = nitrogen extinction coefficient (m² soil m⁻² leaf),

LAI = leaf area index (m² leaf m⁻² soil)

Bottom leaf nitrogen content follows from that of the top leaves by multiplying by: $\exp(-k_N \cdot LAI)$, according to the exponential extinction function (Equation 4.2) (Yin *et al.*, 2000). For the 1997 growing season, transmittance fraction (T) for incoming PAR was related to leaf area index, to calculate light extinction coefficients (k_L) (Equation 4.1). Similarly, nitrogen extinction coefficients (k_N) were established by relating the transmittance fraction (T) to leaf organic nitrogen content (g N m⁻² soil) (Equation 4.2).

Recapitulating, we used the following measurements:

Field measurements: leaf area index (LAI, m² m⁻²), leaf dry weight (g m⁻²), leaf organic nitrogen content (LeafN, expressed as: g N g⁻¹ leaf; g N m⁻² leaf and g N m⁻² soil), incoming PAR above the canopy and PAR intensity at soil level.

Near and remote sensing measurements: SPAD-502 chlorophyll readings and CropScan™ reflectance measurements.

Calculated variables: radiation transmittance fraction (T, -), red edge position wavelength (λ_{rep} , nm). Near and remote sensing observations were correlated to field and laboratory measurements and statistical regression was performed to evaluate theories on canopy nitrogen distribution.

4.4 Results

4.4.1 Field measurements

Both varieties *Eersteling* and *Bintje* followed a normal development and growth pattern, as shown in Table 4.1. Crops did not suffer from water shortage, due to supplementary irrigation during periods with precipitation deficits. Different nitrogen treatments resulted in different chlorophyll and nitrogen contents. SPAD-readings had average standard deviations of 1.05 (*Bintje*) and 1.89 (*Eersteling*). Average standard deviations for red edge position measurements were 0.63 nm (*Bintje*) and 0.79 nm (*Eersteling*). WDVI observations had average standard deviations of 2.5 % for both varieties. Organic nitrogen measurements had average standard deviations of 0.56 g N m⁻² soil.

Table 4.1 Average potato growth characteristics for 1997 and 1998 experiments^{a,b,c}. Potato varieties: E = *Eersteling*, B = *Bintje*. Numbers 97 and 98 refer to experiment year. LAI = leaf area index, LeafN = organic nitrogen in leaves, SPAD = SPAD-502 chlorophyll reading, λ_{rep} = red edge position wavelength, WDVI = Weighted Difference Vegetation Index (Clevers, 1989). Leaves and tubers are expressed in dry weights. Unless indicated otherwise, values refer to observations at maximum LAI^b.

	N supply ^{a)} (kg N ha ⁻¹)	LAI _{max} ^{b)} (m ² m ⁻²)	LeafN (g N m ⁻² soil)	SPAD (-)	λ_{rep} (nm)	WDVI (%)	Leaves (g m ⁻²)	Tubers ^{c)} (g m ⁻²)
E97	0	2.37	2.80	35.7	727.4	32.9	95.2	827.9
	100	4.41	5.48	40.3	730.0	48.3	171.2	1204.8
	200	5.03	8.36	42.8	731.2	56.0	207.3	1262.1
	300	5.86	10.51	43.5	731.7	55.8	247.5	1410.2
B97	0	2.45	3.22	34.8	727.3	37.9	96.9	1168.9
	100	5.16	9.12	43.6	732.5	54.2	215.7	1382.8
	200	5.35	11.94	46.5	731.9	56.2	208.2	1408.7
	300	5.31	12.00	47.0	731.8	53.9	201.3	1347.0
B98	0	2.48	2.70	32.1	727.0	21.7	85.5	1116.8
	100	4.79	5.48	37.2	729.8	54.8	153.5	1384.6
	200	6.98	8.59	43.1	731.6	50.0	187.0	1541.7
	300	7.51	12.12	45.9	731.9	51.7	225.9	1631.7

a) Fertilization at planting for E97 and B97: April 17th 1997, B98: May 11th 1998

b) Maximum LAI for E97: June 30th 1997, B97: June 24th 1997, B98: July 14th 1998

c) Harvest dates for E97: August 26th 1997, B97: September 16th 1997, B98: September 28th 1998

4.4.2 Vertical light and leaf nitrogen distribution

Light extinction coefficients (k_L) varied over the 1997 growing season (Figure 4.2) and averaged 0.66 ± 0.17 for early variety *Eersteling* (E) and 0.73 ± 0.14 for late variety *Bintje* (B). Under similar nitrogen supply, early variety *Eersteling* produced fewer leaves than late variety *Bintje*, resulting in lower LAI and higher PAR absorption efficiency per unit leaf area, as PAR interception did not decrease linearly with LAI reduction. For both varieties, k_L values decreased with increasing nitrogen supply, indicating more uniform light distributions, i.e. less steep light gradients. Relatively high k_L values imply steep light gradients, i.e. relatively low light intensities deeper in the canopy, which is characteristic for potato crops. The higher k_L for early *Eersteling* and the higher values in the lower nitrogen treatments for both varieties, result from lower LAI and more planophile leaf orientation.

Nitrogen extinction coefficients (k_N) showed greater variation than k_L over the 1997 growing season and averaged 0.41 ± 0.10 (0.39 ± 0.11 for early variety *Eersteling* and 0.42 ± 0.10 for late variety *Bintje*; Figure 4.3). Lower nitrogen supply resulted in higher k_N values with time, indicating translocation of leaf nitrogen from lower leaf layers to top layers in the course of the growing season. Potato crops that received higher nitrogen doses showed more stable values for k_N over time, indicating less translocation of nitrogen to upper leaf layers, as nitrogen supply was sufficient to maintain high nitrogen contents throughout.

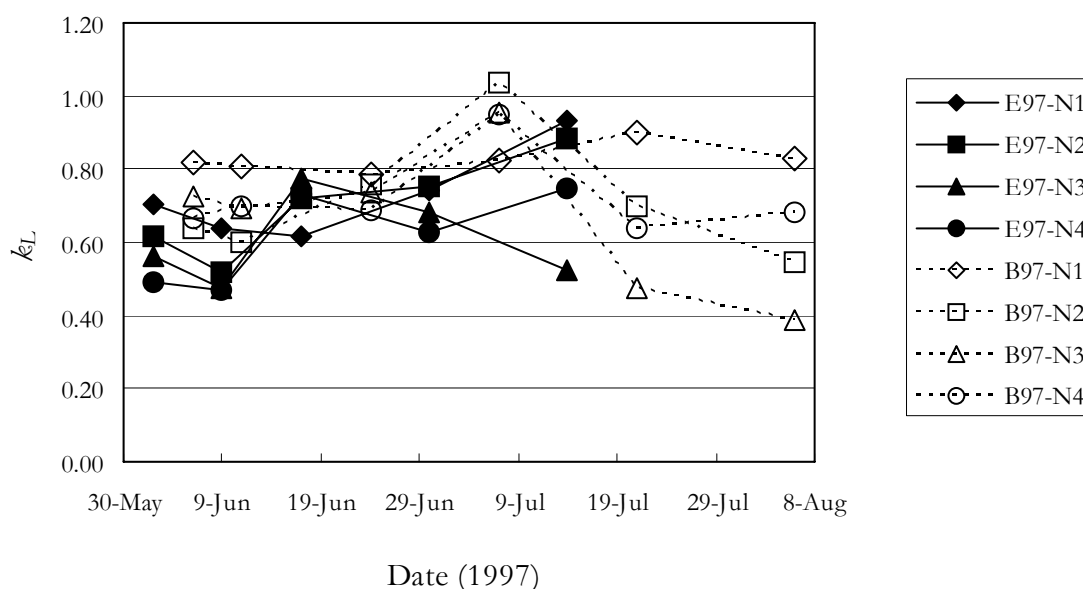


Figure 4.2 Light extinction coefficient (k_L) in the 1997 experiment for potato varieties *Eersteling* (E) and *Bintje* (B) with different nitrogen treatments supplied at planting (N1=0, N2=100, N3=200 and N4=300 kg N ha⁻¹).

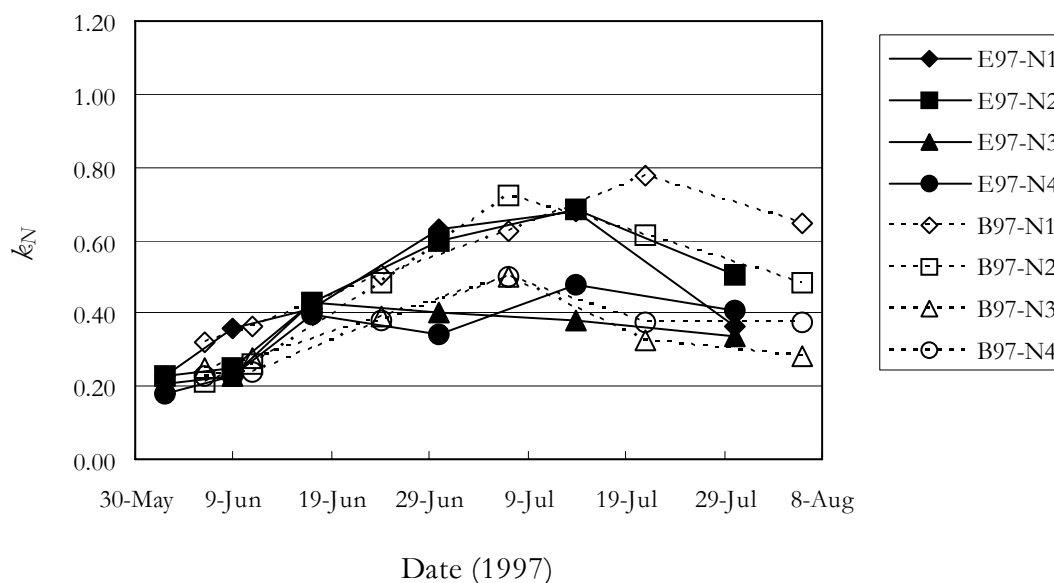


Figure 4.3 Nitrogen extinction coefficient (k_N) in the 1997 experiment for potato varieties Eersteling (E) and Bintje (B) with different nitrogen treatments supplied at planting (N1=0, N2=100, N3=200 and N4=300 kg N ha⁻¹).

4.4.3 Relating SPAD-502, red edge position and nitrogen contents

SPAD-502

Based on leaf surface area, total leaf nitrogen contents (g N m⁻² leaf) could be estimated more accurately from SPAD-502 readings if vertical nitrogen distribution (k_N) was integrated in the calculation procedure for both varieties and both years (Table 4.2, columns 2-4). If k_N was taken into account, correlation coefficients for the correlation of SPAD-502 readings (taken at the upper leaves of the canopy) to average total leaf nitrogen contents as measured in the laboratory for all leaves, were significantly higher. A value of $k_N = 0.41$ yielded the best results. Higher k_N values resulted in lower correlation coefficients. Calculating k_N and k_L separately for each observation date resulted in lower correlation coefficients. Figure 4.4 shows the exponential fit for the *Bintje* 1997 experiment, corrected for vertical nitrogen distribution ($k_N = 0.41$): $\text{LeafN}_{\text{org}} = 0.46 \cdot \exp(0.047 \cdot \text{SPAD})$ with an $r^2 = 0.91$.

Using leaf nitrogen contents on a dry weight basis (g N g⁻¹ leaf) yielded slightly lower correlation coefficients for most k_N values (Table 4.2, columns 5-7).

Leaf nitrogen contents on soil surface area basis (g N m⁻² soil) yielded the lowest correlation coefficients with SPAD-502 readings for all situations (Table 4.2, columns 8-10).

Table 4.2 Effect of selected k_N values on squared correlation coefficient (r^2) for exponential relation between SPAD-502 measurements and leaf nitrogen contents expressed as: g N m^{-2} leaf, g N g^{-1} leaf and g N m^{-2} soil. Potato varieties: E= Eersteling, B= Bintje. 97 and 98 refer to experiment years. Highest r^2 values per column are shown in bold.

k_N	Leaf nitrogen contents								
	(g N m ⁻² leaf)			(g N g ⁻¹ leaf)			(g N m ⁻² soil)		
	E97	B97	B98	E97	B97	B98	E97	B97	B98
0.00	0.35	0.53	0.54	0.90	0.84	0.77	0.22	0.52	0.27
0.41	0.53	0.91	0.70	0.68	0.85	0.75	0.13	0.39	0.18
0.55	0.48	0.84	0.60	0.59	0.79	0.66	0.12	0.37	0.16
0.70	0.20	0.77	0.50	0.54	0.72	0.57	0.11	0.35	0.15
k_N calc ^{a)}	0.21	0.57	n.a. ^{b)}	0.59	0.78	n.a. ^{b)}	0.04	0.26	n.a. ^{b)}
k_L calc ^{c)}	0.20	0.61	n.a. ^{b)}	0.53	0.77	n.a. ^{b)}	0.06	0.32	n.a. ^{b)}

a) k_N value was calculated at each observation date

b) n.a. = not available. In 1998 radiation transmittance data were not collected and as a result k_N and k_L values could not be calculated

c) k_N was set to k_L , which was calculated at each observation date

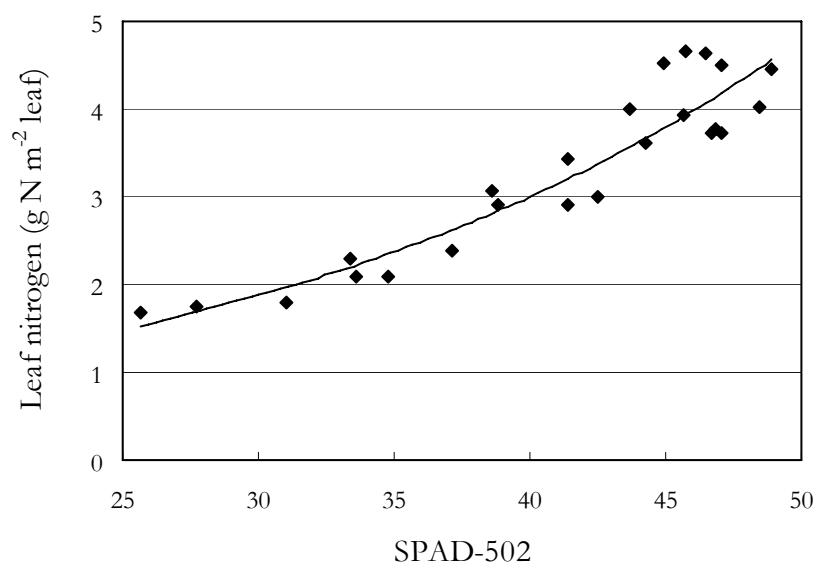


Figure 4.4 Relation between SPAD-502 readings (-) and leaf nitrogen contents (g N m^{-2} leaf) after correction for vertical nitrogen distribution ($k_N = 0.41$) for the Bintje 1997 trial. Bold line is exponential fit: $0.46 \cdot \exp(0.047 \cdot \text{SPAD})$ with $r^2 = 0.91$.

Red edge position (λ_{rep})

If in the correlation analyses between CropScan™ reflectance measurements (λ_{rep}) and nitrogen contents the latter were expressed per unit leaf area (g N m⁻² leaf) or per unit dry weight (g N g⁻¹ leaf), k_N values similar to average k_L values (≈ 0.70) yielded the highest correlation coefficients (Table 4.3). For nitrogen content expressed per unit soil area (g N m⁻² soil), no correction for vertical nitrogen distribution (i.e. $k_N = 0.00$) yielded good and stable results.

Accurately estimating leaf nitrogen contents in g N m⁻² leaf (Table 4.3, columns 2-4) or in g N g⁻¹ leaf (columns 5-7) from reflectance measurements over a canopy, requires knowledge of the vertical nitrogen distribution. Except for variety *Eersteling*, which has fewer leaves with a more planophile orientation, squared correlation coefficients (r^2) are very low (Table 4.3).

Leaf nitrogen contents per unit leaf surface area (g N m⁻² leaf) and per unit dry weight (g N g⁻¹ leaf) were estimated more accurately from CropScan™ reflectance measurement at higher k_N values. Such higher values imply steeper vertical gradients in leaf nitrogen, as a relatively larger proportion of total nitrogen is located in the upper canopy layers. As k_N continues to increase, eventually a situation will be reached where all leaf nitrogen appears located in the top canopy layer, thereby approaching the value of leaf nitrogen expressed per unit soil surface (g N m⁻² soil).

Leaf nitrogen contents per unit soil surface, (g N m⁻² soil) were accurately estimated, as CropScan™ reflectance measurements penetrated deeply into the canopy, thus recording all organic nitrogen. Therefore, correction for vertical nitrogen distribution

Table 4.3 Effect of selected k_N values on squared correlation coefficient (r^2) for exponential relation between CropScan™ reflectance measurements (λ_{rep}) and leaf nitrogen contents expressed as: g N m⁻² leaf, g N g⁻¹ leaf and g N m⁻² soil. Potato varieties: E= Eersteling, B= Bintje. 97 and 98 refer to experiment years. Highest r^2 values per column are shown in bold.

k_N	Leaf nitrogen contents								
	(g N m ⁻² leaf)			(g N g ⁻¹ leaf)			(g N m ⁻² soil)		
	E97	B97	B98	E97	B97	B98	E97	B97	B98
0.00	0.14	0.06	0.03	0.52	0.19	0.05	0.59	0.82	0.80
0.41	0.74	0.66	0.68	0.87	0.62	0.53	0.49	0.77	0.74
0.55	0.81	0.74	0.75	0.85	0.67	0.60	0.47	0.76	0.73
0.70	0.83	0.79	0.79	0.83	0.70	0.65	0.46	0.75	0.72
k_N calc ^{a)}	0.66	0.56	n.a. ^{b)}	0.91	0.64	n.a. ^{b)}	0.35	0.66	n.a. ^{b)}
k_N calc ^{c)}	0.68	0.60	n.a. ^{b)}	0.87	0.65	n.a. ^{b)}	0.39	0.69	n.a. ^{b)}

a) k_N was calculated at each observation date

b) n.a. = not available. In 1998 radiation transmittance data were not collected and as a result k_N and k_L values could not be calculated

c) k_N was set to k_L , which was calculated at each observation date

Table 4.4 Squared correlation coefficient (r^2) for exponential relation between CropScan™ reflectance measurements (λ_{rep}) and nitrogen contents of leaves, stems and leaves + stems, expressed as g N m^{-2} soil. Potato varieties: E= Eersteling, B= Bintje. 97 and 98 refer to experiment years.

Nitrogen source	Nitrogen contents		
	(g N m^{-2} soil)		
	E97	B97	B98
Leaves	0.59	0.82	0.80
Stems	0.48	0.70	0.67
Leaves + Stems	0.56	0.83	0.78

by introducing k_N in the correlation equation results in overestimation of leaf nitrogen content per unit soil surface and thus to lower correlation coefficients. As nitrogen in green stems may contribute to observed reflectance patterns, it was included in the correlation calculations between CropScan™ reflectance measurements (λ_{rep}) and nitrogen contents (g N m^{-2} soil), but that did not improve the correlations (Table 4.4). This can be attributed to the fact that potato stems are oriented more vertically than leaves, which reduces their contribution to the reflectance signal. Figure 4.5 shows the exponential fit for the *Bintje* 1997 experiment, without correction for vertical nitrogen distribution ($k_N = 0.00$): $LeafN_{org} = 0.1131 \cdot \exp(0.1878 \cdot (\lambda_{rep} - 710))$, with an $r^2 = 0.82$. It must be noted that year-to-year variability in SPAD-502 readings is substantial (Table 4.2), but that reflectance measurements (λ_{rep}) are more stable (Table 4.3).

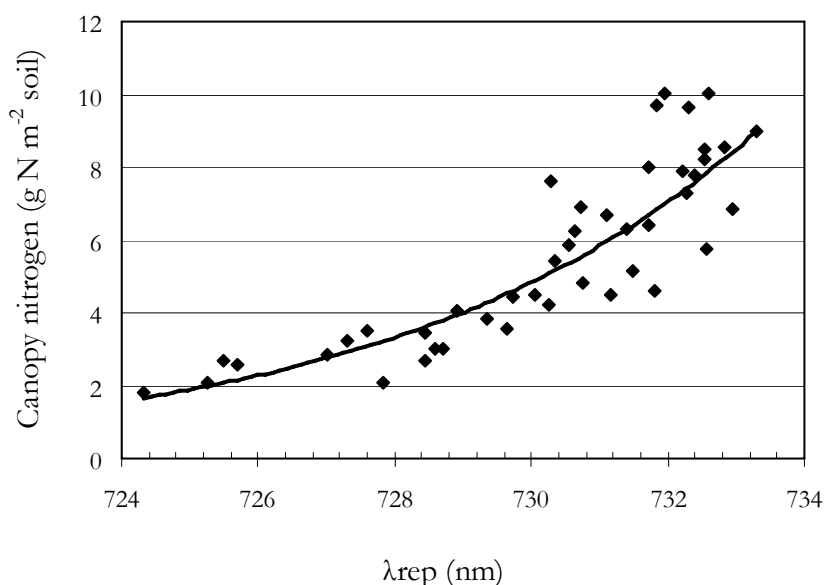


Figure 4.5 Relation between λ_{rep} (nm) and leaf nitrogen content (g N m^{-2} soil) in the *Bintje* 1997 trial. Bold line is exponential fit: $0.1131 \cdot \exp(0.1878 \cdot (\lambda_{rep} - 710))$ with $r^2 = 0.82$.

4.5 Discussion and conclusions

In this paper it is shown that leaf, plant and canopy nitrogen contents can be estimated accurately from observation techniques at leaf, plant and canopy level and that they can be linked via assumptions on vertical nitrogen distribution in a crop. SPAD-502 readings, if recorded at upper leaves only, do not account for vertical nitrogen distribution and are therefore less reliable in establishing crop nitrogen status. Results improve significantly if vertical nitrogen distribution is accounted for through adapted sampling techniques, i.e. by avoiding sampling upper leaves only and by using k_N to correct SPAD-502 readings. The best fit was obtained with $k_N = 0.41$, with $r^2=0.91$, which is similar to other potato SPAD models, such as reported by Vos and Bom (1993).

If red edge position (λ_{rep} , nm) can be established from reflectance measurements, nitrogen contents in potato canopies can be estimated with good accuracy. The results in this study show higher correlation coefficients than reported so far (in other crops) and gain in value, considering that the results were obtained with discontinuous medium-broad spectral bands and not with continuous high-spectral data, such as reported by Broge and Mortenson (2002). They used high-spectral field data and reported low correlation coefficients (r^2) for relations between λ_{rep} and wheat canopy organic nitrogen contents, ranging from 0.24-0.53. Relations between λ_{rep} and canopy chlorophyll contents resulted in $r^2=0.71$ for field spectral data in grass and $r^2=0.66$ for wheat canopies, whereas for airborne spectral data these values were $r^2=0.53$ for grass and $r^2=0.67$ for wheat canopies (Jago *et al.*, 1999). A big advantage of reflectance measurements is that they represent an integrated measure of nitrogen contents over total canopy depth, which gives direct values for crop nitrogen status.

Vertical nitrogen distribution should be taken into account in estimating nitrogen contents of potato leaves, plants and/or canopy from observations at leaf (SPAD-502) or canopy (reflectance measurements) level. In fact, this study shows that accuracy of these estimates can be increased significantly, the magnitude depending on observation scale (leaf, plant or canopy) and observation technique (SPAD-502 or reflectance measurements).

For (nitrogen) fertilizer management it makes no difference whether nitrogen status is expressed per unit soil area (g N m^{-2} soil), or per unit plant area (g N m^{-2} leaf). Classical field observation techniques take measurements at leaf scale, and are therefore mostly expressed per unit plant area. Remote sensing observations seem to operate best per unit soil area (Table 4.3). Integrating leaf area index (LAI, m^2 leaf m^{-2} soil) measurements enables interchange between units. Exponential fits of λ_{rep} to relatively higher organic nitrogen levels ($>6 \text{ g N m}^{-2}$ soil) seem to saturate. However, for (nitrogen) fertilizer management, the most interesting part of the relation is that below 6 g N m^{-2} soil, where nitrogen contents may be limiting crop growth. Crop production is limited if observed canopy nitrogen contents are below critical values. Greenwood *et al.* (1990) report that critical nitrogen contents decrease with increasing plant biomass, but it is more likely that a minimum amount of organic nitrogen is needed to efficiently intercept incoming radiation. This gives remote sensing observations an advantage over SPAD-502 readings, as remote sensing integrates canopy nitrogen over canopy depth, whereas SPAD-502 readings should be corrected for vertical nitrogen distributions.

The effect of vertical nitrogen distribution on radiation interception efficiency should be investigated further. Evans (1983) and Bindraban (1999) already reported non-linearity between radiation intensity and assimilation efficiency. Yin *et al.* (2000) use vertical nitrogen attenuation (k_N) and light attenuation (k_L) to calculate radiation interception capacity to quantify leaf senescence and (reduced) assimilation capacity. If nitrogen shortage is identified by one of these methods, appropriate fertilization techniques should be applied to remedy nitrogen deficits.

The most important conclusions from this study are:

- Relations between SPAD-502 readings and leaf nitrogen contents are best expressed in exponential equations and yield squared correlation coefficients (r^2) up to 0.91. For potato plants with high k_N values (i.e. low nitrogen contents, low LAI), SPAD-502 readings need minimal correction, as most of their organic nitrogen is located in upper leaf layers.
- The relation between SPAD-502 readings and organic nitrogen contents of potato leaves (g N m^{-2} leaf) is given by $0.46 \cdot \exp(0.047 \cdot \text{SPAD})$.
- If λ_{rep} can be determined from reflectance measurements, the correlations between λ_{rep} and canopy nitrogen contents are strongest if nitrogen contents are expressed per unit soil area (e.g. g N m^{-2} soil). To estimate canopy nitrogen contents from observations at leaf level, vertical nitrogen distribution should be integrated in the calculation procedure to assign total amounts of organic nitrogen to top and bottom leaves of the canopy.
- The relation between λ_{rep} and organic nitrogen contents of potato leaves (g N m^{-2} soil) is given by $0.1131 \cdot \exp(0.1878 \cdot (\lambda_{\text{rep}} - 710))$.
- SPAD-502 readings can be related to canopy nitrogen status instead of leaf nitrogen status. Integration of vertical nitrogen distribution, assuming exponential extinction with depth, increases the accuracy of estimates of canopy nitrogen contents (expressed as g N m^{-2} leaf, or g N g^{-1} leaf) based on SPAD-502 readings.
- Relations between canopy reflectance measurements (λ_{rep}) and canopy nitrogen contents expressed per unit leaf improved, if vertical nitrogen profiles were assumed.
- Relations between canopy reflectance measurements (λ_{rep}) and canopy nitrogen contents expressed per unit soil do not need to account for vertical nitrogen distribution, as canopy remote sensing integrates nitrogen contents over total canopy depth.
- Relations between canopy reflectance measurements (λ_{rep}) and canopy nitrogen contents (g N m^{-2} soil) become less accurate at higher values of λ_{rep} . As these values occur in situations where nitrogen is not limiting crop growth (i.e. $\text{LeafN}_{\text{org}} > 6 \text{ g N m}^{-2}$ soil), this technique is suitable for monitoring in support of potato crop management.
- For extrapolation to other crops, theoretical assumptions on vertical nitrogen distribution in potato should be verified experimentally. For extrapolation to other spatial scales and to other sensor resolutions, this point-based approach may be further explored by reflectance measurements taken by airborne or by space born sensors. We hope that these results will stimulate the use of remote sensing for these types of applications.

4.6 Acknowledgements

The Dutch Ministry of Agriculture, Nature Management and Fisheries financed this project in their programmes on precision agriculture. We are grateful to Prof. Dr. Steven M. de Jong, Prof. Dr. Herman van Keulen and Dr. Prem S. Bindraban for useful comments on the manuscript. Further acknowledgements are for Dik Uenk of *Plant Research International* who supervised all field operations and was able to recall small but important details of the field experiments. We would like to thank two anonymous referees for their constructive comments on an earlier draft of the paper.

4.7 References

- Anten, N.P.R., F. Schieving, M.J.A. Werger, 1995.
Patterns of light and nitrogen distribution in relation to whole canopy carbon gain in C₃ and C₄ mono- and dicotyledoneous species. *Oecol.* 101, 504-513.
- Bindraban, P.S., 1999.
Impact of canopy nitrogen profile in wheat on growth. *Field Crops Res.* 63, 63-77.
- Bouman, B.A.M., 1992.
Accuracy of estimating the leaf area index from vegetation indices derived from crop reflectance characteristics, a simulation study. *Int. J. Rem. Sens.* 13, 3069-3084.
- Bouman, B.A.M., D. Uenk, A.J. Haverkort, 1992a.
The estimation of ground cover of potato by reflection measurements. *Pot. Res.* 35, 111-125.
- Bouman, B.A.M., H.W.J. van Kasteren, D. Uenk, 1992b.
Standard relations to estimate ground cover and LAI of agricultural crops from reflection measurements. *Eur. J. Agron.* 1, 249-262.
- Broge, N.H., J.V. Mortensen, 2002.
Deriving green crop area index and canopy chlorophyll density of winter wheat from spectral reflectance data. *Rem. Sens. Environ.* 81, 45-57.
- Büker, C., J.G.P.W. Clevers, 1992.
Imaging spectroscopy for agricultural applications. Wageningen Agricultural University, Department of Landsurveying and Remote Sensing, Report 199206, Wageningen, the Netherlands, 88 pp.
- Clevers, J.G.P.W., 1989.
The application of a weighted infrared-red vegetation index for estimating Leaf Area Index by correcting for soil moisture. *Rem. Sens. Environ.* 29, 25-37.
- Clevers, J.G.P.W., C. Büker, 1991.
Feasibility of the red edge index for the detection of nitrogen deficiency. In: *Proc. 5th International Colloquium Physical measurements and Signatures in Remote Sensing.* 14-18 January 1991, Courchevel, France, ESA SP-319, pp. 165-168.

- Clevers, J.G.P.W., R.E.E. Jongschaap, 2001.
Imaging spectrometry for agricultural applications. In: F.D. van der Meer, S.M. de Jong (Eds.). *Imaging spectrometry: Basic principles and prospective applications*, Vol 4, Chapter 6, pp. 157-199. Kluwer Academic Publ., Dordrecht, the Netherlands, 425 pp.
- CropScan™, 1993.
Multi-Spectral Radiometer (MSR): Users manual and technical reference. CropScan™, Rochester, MN, USA.
- Dreccer, M.F., 1999.
Radiation and nitrogen use in wheat and oilseed rape crops. Ph. D. Thesis, Wageningen Agricultural University, Wageningen, the Netherlands, 135 pp.
- Dreccer, M.F., A.H.C.M. Schapendonk, M. van Ooijen, C.S. Pot, R. Rabbinge, 2000.
Radiation and nitrogen use at the leaf and canopy level by wheat and oil seed rape during the critical period for grain number definition. *Austr. J. Plant Phys.* 27, 899-910.
- Evans, J.R., 1983.
Nitrogen and photosynthesis in the flag leaf of wheat. *Plant Phys.* 72, 297-302.
- Goudriaan, J., 1995.
Optimization of nitrogen distribution and leaf area index for maximum canopy assimilation rate. In: T.M. Thiyagarajan, H.F.M. ten Berge, M.C.S. Wopereis (Eds.). *Nitrogen management studies in irrigated rice*. International Rice Research Institute (IRRI), Los Baños, Philippines, pp. 85-97.
- Greenwood, D.J., G. Lemaire, G. Gosse, P. Cruz, A. Draycott, J.J. Neeteson, 1990.
Decline in percentage N of C₃ and C₄ crops with increasing plant mass. *Ann. Bot.* 66, 425-436.
- Groot, J.J.R., 1988.
Post-floral nitrogen behaviour in grain crops: Measurements and simulation. In: M.L. Jorna, L.A.J. Sloodmaker (Eds.). *Cereal breeding related to integrated cereal production*. In: Proc. EUCARPIA. 24-26 February 1988, Wageningen, the Netherlands, pp. 93-97.
- Guyot, G., F. Baret, 1988.
Utilisation de la haute résolution spectrale pour suivre l'état des couverts végétaux. In: T.D. Guyenne, J.J. Hunt (Eds.). *Proc. 4th International Colloquium on Spectral Signatures of Objects in Remote Sensing*. 18-22 January 1988, Aussois, France, ESA SP-287, pp. 279.
- Jago, R.A., M.E.J. Cutler, P.J. Curran, 1999.
Estimating canopy chlorophyll concentration from field and airborne spectra. *Rem. Sens. Environ.* 68, 217-224.
- LI-COR, 2001.
Leaf Area Meters. LI-3100 Area Meter, Lincoln, USA, 6-7.
- Meurs, E.J.J., A.D.H. Kreuzer, 1995.
Measuring equipment in crop physiology research (in Dutch). DLO Institute for Agrobiolgy and Soil Fertility Research (AB-DLO), Note 14, Wageningen, the Netherlands, 77 pp.

Minolta, 2003.

Chlorophyll meter SPAD-502. Instruction Manual. Minolta Camera BeNeLux BV, Maarssen, the Netherlands.

Monsi, M., T. Saeki, 1953.

Über den Lichtfaktor in den Pflanzengesellschaften und seine Bedeutung für die Stoffproduktion. *Jap. J. Bot.* 14, 22-52.

Mooney, H.A., S.L. Gulmon, 1979.

Environmental and evolutionary constraints on the photosynthetic characteristics of higher plants. In: O.T. Solbrig, S. Jain, G.B. Johnson, P.H. Raven (Eds.). *Topics in plant population biology*. MacMillan, London, UK, pp. 316-337.

Ono, K., I. Terashima, A. Watanabe, 1996.

Interaction between nitrogen deficit of a plant and nitrogen content in the old leaves. *Plant Cell Phys.* 37, 1083-1089.

Thenkabail, P.S., R.B. Smith, E. de Pauw, 2000.

Hyperspectral vegetation indices and their relationships with agricultural crop characteristics. *Rem. Sens. Environ.* 71, 158-182.

Vos, J., M. Bom, 1993.

Hand-held chlorophyll meter: a promising tool to assess the nitrogen status of potato foliage. *Pot. Res.* 36, 301-308.

Vos, J., P.E.L. van der Putten, 2001.

Effects of partial shading of the potato plant on photosynthesis of treated leaves, leaf area expansion and allocation of nitrogen and dry matter in component plant parts. *Eur. J. Agron.* 14, 209-220.

Yin, X., A.H.C.M. Schapendonk, M. Kropff, M. van Ooijen, P.S. Bindraban, 2000.

A generic equation for nitrogen-limited leaf area index and its application in crop growth models for predicting leaf senescence. *Ann. Bot.* 85, 579-585.

Yin, X., J. Verhagen, R.E.E. Jongschaap, A. Schapendonk, 2001.

A model to simulate responses of the crop-soil system in relation to environmental change. *Plant Research International, Note 129*, Wageningen, the Netherlands, 46 pp. + appendices.

Chapter 5

Run-time calibration of simulation models by integrating remote sensing estimates of leaf area index and canopy nitrogen

Raymond. E.E. Jongschaap

*Wageningen University and Research centre, Plant Sciences Group,
Plant Research International, P.O. Box 16, NL-6700AA Wageningen, the Netherlands.
Tel.: +31-317-475953, Fax: +31-317-423110, E-mail: raymond.jongschaap@wur.nl*

© 2006 *Eur. J. Agron.* 24, 328-336. Reprinted with permission from Elsevier.

5.1 Abstract

Dynamic simulation models may enable for farmers the evaluation of crop and soil management strategies, or may trigger crop and soil management strategies if they are used as warning systems, e.g. for drought risks and for nutrient shortage. Predictions by simulation models may differ from field observations for a variety of reasons, and such deviations can be revealed instantly by traditional or by new field monitoring techniques. The objective of this study was to improve simulation results by integrating remote sensing observations during the growing season in the simulation (i.e. *run-time calibration*). The *Rotask 1.0* simulation model was used as it simulates daily interactions between climate (radiation, temperature, vapour pressure, wind speed, precipitation), soils (water holding capacities, soil organic matter dynamics, evaporation) and crops (light interception, dry matter production, nitrogen uptake, transpiration). Various run-time calibration scenarios for replacing simulated values by remotely observed values were tested. For a number of times in the growing season, simulated values of leaf area index (LAI) and canopy nitrogen contents were replaced with values estimated from remote sensing. Field experiments were carried out in the Netherlands in 1997 (validation) and 1998 (calibration) with potato variety *Bintje*. Destructive field samplings

were performed to follow LAI and canopy nitrogen development in the growing season. Remote sensing observations at canopy level were taken by CropScan™ equipment, covering the electromagnetic spectrum between 460-810 nm in 8 spectral bands. LAI and canopy nitrogen were monitored at various moments throughout the growing season by relating them with Vegetation Indices (VI) that were calculated from the combination of specific remote sensing bands. The results of this study show that run-time calibration of mechanistic simulation models may enhance simulation accuracy, depending on the method how additional information is integrated. It is advised to synchronize dry matter balances and internal nitrogen balances in accordance with adjustments to observed calibration variables (in this case LAI and canopy nitrogen content). It is shown that an integrated approach follows the actual crop-soil system more closely, which is helpful for specific crop management and precision agriculture in general. Run-time calibration with variables that can be estimated from remote sensing observations gives more accurate simulation results of variables that can not be observed directly, e.g. the evolution of soil inorganic nitrogen contents. High frequencies of remote sensing observations and interpolation in between them, allow reconstructing the evolution of LAI and canopy nitrogen contents to be integrated in the simulation, thereby increasing simulation accuracy of other model variables.

Keywords: calibration, remote sensing, simulation model, canopy nitrogen, LAI, potato, precision agriculture

5.2 Introduction

Mechanistic crop growth simulation modelling has a history of more than 50 years, with the 3 major ‘schools of development’ based in Australia, the Netherlands and the United States (Jones *et al.*, 2001). These models have proven to be valuable tools in yield forecasting both on the regional scale (e.g. Supit *et al.*, 1996) and at plot level (e.g. Keating *et al.*, 2003; MacKerron and Haverkort, 2004; Paz *et al.*, 2004). For useful applications in agricultural management however, further developments are necessary (Landau *et al.*, 1998; van Ittersum *et al.*, 2003). Increased process knowledge and improved computer technology have contributed to better understanding and description of complex systems such as the crop-soil system. In a systems approach the behaviour of the system is explained from quantitative description of the underlying processes. This approach is followed in dynamic and mechanistic crop growth simulation models in analyzing, predicting and exploring the integrated effects of the environment on crop performance. Such models are therefore suitable for analyzing effects of crop and soil management and their interactions with the aerial and soil environment. Crop growth simulation modelling hitherto mainly focussed on crop production and yield, with both satisfactory, as well as unsatisfactory results (Bouman *et al.*, 1996; Landau *et al.*, 1998). Dynamic simulation models need detailed information on environmental conditions and have to be calibrated under local conditions to

generate reliable results. Even if all input data are available, which is often difficult to realize, deviations from reality may always occur because of processes that are insufficiently understood, due either to conditions outside the model boundaries, or to situations that are not included (e.g. random attacks by pests and diseases).

Remote sensing may provide an attractive alternative to monitor crop and soil status, as it can be applied easily at a large spatial scale (especially with airborne and spaceborn sensors). Additionally, remote sensing does not need destructive sampling and time-consuming laboratory analyses. Remote sensing data may be useful in the calibration process of simulation models, if important crop characteristics can be retrieved temporarily from remote sensing images, in order to reconstruct growth curves (Prévoit *et al.*, 2003). An alternative option to incorporate additional information during run time (i.e. 'run-time calibration') offers the possibility to generate model output in more close agreement with observed values.

It is hypothesized that run-time calibration through integration of real-time (remote sensing) measurements for estimating LAI and canopy nitrogen, is a valuable method for more accurate model simulations. This requires integration of a continuous simulation system with a run-time, discrete calibration technique. The underlying hypotheses are therefore, that the physiological condition of the crop (LAI, canopy nitrogen) can be quantified using remotely sensed information, and that the information gathered by the sensors has greater accuracy than the simulated ones.

The objective of this study is to achieve such a system and to find an integration method that does not violate the mechanistic simulation processes, and eventually yields more accurate simulation results.

In precision agriculture, prediction of final yield is still important, but synchrony between soil supply of and crop demand for water and nutrients is the key in realizing that yield. Useful simulation models should be able to give reliable information on the evolution of crop-soil systems, especially in between field observations, or on crop-soil variables that can not be measured easily, such as soil inorganic nitrogen contents. Evidently, accurate prediction of the temporal and spatial dynamics of the crop-soil system is also of interest to allow adequate management interventions to avoid economic losses and reduce risks of environmental pollution. In this study it is investigated if simulation of the crop-soil system can be minimized, by interpolating remote sensing observations of important model drivers, such as LAI and canopy nitrogen contents and to integrate these interpolations in the model.

5.3 Material and methods

5.3.1 Field experiment

Both in 1997 and 1998, a field experiment was conducted at *Plant Research International* in the Netherlands (51° 58' N and 5° 40' E). Tubers of 35-45 mm of potato (*Solanum tuberosum* L.) variety *Bintje* were planted at an approximate density of 44,444 plants ha⁻¹ (0.75 m between rows and 0.30 m within rows). A base fertilizer application of 10 kg N

ha⁻¹ (KAS), 115 kg P ha⁻¹ (Triple Super Phosphate) and 120 kg K ha⁻¹ (Kali) was followed by four nitrogen doses (0, 100, 200 and 300 kg N ha⁻¹) to create different canopy nitrogen levels in the course of the growing season. Each treatment was replicated three times and was assigned randomly to plots of ca. 25 m².

In both 1997 and 1998, 10 periodic samplings were carried out, consisting of 12 plants per plot (30 plants at final harvest), removed from inner rows to avoid disturbing effects from adjacent plots. Samples were taken at predetermined soil cover stages (5-10 %, 25 %, 50 %, 75 % and 100 %) and at fixed time-intervals after the 100 % cover date (at 2, 4 and 6 weeks after 100 % cover). The last sampling date was at crop harvest. Leaf area of young, full-grown fresh leaves was measured by LI-COR 3100 equipment (Lincoln, USA). Fresh weight of all leaves in the sample was determined, as well as dry weight of sub-samples of leaves after 24 hours in an oven at 105 °C. Sub-samples of leaves were chemically analyzed for total nitrogen according to the Dumas method on Vario-EL equipment (Hereaus, NL), and for nitrate on a Bran and Luebbe Traacs 800 continuous flow system (Maarssen, NL) (Meurs and Kreuzer, 1995). Leaf organic nitrogen contents (g N m⁻²) were calculated as the difference between total nitrogen and nitrate contents.

At each sampling date, 3 canopy reflectance readings (percentage of incoming solar radiation in each wavelength band) per plot were taken with CropScan™ equipment (CropScan™, 1993), equipped with 8 spectral bands, each covering approximately 20 nm, centred at 460, 510, 560, 610, 660, 710, 760 and 810 nm, and averaged per plot. CropScan™ equipment was positioned horizontally at about 1.5 m above the potato canopy, with a viewing angle of ca. 28 °, resulting in an area of view of about 0.44 m². Reflectance measurements of bare soil were taken at each sampling date to enable calculation of specific spectral vegetation indices (Table 5.1), such as Weighted Difference Vegetation Index (WDVI (%); Clevers, 1989) and red edge position (λ_{rep}; Guyot *et al.*, 1988). Potato LAI (m² m⁻²) can be estimated from WDVI using growth stage-specific relations as derived from potato trials in the Netherlands (Equations 5.2 and 5.3: Bouman, 1992; Bouman *et al.*, 1992a; Bouman *et al.*, 1992b; Uenk *et al.*, 1992).

$$WDVI = R_{nir} - R_{vis} \cdot \left(\frac{R_{s_{vis}}}{R_{s_{nir}}} \right) \quad (\text{Equation 5.1})$$

With R = canopy reflectance (%), R_s = bare soil reflectance (%), *nir* = near infrared and *vis* = visible.

Table 5.1 Vegetation indices (and wavelengths (nm) of the CropScan™ field-spectrometer to calculate them) for the determination of potato canopy variables.

Canopy variable	Vegetation index	CropScan™ bands	Reference
Biomass	NDVI, WDVI	680, 810 nm	(Bouman <i>et al.</i> , 1992)
Leaf area index	WDVI	680, 810 nm	(Clevers, 1989), (Bouman, 1992)
Nitrogen content	Red Edge Position	660, 710, 760, 810 nm	(Guyot <i>et al.</i> , 1988), (Jongschaap and Booij, 2004)

$$LAI = 0.048 \cdot WDVI \quad \text{for } WDVI < 29 \quad (r^2=0.69) \quad (\text{Equation 5.2})$$

$$LAI = -0.867 + 0.091 \cdot WDVI \quad \text{for } WDVI \geq 29 \quad (r^2=0.57) \quad (\text{Equation 5.3})$$

Potato canopy nitrogen (g N m⁻²) can be estimated from red edge position measurements (Jongschaap and Booij, 2004):

$$\text{Canopy nitrogen} = 0.1131 \cdot \exp(0.1878 \cdot (\lambda_{\text{rep}} - 710)) \quad (r^2=0.82) \quad (\text{Equation 5.4})$$

With λ_{rep} in nm.

5.3.2 *Rotask* 1.0 simulation model

The dynamic simulation model *Rotask* 1.0 (Jongschaap, 1996), developed in the 1990s was used as a tool in scientific research and decision support for global environmental change and crop management (Yin *et al.*, 2001; Jongschaap *et al.*, 2002). The model consists of separate modules to perform model simulations for various crop and soil processes. Tools have been added for quick result viewing and calibration procedures in a modelling framework (Hillyer *et al.*, 2003).

Rotask 1.0 is a mechanistic simulation model, using (simple) algorithms based on knowledge of the underlying physical, physiological and biochemical processes that are described in individual modules that can, if required, be replaced by modules with different complexity. For fallow or field crop rotation systems, the model quantifies water fluxes (precipitation, irrigation, run-off, soil evaporation, transpiration and drainage), nitrogen fluxes (soil organic nitrogen flows, i.e. mineralization/immobilization, mineralization from dead plant material, (in-) organic fertilization, wet deposition, leaching and root nitrogen uptake by mass flow and diffusion), light interception and thermal heat accumulation direct crop growth and development, respectively. Crop nitrogen contents may vary as a result of variations in nitrogen availability, caused by mineralization, immobilization and fertilizer applications. Management decisions refer to ploughing (date, depth), incorporation of organic fertilizer (date, rate, type), and application of inorganic fertilizer (date, rate, type), sowing (rate, depth), irrigation (date, rate) and harvest (date, method). Crops currently included in the model are wheat, sugar beet, potato, barley, rape-seed and maize. For the current study, simulations were performed for potato only.

Crop growth is driven by light interception of the canopy (LAI). The negative feedback on crop growth due to water shortage is accounted for by stomatal closure, which reduces the potential assimilation rates proportionally. The negative feedback on crop growth for nitrogen shortage is coupled with ‘functional LAI’ development. ‘Functional LAI’ is defined as green tissue that is able to efficiently intercept incoming radiation. The amount of canopy nitrogen then determines the magnitude of ‘functional LAI’ as a minimum concentration of nitrogen required to be functional. ‘Non-functional LAI’ enters the senescence pool more quickly than ‘functional LAI’.

Five categories of input parameters were used in the model: 1) **control data**: start day and year of simulation, end day and year of simulation, location, output variables, 2) **environmental data**, i.e. climate: daily values of radiation, minimum and maximum temperature, vapour pressure, wind speed and precipitation and nitrogen concentration in precipitation, 3) **crop data**: crop type, initial values for LAI and organ dry matter weights at emergence, minimum, optimum and maximum nitrogen concentrations, temperature sums for phenological development stages (emergence, vegetative phase, reproductive phase), base temperatures for phenological development rates, maximum rooting depth and extinction coefficients for radiation, 4) **soil data**: soil moisture contents at specific pF-values, soil organic matter pools (stable and labile), initial carbon and organic nitrogen contents, bulk density, initial inorganic nitrogen content, 5) **management data**: decision variables on ploughing, sowing/planting, organic and inorganic fertilizer application, irrigation and harvesting.

Output of the model can be selected from all available variables in the separate process modules. For the current study, LAI ($\text{m}^2 \text{m}^{-2}$), leaf nitrogen content (g m^{-2}) and soil inorganic nitrogen content (g m^{-2}) were selected.

Calibration parameters identified by sensitivity analyses were established by using data from various sites in temperate regions in Europe (Jongschaap, 1996; Yin *et al.*, 2001; Jongschaap *et al.*, 2002). Sensitivity was expressed as the ‘elasticity’ of output parameters: percentile change in output parameter per percentile change of input parameter. The input parameters were varied by -10 % and +10 % and the sensitivity of selected model output parameters was calculated (Table 5.2). The model was calibrated on the 1998 data set for environmental conditions (climate) and soil characteristics in Wageningen, the Netherlands to obtain initial values for the sensitive input parameters and then applied to the 1997 dataset for validation.

Model initialization comprised attuning the crop, soil and management data files for the potato trials in 1997 and 1998. For crop and management data: LAI at emergence ($0.059 \text{ m}^2 \text{m}^{-2}$); row distance (0.75 m); temperature sum between emergence and tuber initiation (125 degree-days) and between tuber initiation and maturity (1675 degree-days); initial dry weight at planting (75 kg ha^{-1}); nitrogen extinction coefficient (0.55 m^{-1}); biomass carbon fraction (0.4603 g g^{-1}); minimum nitrogen leaf weight concentration (0.4 g m^{-2}). The soil module was initialized for soil moisture holding capacity at saturation ($0.5090 \text{ cm}^3 \text{cm}^{-3}$), at field capacity ($0.3587 \text{ cm}^3 \text{cm}^{-3}$), at wilting point ($0.1084 \text{ cm}^3 \text{cm}^{-3}$), at air dry ($0.0365 \text{ cm}^3 \text{cm}^{-3}$) and the initial soil moisture holding capacity at $0.2030 \text{ cm}^3 \text{cm}^{-3}$; soil evaporation extinction coefficient (0.2 m^{-1}). Several soil fertility input parameters were measured: initial soil inorganic nitrogen (40 kg ha^{-1}); initial carbon percentage in top soil layer (1.75 %); initial organic nitrogen content in top soil layer (0.25 %) and bulk density (1.2 g cm^{-3}).

The model was started on January 1st, 1997 (day 1) and continued until harvest at day 259 (September 16th). In correspondence with the field experiments, simulated fields were ploughed 0.25 m deep on day 65 (March 6th); at day 100 (April 10th) 10 kg N ha^{-1} was applied as base fertilizer rate, followed on day 107 (April 17th) by the remainder of the fertilizer at planting. Emergence of the potato crop was set at day 137 (May 17th) in accordance with field observations.

Table 5.2 Sensitivity analysis results (% %⁻¹) for input parameters affecting model output variables Leaf Area Index (LAI, m² m⁻²) and Leaf Nitrogen Content (LeafNWt, kg ha⁻¹).

LAI (m ² m ⁻²)	(% % ⁻¹)	LeafNWt (kg ha ⁻¹)	(% % ⁻¹)
Water content at field capacity	1.23	Nitrogen extinction coefficient	-0.82
Water content at wilting point	-0.81	Biomass carbon fraction	0.62
Nitrogen extinction coefficient	-0.68	Minimum Leaf Nitrogen Weight Concentration	-0.55
		Water content at field capacity	0.53

5.3.3 Model integration with remote sensing observations

Model reset on observation dates

A first method (A) for model adjustment with remote sensing observations was to reset model variables on each observation date with the value estimated from remote sensing.

The canopy variables derived from remote sensing (LAI and/or canopy nitrogen status) were compared with simulated values, and if deviations exceeded 10 % (the maximum error in traditional field observation techniques), the variables in the simulation model were adjusted to the remote sensing estimate. This was done for LAI and canopy nitrogen contents separately, as well as for their combination (Table 5.3, scenarios 1-6).

Table 5.3 Scenario specifications for integration of remote sensing estimates of leaf area index (♣) and canopy nitrogen contents (♣n), together with options for the adjustment of internal dry matter and nitrogen ratios for shoot and roots (%) and the adjustment of the soil inorganic nitrogen pool (Sn).

Scenario	Adjusted variables			
	Leaf area index ♣	Canopy nitrogen ♣n	DMShoot/DMRoot ratios %	Soil nitrogen pool Sn
0	-	-	-	-
1	+	-	-	-
2	-	+	-	-
3	+	+	-	-
4	+	-	-	+
5	-	+	-	+
6	+	+	-	+
7	+	-	+	-
8	-	+	+	-
9	+	+	+	-
10	+	-	+	+
11	-	+	+	+
12	+	+	+	+

The 0-scenario was used for comparison with other scenarios.

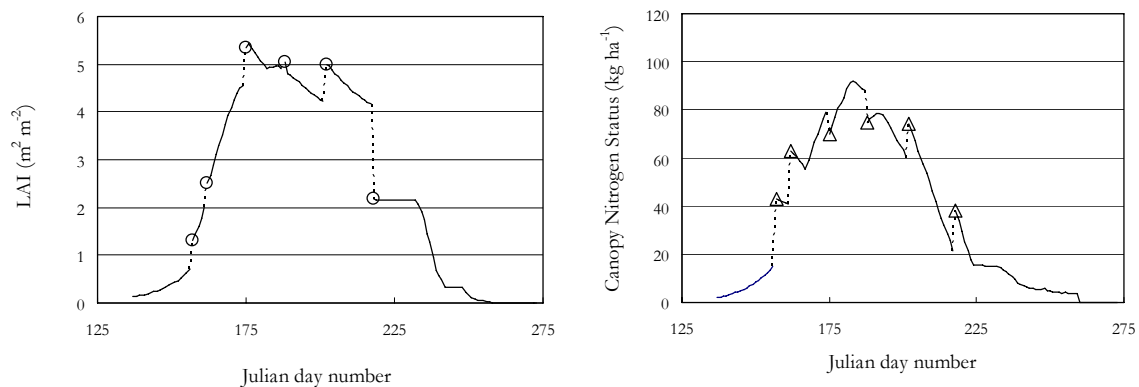


Figure 5.1 Example of method A (potato 1997 at 200 kg N ha⁻¹) for the integration of leaf area index values estimated from remote sensing observations (○, m² m⁻², scenario 10) and for the integration of canopy nitrogen values estimated from remote sensing observations (Δ, kg ha⁻¹, scenario 11). Solid line represents simulated values; dashed lines represent the run-time calibration ('model-reset').

An additional strategy was introduced to evaluate the effect of synchronizing internal crop balances between root/shoot dry matter and root/shoot nitrogen contents (Table 5.3, scenarios 7-12). These balances govern crop nitrogen demand and dry matter partitioning during crop growth, and should, in principle, not be disturbed when resetting individual model variables. This phenomenon was acknowledged by Boegh *et al.* (2004) who, for the 1st remote sensing observation and LAI adjustment date, synchronized all vegetation parameters in order to maintain the congruity of the model canopy representation. Afterwards at subsequent satellite passages, only LAI was adjusted. In our approach we synchronize root and shoot dry matter (including maintaining the ratio between dry matter in stems and leaves) and we synchronize the aboveground and belowground nitrogen contents (including the ratio between nitrogen contents in stems and leaves). In Figure 5.1 an example of method A is given for the integration of LAI (scenario 10) and canopy nitrogen values (scenario 11).

By following this synchronization approach, it is possible that during run-time calibration scenarios an additional nitrogen demand is created from the modelled soil system (if canopy nitrogen content derived from remote sensing exceeded the simulated value). If this occurred, it was taken from the soil inorganic nitrogen pool. Alternatively, 'surplus' nitrogen is then returned to the modelled soil system (if canopy nitrogen content from remote sensing was below the simulated value). These situations and their consequences were examined in scenarios 4-6 and 9-12 (Table 5.3).

The 0-scenario (running the simulation model without integration of remote sensing observations) was used for comparison with the other scenarios.

Model interpolation between observation dates

In method (B) of model integration with remote sensing observations, canopy variables were reset on observation dates and interpolated between those dates (Figure 5.2), as

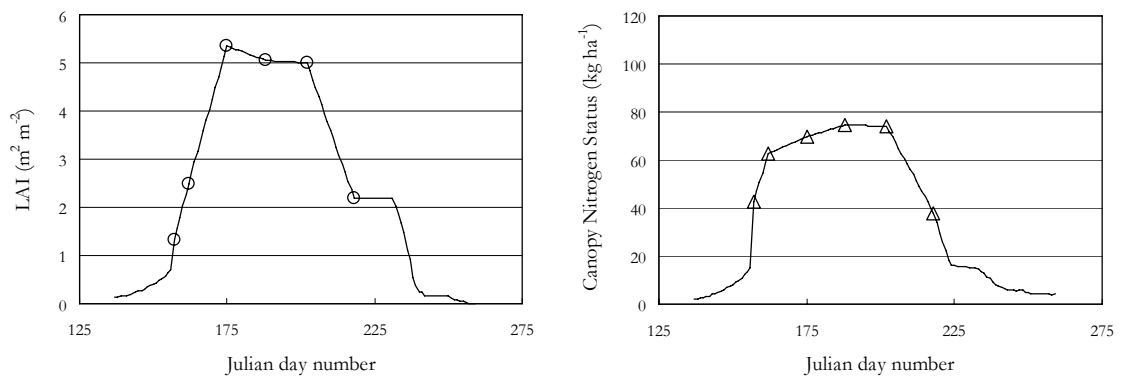


Figure 5.2 Example of method B (potato 1997 at 200 kg N ha⁻¹) for the integration and interpolation of leaf area index values estimated from remote sensing observations (\circ , m² m⁻², scenario 10) and for the integration and interpolation of canopy nitrogen values estimated from remote sensing observations (Δ , kg ha⁻¹, scenario 11). Solid line is simulated to 1st remote sensing estimate, and from last remote sensing estimate; values in between are interpolated between remote sensing estimates.

the frequency and timing of remote sensing observations allowed reconstructing the dynamics of LAI and canopy nitrogen content throughout the growing season. Model accuracy will be reduced, if this method (B) is applied at observation frequencies that do not allow reconstructing the dynamics of LAI and canopy nitrogen content adequately. The consequences of reduced observation frequencies for this method will be described in a future paper (Jongschaap, 2006). All scenarios in Table 5.3 were used for integration method B.

In method B, simulation proceeds until the 1st remote sensing observation date, after which the relevant variables are derived from interpolation between observations, and so forth. After the last remote sensing observation, simulation is resumed until crop harvest.

5.3.4 Evaluation procedure

The integration methods A and B, each comprising 12 scenarios, were evaluated by calculating the Root Mean Square Errors (RMSE) of the simulated results against field measurements. LAI (m² m⁻²) and canopy nitrogen contents (kg ha⁻¹) were selected as important crop characteristics, as they govern the light interception and canopy photosynthesis processes. In addition, nitrate contents (kg ha⁻¹) in the top 0.60 m of the soil profile (i.e. potato root zone) were evaluated. Soil inorganic nitrogen content cannot be estimated directly from remote sensing, but is an important characteristic both for management (fertilization) and for environmental impact, such as the risk of pollution.

5.4 Results and discussion

5.4.1 Simulation results

Validation results for 1997 without the use of remote sensing information (0-scenario) can be read from Table 5.4 and Figure 5.3. Model performance for LAI and canopy nitrogen content is satisfactory (low RMSE) for large parts of the growing season, especially in the early growth phase. LAI simulations deviated from reality in the later stages when leaf senescence was increasing. Canopy nitrogen uptake is simulated satisfactorily, although with a slight lag in the early phase, while translocation is overestimated in the final growth phase. Soil inorganic nitrogen is simulated most accurately towards the end of the growing season, when the model ‘catches up’ with the observed values. The step increase in soil inorganic nitrogen around day 107 reflects the fertilizer applications (Figure 5.4).

5.4.2 Remote sensing estimates of LAI and canopy nitrogen contents

Estimates of LAI from WDVI relations were satisfactory, when a distinction was made between early and late phases of potato growth ($r^2=0.87$), although LAI estimates were somewhat too high, which might have been avoided if WDVI relations would have been calibrated on the dataset. The current procedure reflects situations where no extra data are available for such calibrations.

Canopy nitrogen contents were satisfactorily estimated from red edge position relations ($r^2=0.82$), although field observations were higher at mid-season. Interference of high leaf area indices might have caused the underestimation, as these interact with canopy nitrogen estimations using red edge position values.

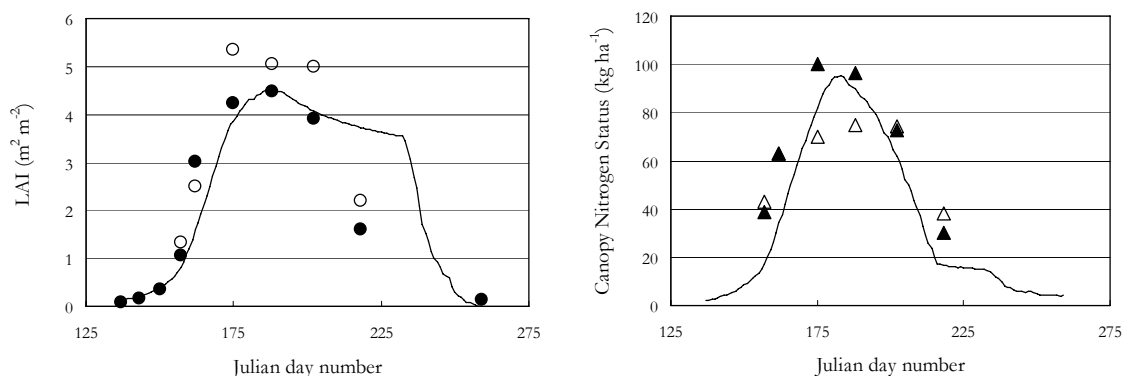


Figure 5.3 0-scenario (see text for explanation) simulation results (solid line) for potato trial in 1997 with fertilizer application of 200 kg N ha^{-1} at planting, with observed values (solid) and remote sensing estimates (open) for leaf area index (\circ, \bullet ; $\text{m}^2 \text{ m}^{-2}$) and canopy nitrogen content (Δ, \blacktriangle ; kg ha^{-1}).

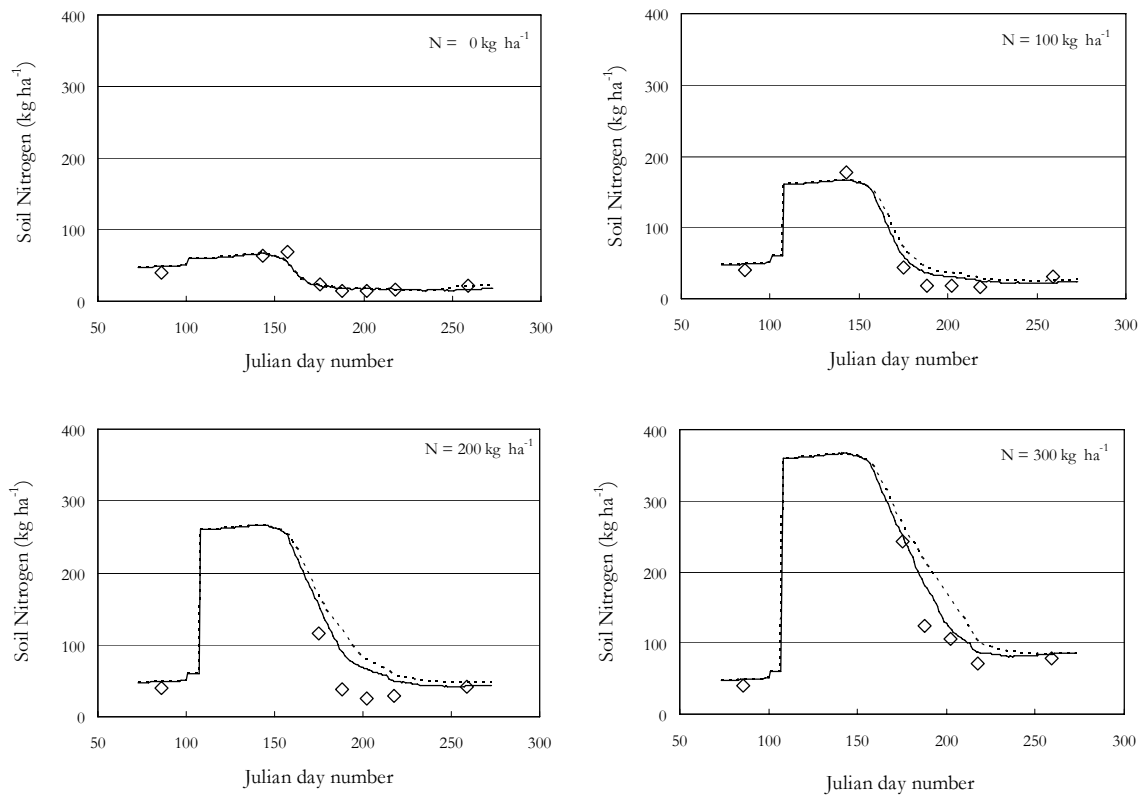


Figure 5.4 Observed (\diamond) and simulated inorganic nitrogen content (kg N ha^{-1}) over top 0.60 m of soil profile for 0-scenario (---) and best integration scenario (B7 —) (see text for explanation). Fertilization treatments are indicated in topright of each graph.

5.4.3 Method A: Integration of remote sensing observations at observation dates

Introduction of remote sensing estimates at observation dates (method A) improved simulation accuracy in the majority of scenarios, but not in all. Table 5.4 summarizes the scenario results for method A. If in a column, the number between parentheses is lower than 100 %, the scenario produced better results than the simulation model alone (scenario 0) and thus validates the hypothesis of this study. Resetting LAI only, improved simulation results for all selected variables under all scenarios. Resetting canopy nitrogen content only, improved canopy nitrogen simulations, but reduced simulation accuracy for LAI and soil nitrogen. Integrating canopy nitrogen or integrating LAI alone resulted in similar improvements for model accuracy of canopy nitrogen simulations. The reason for this is that the leaf nitrogen concentration (%) was maintained at changing LAI values, thereby proportionally changing the canopy nitrogen content (kg ha^{-1}). Resetting LAI and canopy nitrogen content simultaneously, improved simulation accuracy for all selected variables, although less than for LAI only. Synchronizing the root/shoot dry matter and nitrogen ratios (scenarios 7-12) hardly affected the accuracy of LAI estimates, but resulted in slightly higher accuracy of soil

Table 5.4 *A-scenario results (reset on remote sensing observation dates) expressed as Root Mean Square Error (RMSE) of leaf area index ($m^2 m^{-2}$), canopy nitrogen ($kg ha^{-1}$) and soil inorganic nitrogen over first 0.60 m of soil profile ($kg ha^{-1}$).*

Scenario	Integration ^{a)}				Leaf area index ($n=40$)		Canopy nitrogen ($n=34$)		Soil inorganic nitrogen ($n=27$)	
	♣	♣ _n	%	Sn						
0	-	-	-	-	0.84	(100)	13.7	(100)	30.4	(100)
1	+	-	-	-	0.61	(73)	12.2	(89)	24.1	(79)
2	-	+	-	-	0.86	(102)	12.0	(88)	33.3	(110)
3	+	+	-	-	0.61	(73)	12.0	(88)	26.0	(86)
4	+	-	-	+	0.61	(73)	12.2	(89)	24.2	(80)
5	-	+	-	+	0.85	(101)	12.0	(88)	34.7	(114)
6	+	+	-	+	0.61	(73)	12.0	(88)	29.3	(96)
7	+	-	+	-	0.61	(73)	12.7	(93)	23.3	(77)
8	-	+	+	-	0.85	(101)	12.0	(88)	33.3	(110)
9	+	+	+	-	0.61	(73)	12.0	(88)	24.9	(82)
10	+	-	+	+	0.61	(73)	12.7	(93)	23.3	(77)
11	-	+	+	+	0.85	(101)	12.0	(88)	34.7	(114)
12	+	+	+	+	0.61	(73)	12.0	(88)	28.9	(95)

The 0-scenario is simulation run without forcing remote sensing variables. Numbers in parenthesis refer to relative value of RMSE (%) compared to 0-scenario (100 %).

^a Integration scenarios: + (integrated) and - (omitted). ♣ = Leaf area index integration, ♣_n = canopy nitrogen integration, % = synchronizing internal dry matter and nitrogen balances, Sn = adjusting soil inorganic nitrogen pools

inorganic nitrogen estimates compared to scenarios 1-6, where synchronization of root/shoot dry matter and nitrogen ratios were omitted.

Adjusting the soil inorganic nitrogen pools by putting back crop surplus nitrogen or by uptake of crop shortage nitrogen (scenarios 4-6, 10-12) reduced simulation accuracy for soil inorganic nitrogen, without affecting LAI and canopy nitrogen estimates.

When integrated together, LAI estimates and canopy nitrogen estimates gave the highest accuracy for soil inorganic nitrogen simulations if internal root/shoot dry matter and nitrogen ratios were synchronized. When the soil inorganic nitrogen pool was adjusted in addition, accuracy was lower, although more accurately than without any re-adjustment.

5.4.4 Method B: Integration of interpolated remote sensing observations

In general, method B (integration of interpolated remote sensing observations) showed higher RMSE values (i.e. lower accuracy) for LAI, canopy nitrogen content and soil inorganic nitrogen content than method A (Table 5.5).

Table 5.5 B-scenario results (interpolation between remote sensing observation dates) expressed as Root Mean Square Error (RMSE) of leaf area index ($m^2 m^{-2}$), canopy nitrogen ($kg ha^{-1}$) and soil inorganic nitrogen over first 0.60 m of soil profile ($kg ha^{-1}$).

Scenario	Integration ^{a)}				Leaf area index ($n=40$)		Canopy nitrogen ($n=34$)		Soil inorganic nitrogen ($n=27$)	
	♣	♣ _n	%	Sn						
0	-	-	-	-	0.84	(100)	13.7	(100)	30.4	(100)
1	+	-	-	-	0.62	(74)	14.1	(103)	21.7	(71)
2	-	+	-	-	0.90	(107)	12.0	(88)	56.8	(187)
3	+	+	-	-	0.61	(73)	12.0	(88)	41.6	(137)
4	+	-	-	+	0.62	(74)	14.1	(103)	21.7	(71)
5	-	+	-	+	0.86	(102)	12.0	(88)	38.3	(126)
6	+	+	-	+	0.61	(73)	12.0	(88)	34.8	(114)
7	+	-	+	-	0.62	(74)	15.4	(112)	20.9	(69)
8	-	+	+	-	0.90	(107)	12.0	(88)	56.8	(187)
9	+	+	+	-	0.61	(73)	12.0	(88)	39.0	(128)
10	+	-	+	+	0.62	(74)	15.4	(112)	20.9	(69)
11	-	+	+	+	0.86	(102)	12.0	(88)	38.3	(126)
12	+	+	+	+	0.61	(73)	12.0	(88)	35.7	(117)

The 0-scenario is simulation run without forcing remote sensing variables. Numbers in parentheses refer to relative value of RMSE (%) compared to 0-scenario (100 %).

^a Integration scenarios: + (integrated) and - (omitted). ♣ = Leaf area index integration, ♣_n = canopy nitrogen integration, % = synchronizing internal dry matter and nitrogen balance, Sn = adjusting soil inorganic nitrogen pools

Resetting LAI only increased simulation accuracy, especially for soil inorganic nitrogen content, especially if root/shoot dry matter and nitrogen ratios were synchronized, and soil inorganic pools were adjusted. Canopy nitrogen content estimates were less accurate, whereas they were positively affected in method A. Resetting canopy nitrogen only, never increased model accuracy for LAI and soil inorganic nitrogen. Resetting both variables simultaneously reduced accuracy of soil inorganic nitrogen estimates. Synchronizing root/shoot dry matter and nitrogen balances had little effect on the accuracy of leaf area and canopy nitrogen estimates, whereas soil inorganic nitrogen estimates were slightly higher in accuracy.

Adjusting soil nitrogen pools increased the accuracy of soil inorganic nitrogen estimates, both without and with synchronized internal root/shoot dry matter ratios (scenarios 4-6 and 10-12 vs. 1-3 and 7-9).

5.5 Discussion

This paper illustrates a method to integrate frequent remote sensing observations with a mechanistic and dynamic crop growth model and apply run-time calibration of LAI and canopy nitrogen content. It should be noted that when remote sensing estimates of model variables are used to redirect the model, the effect on other model variables should be studied. Boegh *et al.* (2004) synchronized all model vegetation parameters at the 1st remote sensing observation date to maintain canopy congruity of the model representation. In our study, this approach was extended to subsequent remote sensing estimates of LAI and canopy nitrogen contents, including the daily interpolation of LAI and canopy nitrogen contents in between observation dates.

The results of this study show that run-time adjustment of LAI by remote sensing estimates in a mechanistic and dynamic crop growth simulation model, increases simulation accuracy, while simultaneous adjustment of canopy nitrogen content reduces this accuracy. These results may be specific for the type of model used. In *Rotask* 1.0, as in many other crop models, dry matter accumulation is driven by light interception of the canopy. Canopy nitrogen content plays a less significant role, as it has no direct feedback on dry matter production, except that it may accelerate leaf senescence, if it falls below a threshold level.

Maintaining internal balances (both dry matter and nitrogen) in the canopy results in higher simulation accuracies for soil inorganic nitrogen simulations and LAI and less simulation accuracies for canopy nitrogen contents, for both method A and method B. This may be explained by the fact that crop growth in favourable and less favourable conditions follows a well-balanced growth pattern for roots and shoots (Brouwer, 1993). Hence, higher LAI values are associated with higher stem and root dry weights, and *vice-versa*. However, in extreme situations, such as hailstorms, fires, and the occurrence of pests and diseases, the functional balance may not be maintained. The simulation model in this study was not designed to simulate re-growth after such events.

This study has shown that combining crop growth simulation models with remote sensing observations can increase simulation accuracy of environmental variables that can not directly be derived from remote sensing, such as soil inorganic nitrogen content.

For situations where model calibration is impossible, because of lack of ground truth data, interpolated values of remote sensing observations may be used as forcing functions in dynamic simulation models, to increase simulation accuracies of other variables, such as e.g., soil inorganic nitrogen contents.

If remote sensing and field observations are taken on the same day, as in the experiments reported in this paper, the calculated accuracy (of the simulated variable, which reflects the remote sensing estimate after a reset) will result in the accuracy of the remote sensing estimation method and not in the accuracy of the simulation model. It would therefore be more interesting to evaluate the accuracy on other model variables that are not estimated by remote sensing, such as soil inorganic nitrogen content.

5.6 Conclusions

It may be concluded that introduction of field-based remote sensing observations for run-time adjustment of mechanistic and dynamic crop growth simulation models enhances simulation accuracy of important variables in precision agriculture (such as LAI, canopy nitrogen status and soil inorganic nitrogen content). More specifically:

- To estimate canopy nitrogen content, best results are obtained by forcing LAI on the simulation model by resetting it on observation dates. This only holds, if the simulation model uses LAI as main driver for radiation interception and dry matter production. Different type models may benefit from other run-time adjustment variables.
- To estimate soil inorganic nitrogen content, best results are obtained by forcing both, LAI and canopy nitrogen content on the simulation model, and maintaining root/shoot ratios for dry matter and nitrogen content.
- Temporal interpolation of LAI and canopy nitrogen contents estimated by remote sensing between observation dates does not improve simulation accuracy, if observation frequencies are low. In these cases, simulation between remote sensing observations remains necessary.

5.7 Acknowledgements

The Dutch Ministry of Agriculture, Nature Management and Fisheries financed this project through their programmes on precision agriculture. I am grateful to Prof. Dr. Steven M. de Jong and Prof. Dr. Herman van Keulen for useful comments on the manuscript. I am grateful to the anonymous reviewers for reviewing this manuscript. Further acknowledgements are for Dr. ir. Remmie Booijt† and Dik Uenk of *Plant Research International*, who were in charge of the potato experiments.

5.8 References

- Boegh, E., M. Thorsen, M.B. Butts, S. Hansen, J.S. Christiansen, P. Abrahamsen, C.B. Hasager, N.O. Jensen, P. van der Keur, J.C. Refsgaard, K. Schelde, H. Soegaard, A. Thomsen, 2004.
Incorporating remote sensing data in physically based distributed agro-hydrological modelling. *J. Hydrol.* 287, 279–299
- Bouman, B.A.M., 1992.
Accuracy of estimating the leaf area index from vegetation indices derived from crop reflectance characteristics, a simulation study. *Int. J. Rem. Sens.* 13, 3069-3084.

† deceased

- Bouman, B.A.M., D. Uenk, A.J. Haverkort, 1992a.
The estimation of ground cover of potato by reflection measurements. *Pot. Res.* 35, 111-125.
- Bouman, B.A.M., H.W.J. van Kasteren, D. Uenk, 1992b.
Standard relations to estimate ground cover and LAI of agricultural crops from reflectance measurements. *Eur. J. Agron.* 1, 249-262.
- Bouman, B.A.M., H. van Keulen, H. van Laar, R. Rabbinge, 1996.
The 'School of de Wit' crop growth simulation models: A pedigree and historical overview. *Agric. Syst.* 52, 171-198.
- Brouwer, R., 1993.
Functional equilibrium: sense or nonsense? *Neth. J. Agric. Sci.* 31, 335-348.
- Clevers, J.G.P.W., 1989.
The application of a weighted infrared-red vegetation index for estimating Leaf Area Index by correcting for soil moisture. *Rem. Sens. Environ.* 29, 25-37.
- CropScan™, 1993.
Multi-Spectral Radiometer (MSR): Users manual and technical reference, CropScan™, Rochester, U.K.
- Guyot, G., F. Baret, D.J. Mayor, 1988.
High spectral resolution: Determination of spectral shifts between the red and the near infrared. *Int. Arch. of Photogr. and Rem. Sensing* 27, 750-760.
- Hillyer, C., J. Bolte, F. van Evert, A. Lamaker, 2003.
The *ModCom* modular simulation system. *Eur. J. Agron.* 18, 333-343.
- Ittersum, M.K. van, P.A. Leffelaar, H. van Keulen, M.J. Kropff, L. Bastiaans, J. Goudriaan, 2003.
On approaches and applications of the Wageningen crop models. *Eur. J. Agron.* 18, 201-234.
- Jones, J.W., B.A. Keating, C.H. Porter, 2001.
Approaches to modular model development. *Agric. Syst.* 70, 421-443.
- Jongschaap, R.E.E., 1996.
Rotask 1.0 - a simulation model for continuous cropping and tillage systems. Reference manual. DLO Institute for Agrobiology and Soil Fertility Research (AB-DLO), Report 70, Haren/Wageningen, the Netherlands, 40 pp. + annexes.
- Jongschaap, R.E.E., 2006.
The effect of LAI and N parameter variability used in run-time calibration of mechanistic and dynamic crop growth simulation models. Chapter 6, pp. 90-109. Ph. D. Thesis, Wageningen University, Wageningen, the Netherlands, 130 pp.
- Jongschaap, R.E.E., R. Booij, 2004.
Spectral measurements at different spatial scales in potato: relating leaf, plant and canopy nitrogen status. *Int. J. Appl. Earth Obs. Geoinform.* 5, 205-218.
- Jongschaap, R.E.E., P. Henstra, J. Verhagen, B. Rutgers, 2002.
Calibration, temporal and spatial application of the *PlantSys* 1.0 simulation model. Integrating forcing methods of remote sensing data. EU-Croma (EVG1-2000-000027), Report D12 and D22, Wageningen, the Netherlands.
- Keating, B.A., P.S. Carberry, G.L. Hammer, M.E. Probert, M.J. Robertson, D. Holzworth, N.I. Huth, J.N.G. Hargreaves, H. Meinke, Z. Hochman,

- G. McLean, K. Verburg, V. Snow, J.P. Dimes, M. Silburn, E. Wang, S. Brown, K.L. Bristow, S. Asseng, S. Chapman, R.L. McCown, D.M. Freebairn, C.J. Smith, 2003.
An overview of *APSIM*, a model designed for farming systems. *Eur. J. Agron.* 18, 267-288.
- Landau, S., R.A.C. Mitchell, V. Barnett, J.J. Colls, J. Craigon, K.L. Moore, R.W. Payne, 1998.
Testing winter wheat simulation models' predictions against observed UK grain yields. *Agric. Forest Meteorol.* 89, 85-99.
- MacKerron, D.K.L., A.J. Haverkort (Eds.), 2004.
Decision support systems in potato production: bringing models to practice. Wageningen Academic Publ., Wageningen, the Netherlands, 238 pp.
- Meurs, E.J.J., A.D.H. Kreuzer, 1995.
Measuring equipment in crop physiology research (in Dutch). DLO Institute for Agrobiology and Soil Fertility Research (AB-DLO), Note 14, Wageningen, the Netherlands, 77 pp.
- Paz, J.O., W.D. Batchelor, P. Pedersen, 2003.
WebGro - A Web-Based Soybean Management Decision Support System. *Agron. J.* 96, 1771-1779.
- Prévot, L., H. Chauki, D. Troufleau, M. Weiss, F. Baret, N. Brisson, 2003.
Assimilating optical and radar data into the STICS crop model for wheat. *Agronomie* 23, 297-303.
- Supit, I., A.A. Hooijer, C.A. van Diepen, 1994.
System Description of the *WOFOST* 6.0 Crop Simulation Model Implemented in CGMS, Volume 1: Theory and Algorithms. An Agricultural Information System for the European Community, EUR 15956 EN, 144 pp.
- Uenk, D., B.A.M. Bouman, H.W.J. van Kasteren, 1992.
Reflection measurements in arable crops (In Dutch). DLO Centre for Agrobiological Research (CABO-DLO), Note 156, Wageningen, the Netherlands, 56 pp.
- Yin, X., J. Verhagen, R. Jongschaap, A. Schapendonk, 2001.
A model to simulate responses of the crop-soil system in relation to environmental change. *Plant Research International*, Note 129, Wageningen, the Netherlands, 46 pp.

Chapter 6

The effect of LAI and N parameter variability used in run-time calibration of mechanistic and dynamic crop growth simulation models

Raymond E.E. Jongschaap

*Wageningen University and Research centre, Plant Sciences Group,
Plant Research International, P.O. Box 16, NL-6700 AA Wageningen, the Netherlands.
Tel.: +31-317-475953; Fax: +31-317-423110; E-mail: raymond.jongschaap@wur.nl*

© 2006 *Ecol. Mod. (submitted)*

6.1 Abstract

Run-time calibration, i.e. adjusting simulation results for field observations of model driving variables during run-time, may allow correcting for deviations between complex mechanistic simulation model results and actual field conditions. Leaf area index (LAI) and canopy nitrogen contents (LeafNWt) are the most important driving variables for these models, as they govern light interception and photosynthetic production capacity of the crop. Remote sensing may provide (spatial) data from which such information can be estimated. How, when and at what frequency such additional information is integrated in the simulation process may have various effects on the simulations. The objective of this study was to quantify the effects of different run-time calibration scenarios for Final Grain Yield (FGY) simulations in order to optimize remote sensing image (RS) acquisition. The *PlantSys* model was calibrated on LAI and LeafNWt for maize in France and used to simulate maize crop growth in Argentina and the USA, for which remote sensing estimates of LAI and leaf chlorophyll contents were available. Leaf chlorophyll data were used to estimate LeafNWt. Due to its structure, the *PlantSys* model was more sensitive to run-time calibration with LeafNWt than with LAI. Run-time calibration with LAI showed the largest effect on FGY before and around flowering, and could mainly be related to maintenance respiration

costs. Run-time calibration with LeafNWt showed the largest effect on FGY at and after flowering and could mainly be related to the change in effective radiation interception due to changes in leaf life-span. The accuracy of LAI estimates showed a major effect on FGY for underestimations but was small in absolute sense. The accuracy of LeafNWt estimates had significant impact at all crop development stages, but was the strongest after flowering where crop growth and nitrogen uptake are less able to recuperate from changes in LeafNWt. In absolute sense, the effect on FGY was as strong as the accuracy of the LeafNWt estimates when applied in the early reproductive stages. Based on these results it was concluded that remotely sensed in-field variability of LAI and LeafNWt is valuable information that can be used to spatially differentiate model simulations. Run-time calibration at sub-field level may lead to more accurate simulation results for whole fields.

Keywords: simulation model, run-time calibration, remote sensing, LAI, nitrogen, maize

6.2 Introduction

Complex mechanistic crop growth simulation models are highly data-demanding and have to be calibrated locally to give accurate and reliable simulation results. Even if these requirements are met, simulation results may deviate from actual field observations for a variety of reasons. Especially when input data are difficult to measure accurately or expensive and laborious to collect, they are easily replaced by expert knowledge, inter- or extrapolated data and/or approximations that give reasonable simulation results, but may still deviate from actual field conditions. Run-time calibration, i.e. adjusting simulation results on the basis of field observations of model driving variables during simulation, allows corrections of such deviations. Such additional information about the crop-soil system may come from conventional field sampling methods, or may be derived from other techniques, such as remote sensing observations that would also directly reveal in-field variability of certain crop and soil characteristics in one overview. With a variable degree of success and at different spatial resolutions, remote sensing has been used to estimate crop and soil characteristics (Thenkabail *et al.*, 2000), such as leaf area index (Clevers, 1989; Bouman, 1992), biomass (Turner *et al.*, 2002), chlorophyll contents (Ma *et al.*, 1996; Jago *et al.*, 1999; Jongschaap and Booij, 2004), and evapotranspiration (Bastiaanssen *et al.*, 2000). Best results are described for hyperspectral imagery, however, these data are not always available, or are too expensive for use at high temporal resolution. Vegetation indices are often derived from observations in the visible domain and for satellite and airborne platforms cloud cover may interfere. Furthermore, high resolution and hyperspectral satellite sensors may have a low overpass frequency, further reducing the chance of obtaining images of the desired objects at regular intervals. Cloud cover is a minor problem for airborne observations that can take place upon request, but frequent flights may be restricted by environmental regulations.

Observation frequency, interval, timing and accuracy of the data used in run-time calibration influence simulation results differentially. The objective of this study was to quantify the effects of different run-time calibration scenarios on simulated Final Grain Yield (FGY), to support optimization of remote sensing image acquisition and for predicting the effects of sub-optimal run-time calibration sets.

Run-time calibration was performed with the *PlantSys* simulation model (Jongschaap, 1996; Jongschaap *et al.*, 2002), applying 5 sequential remote sensing (RS) estimates in the course of the growing season of leaf area index (LAI) and leaf chlorophyll content. Leaf chlorophyll contents were used to calculate canopy nitrogen contents (LeafNWt). *PlantSys* was calibrated for maize growth in France (Jongschaap *et al.*, 2002) and used for maize growth simulations in Argentina and the US, for which remote sensing estimates of LAI and leaf chlorophyll were available. The effects were analyzed of number of integrated RS observations (1-5) for run-time calibration, as well as their timing in the growing season, and of RS estimation accuracy (95 %, 90 %, 75 % and 60 %) on simulated FGYs.

6.3 Material and methods

6.3.1 Field experiments

For model calibration, a field experiment with maize (*Zea mays* L.) was executed in 1999 at Avignon-Montfavet, France at 43° 57' N and 4° 5' E. Fertilizer (15-15-15) at 500 kg ha⁻¹ was applied on 13 March 1999 (DoY 72), i.e. 75 kg ha⁻¹ of the elements N, P and K. Variety DK-604 was sown at 0.8 m between rows (oriented north-south) and 0.115 m between plants on 10 May 1999 (DoY 130) and emerged at a density of 9.32 plants m⁻². In June and July 1999 the maize was irrigated (at a rate of 20 mm) once a week and in August 1999 twice a week to restrict growth reduction due to drought stress. Plants were sampled every 5-7 days (18 times between 27 May and 7 October 1999) for determination of fresh and dry weight of leaves, stems and grains. Leaf area index (m² m⁻²) was recorded just before sampling with LAI-2000 equipment (LI-COR Inc., USA). SPAD-meter (Minolta, USA) readings were taken on June 28 (DoY 178), July 23 (DoY 206) and September 16 (DoY 269). A direct relation between SPAD meter readings and leaf nitrogen contents (LeafNWt, kg ha⁻¹ leaf) was used (Equation 6.1; r²=0.92; Blackmer *et al.*, 1994).

$$\text{LeafNWt} = -1.0244 + 0.0469 \cdot \text{SPAD} \quad (\text{Equation 6.1})$$

Additional experimental data were retrieved from maize experiments, originally designed to relate remote sensing observations to field observations, carried out under similar settings in 1997 and 1998 in 'Blue Earth' Minnesota (43° 45' N, 94° 16' W) in the USA, and in Pergamino (34° 07' S, 60° 09' W) and Pehuaro (36° 09' S, 62° 58' W) in Argentina. From these trials, information was available on planting and harvest dates, maize cultivars, fertilizer application (dates and rates), irrigation (dates and rates),

and some information on soil characteristics. These data are further referred to as the ‘EU Croma database’, named after the project through which these data were made available (Croma, 2002).

Five experimental sites from ‘Blue Earth’ (BLE), eight sites from Pergamino (PG) and six sites from Pehuaro (PH) provided data on leaf area index and chlorophyll contents at different crop development stages. Leaf SPAD measurements (Minolta, USA) were related to leaf chlorophyll contents (LeafChl; $\mu\text{mol m}^{-2}$ leaf; Equation 6.2; $r^2=0.96$; Markwell *et al.*, 1995) and then converted to leaf nitrogen contents (LeafNWt, kg ha^{-1} leaf; Equation 6.3; $r^2=0.83$; Ercoli *et al.*, 1993). This two-step approach was needed because original SPAD values were no longer available in the EU Croma database. As a result, LeafNWt estimates may have been less accurate than LeafNWt estimates in the Avignon dataset.

$$\text{LeafChl} = 10^{\text{SPAD}^{0.265}} \quad (\text{Equation 6.2})$$

$$\text{LeafNWt} = -2.797 + 0.0188 \cdot \text{LeafChl} \quad (\text{Equation 6.3})$$

In this study, average values and standard deviations per plot and per observation date were generated. To study the effect of different run-time calibration frequencies and timing in the growing season, five observation dates were selected: 2 in the vegetative phase; 1 around tasseling/flowering; and 2 in the reproductive phase (Table 6.1).

6.3.2 Simulation model

PlantSys 1.0 is a mechanistic simulation model (Jongschaap *et al.*, 2002), consisting of algorithms based on knowledge of the underlying physical, physiological and biochemical processes that are described in individual modules that can, if required, be replaced by modules with different complexity. The *PlantSys* model combines the *Rotask* simulation model (Jongschaap, 1996) and the crop growth and development approach of Yin *et al.* (2001) and Yin and van Laar (2005). *PlantSys 1.0* is written in Fortran90, and runs in the Fortran Simulation Environment (Version 4) developed by van Kraalingen (1995). For fallow or field crop rotation systems, the model quantifies water fluxes (precipitation, irrigation, run-off, soil evaporation, transpiration and drainage) and nitrogen fluxes (soil organic nitrogen flows, i.e. mineralization/immobilization, mineralization from crop residues, (in-) organic fertilization, wet deposition, leaching and root nitrogen uptake by mass flow and diffusion). Light interception and thermal heat accumulation govern crop growth and development, respectively. Crop nitrogen contents may vary as a result of variations in nitrogen availability, resulting from mineralization, immobilization and fertilizer applications. Management decisions refer to ploughing (date, depth), incorporation of organic fertilizer (date, rate, type), and application of inorganic fertilizer (date, rate, type), sowing (rate, depth), irrigation (date, rate) and harvest (date, method). Crops currently included in the model are

Table 6.1 Observed maize development stages according to Ritchie et al. (1997) and available run-time calibration dates for BLE (Blue Earth, USA), PG and PH (Pergamino and Pebuario, Argentina) sites used in the simulation experiments.

	1	2	3	4	5
Crop Stage ^{a)}	V5 – V7 5 th -7 th leaf	V7 - V9 7 th -9 th leaf	V9 - VT 9 th leaf-tasseling	R1 - R2 - R3 Silking-Blister-Milk	R4 - R5 Dough-Dent
	Vegetative				
Field ID				Reproductive	
BLE 14-18-21-29-36	15-Jun-98	2-Jul-98	17-Jul-98	18-Aug-98	2-Sep-98
PG 01-02	26-Nov-97	16-Dec-97	29-Dec-97	26-Jan-98	17-Feb-98
PG 04	n.a. ^{b)}	16-Dec-97	29-Dec-97	20-Jan-98	n.a.
PG 10	1-Dec-97	23-Dec-97	13-Jan-98	26-Jan-98	17-Feb-98
PG 26	n.a.	28-Nov-97	24-Dec-97	23-Jan-98	11-Feb-98
PG 27	n.a.	8-Jan-98	26-Jan-98	12-Feb-98	n.a.
PG 29	8-Jan-98	23-Jan-98	12-Feb-98	25-Feb-98	19-Mar-98
PG 36	n.a.	23-Jan-98	13-Feb-98	23-Feb-98	11-Mar-98
PH 38	3-Dec-97	n.a.	7-Jan-98	27-Jan-98	10-Mar-98
PH 40	3-Dec-97	17-Dec-97	7-Jan-98	27-Jan-98	9 Feb-98
PH 43	n.a.	16-Dec-97	6-Jan-98	28-Jan-98	n.a.
PH 44-45	3-Dec-97	10-Dec-97	6-Jan-98	28-Jan-98	n.a.
PH 47	2-Dec-97	15-Dec-97	5-Jan-98	2-Feb-98	17-Feb-98
PH 51	2-Dec-97	10-Dec-97	30-Dec-97	19-Jan-98	n.a.

^{a)} V = vegetative phase, R = reproductive phase

^{b)} n.a. = not available

wheat, sugar beet, potato, barley, rape-seed and maize. For the current study, simulations were performed for maize only.

Five categories of input data were used in the model:

- 1) **Control data:** start day and year of simulation, end day and year of simulation, location, output variables,
- 2) **Environmental data,** i.e. meteorological input from local weather stations: daily values of radiation, minimum and maximum temperature, vapour pressure, wind speed and precipitation and nitrogen concentration in precipitation
- 3) **Crop data:** crop type, initial values (at emergence) for LAI and organ dry weights, minimum, optimum and maximum nitrogen concentrations in various crop organs, temperature sums for phenological development stages (emergence, vegetative phase, reproductive phase), base temperatures for phenological development rates, maximum rooting depth and extinction coefficients for radiation
- 4) **Soil data:** soil moisture contents at specific pF-values, soil organic matter pools (stable and labile), initial carbon and organic nitrogen contents, bulk density, and initial inorganic nitrogen content

- 5) **Management data:** decision variables on ploughing, sowing/planting, organic and inorganic fertilizer application, irrigation and harvesting

Potential leaf photosynthesis rates are modelled with interactive effects of intercepted photosynthetic active radiation (PAR), CO₂ levels, canopy nitrogen contents and canopy temperatures (Farquhar *et al.*, 1984; Yin and van Laar, 2005). Potential leaf transpiration rates are coupled with potential photosynthesis rates via the Penman-Monteith equation (Monteith, 1973; Yin and van Laar, 2005). Actual transpiration rates depend on the crop's ability to transpire water from the soil that enters the plant through the roots. Actual leaf photosynthesis rates are proportional to actual/potential transpiration rates. The intercepted PAR_i depends on the incoming PAR₀ and the extinction of PAR in the canopy depending on LAI according to Equation 6.4, with $k_L = 0.65$ as PAR extinction coefficient for maize.

$$PAR_i = PAR_0 \cdot (1 - e^{-k_L \cdot LAI}) \quad (\text{Equation 6.4})$$

In Equation 6.4, the effective (green) LAI results from leaf growth and leaf senescence processes. A vertical nitrogen distribution between a minimum leaf nitrogen concentration deeper in the canopy and a nitrogen extinction coefficient ($k_N = 0.36$; Jongschaap *et al.*, 2002) determine which part of the LAI is effective for light interception. Any 'ineffective' LAI is directed towards the senescent pool (Yin *et al.*; 2000; Yin and van Laar, 2005). This marks the importance of using LAI and LeafNWt for model run-time calibration for the *Plantsys* model.

Output of the model can be selected from all variables in the separate process modules. For the current study, Final Grain Yield (kg ha⁻¹) was selected as dynamic crop growth simulation models are mostly used for yield predictions.

6.3.3 Model sensitivity analysis and model calibration

The sensitivity analysis was tailored to the objective of predicting more accurate values over the growing season for Leaf Area Index (LAI, m² m⁻²), aerial biomass dry matter (ShootWt, kg ha⁻¹), canopy nitrogen contents (LeafNWt, kg ha⁻¹) and grain dry matter (GrainWt, kg ha⁻¹). In addition, two other variables are considered important, Final Grain Yield (FGY, kg ha⁻¹) and Total Nitrogen Uptake (TN_{Upt}, kg ha⁻¹). As the EU Croma database contains values of leaf chlorophyll concentration (µg cm⁻²), canopy nitrogen content was derived from its chlorophyll content (Equation 6.3; Markwell *et al.*, 1995). Sensitivity or responsiveness was expressed as the 'elasticity' of output parameters: change in value of the output parameter per unit change in value of the input parameter, both expressed in percentages (Equation 6.5).

$$E_{FGY} = \left(\frac{FGY^{+err} - FGY^{-err}}{FGY^{err=0}} \right) \cdot \left(\frac{100}{2 \cdot err} \right) \quad (\text{Equation 6.5})$$

The input parameters were varied by -10 % and +10 % ($err = 10\%$) and the elasticity of the selected model output parameters was calculated. The most sensitive input parameters were entered into the calibration procedure that consisted of an optimization procedure to minimize the deviation between simulation results and field measurements of leaf area index, grain weight and final grain weight (Hillyer *et al.*, 2003). Values of the sensitive model input parameters were varied randomly over their biologically plausible range (BPR) until the combination with the lowest Root Mean Square Error (RMSE) was found. After calibration on the detailed dataset of Avignon (1999), calibration was continued on the EU Croma database (for Argentina and the USA) to establish cultivar-specific values for the phenological characteristics Base Temperature (TempBase, °C), Optimum Temperature (TempOptim, °C), Temperature Sum for the Vegetative Phase (TempSumVeg, degree-days) and Temperature Sum for the Reproductive Phase (TempSumGen, degree-days). Meteorological data from (nearby) weather stations were used to calculate temperature sums between sowing, emergence, flowering and maturity dates.

6.3.4 Run-time calibration procedures

The model variables LAI and LeafNWt were used in run-time calibration, the most important drivers for dry matter production in the *PlantSys* model. Both variables influence interception of incoming radiation and hence photosynthesis rates and biomass production. During run-time calibration, simulated values of LAI and LeafNWt were replaced by estimates derived from remote sensing, at maximally five dates during the growing season. Three run-time calibration aspects (A, B and C) were considered in the analysis.

Aspect A: Number of remote sensing observations that was integrated. Run time calibration was performed with 1, 2, 3, 4 and 5 estimates for LAI and LeafNWt.

Aspect B: Timing of the run-time calibrations by varying the observation dates integrated in the run-time calibration procedure. All 32 possible combinations for 5 remote sensing dates were tested (Table 6.1).

Aspect C: The effect of under- and overestimation (5 %, 10 %, 25 % and 40 %) of LAI and LeafNWt that are used in the run-time calibration procedure.

To evaluate the value of a specific remote sensing date (target date) in the run-time calibration procedure, the results of scenarios were associated with weight factors that accounted for the number of remote sensing dates that were integrated, and for the distance between the target observation date and other observation dates in the specific scenario. An example may clarify the weight factor assignment: for target remote sensing date 1 (early vegetative stage), the scenario where only 1 remote sensing image was used (at date 1, obviously) obtained weigh factor 1.00. A scenario with N remote sensing observations (including the target date), obtained a weight factor of $1/N$ in the calculations. Additionally, the distance of the supplemental remote sensing

dates (close by or further away from the target date) was accounted for: scenarios with remote sensing dates next to the target date (at distance 1) obtained a weigh factor $1/2$; at distance 2 it was $1/4$; at distance 3 it was $1/8$ and at distance 4 it was $1/16$. Eventually, the cumulative effects were divided by the cumulative weight factors in order to average the impact of each remote sensing scenario per target date.

As the *PlantSys* model was not designed to simulate the effect of disturbances (such as grazing, mowing, cutting or partial harvesting), a number of other model variables were adjusted in association with LAI adjustment: LeafWt, to maintain specific leaf weight ($\text{m}^2 \text{ leaf g}^{-1} \text{ leaf}$); StemWt, to maintain the leaf/stem ratio ($\text{g leaf g}^{-1} \text{ stem}$) and RootWt, to maintain the shoot/root ratio ($\text{g shoot g}^{-1} \text{ root}$). This approach was suggested by Boegh *et al.* (2004) and successfully applied by Jongschaap (2006).

The run-time calibration procedures were evaluated by the elasticity of the simulated FGYs with respect to the accuracy of the remote sensing observations (Equation 6.5).

With E_{FGY} = Elasticity (-); FGY_{err} = Final Grain Yield (kg ha^{-1}) at accuracy level *err* (%) for remote sensing estimates of LAI and/or LeafNWt; *err* = error in remote sensing estimate (0, 5, 10, 25 or 40 %). For analysis of the underestimates and overestimates in LAI and LeafNWt used in run-time calibration at different crop development stages, FGY results were compared with those from simulations where LAI and LeafNWt were accurately estimated ($err=0$).

6.4 Results and discussion

6.4.1 Model sensitivity analysis and calibration

Table 6.2 shows the results of the sensitivity analysis using Equation 6.5. The model variables LAI ($\text{m}^2 \text{ m}^{-2}$), LeafNWt (kg ha^{-1}), ShootWt (kg ha^{-1}) and GrainWt (kg ha^{-1}) were most sensitive to variations in soil moisture characteristics and in phenological characteristics.

Soil moisture characteristics affect moisture availability to the crop, which is linearly related to dry matter production, and phenological characteristics affect the duration of the vegetative and reproductive phases. These input parameters were either measured at the location, or could be estimated from secondary data for each site and cultivar, by taking into account soil texture, organic matter contents, emergence dates, flowering dates, maturity dates and meteorological data. The most sensitive input parameters (Table 6.3) were varied over their biologically plausible range (BPR) and were calibrated to field observations for Avignon (Fr).

Figure 6.1 and Figure 6.2 illustrate simulated model results with field observations for Avignon (calibration) and Argentina/USA (validation). Both, LAI simulations (Figure 6.1) and LeafNWt simulations (Figure 6.2) gave satisfactory results with high correlation coefficients (r^2) and acceptable Root Mean Square Errors (RMSE). In the datasets, the standard deviations for field observations of LAI range from 0.2-0.7 $\text{m}^2 \text{ m}^{-2}$ and for approximations of LeafNWt from 0.5-5.0 kg ha^{-1} . In general, LeafNWt

Table 6.2 Sensitivity analysis results (Equation 6.5; Elasticity, -) for input parameters having the largest effect on seasonal simulation values (at 18 comparison dates) for LAI ($m^2 m^{-2}$), LeafNWt ($kg ha^{-1}$), ShootWt ($kg ha^{-1}$) and GrainWt ($kg ha^{-1}$).

LAI ($m^2 m^{-2}$)	LeafNWt ($kg ha^{-1}$)	ShootWt ($kg ha^{-1}$)	GrainWt ($kg ha^{-1}$)				
WC	1.23	ExtCoefN	-0.82	WC	2.28	TempSum	-3.72
Fieldcapacity				Fieldcapacity		Veg	
WC	-0.81	BiomassCFract	0.61	WC	-1.14	TempBase	-1.70
WiltingPoint				WiltingPoint			
ExtCoefN	-0.68	LeafNWtConc2	-0.55	BiomCFract	-0.68	TempOptim	1.20
		Min					
		WC	0.53			NitDemRate	0.62
		Fieldcapacity				Base	
						WC	-0.58
						Fieldcapacity	
						InitSeedN	-0.51
						Conc1	

Table 6.3 Biologically Plausible Range (Min-Max, with references) and resulting calibrated values (V_{cal}).

Input parameter	Min	Max	V_{cal}	Unit	Reference
BiomassCFract	0.3	0.6	0.4249	$g g^{-1}$	Yin <i>et al.</i> (2001)
ExtCoefN	0.1	0.8	0.3600	m^{-1}	Vleeshouwers and Jongschaap (2001)
InitSeedNConc1	0.01	0.025	0.0117	$g g^{-1}$	Ta and Weiland (1992a, 1992b); Sibma (1987)
LeafNWtConc2Min	0.1	0.6	0.3226	$g m^{-2}$	Lemaire <i>et al.</i> (1997)
NitDemRateBase	0.0	0.5	0.1954	$g m^{-2} d^{-1}$	Yin <i>et al.</i> (2000, 2001)
TempBase	4.	10.	7.9316	$^{\circ}C$	Sibma (1987); Coelho and Dale (1980); McMaster and Wilhelm (1997)
TempOptim	26.	32.	28.0	$^{\circ}C$	Boons-Prins <i>et al.</i> (1993); Coelho and Dale (1980)

seems to be slightly underestimated in the model, which may be due to the fact that the approximation between SPAD meter readings and LeafNWt (Equation 6.1; Blackmer *et al.*, 1994) could not be calibrated on the dataset, or that vertical nitrogen distribution may not be fully accounted for in leaf chlorophyll readings (Vleeshouwers and Jongschaap, 2001; Jongschaap and Booij, 2004). This study put emphasis on the relative effect of run-time calibration methods rather than considering absolute values. Therefore, these standard deviations will not have an important impact on the outcome of this study.

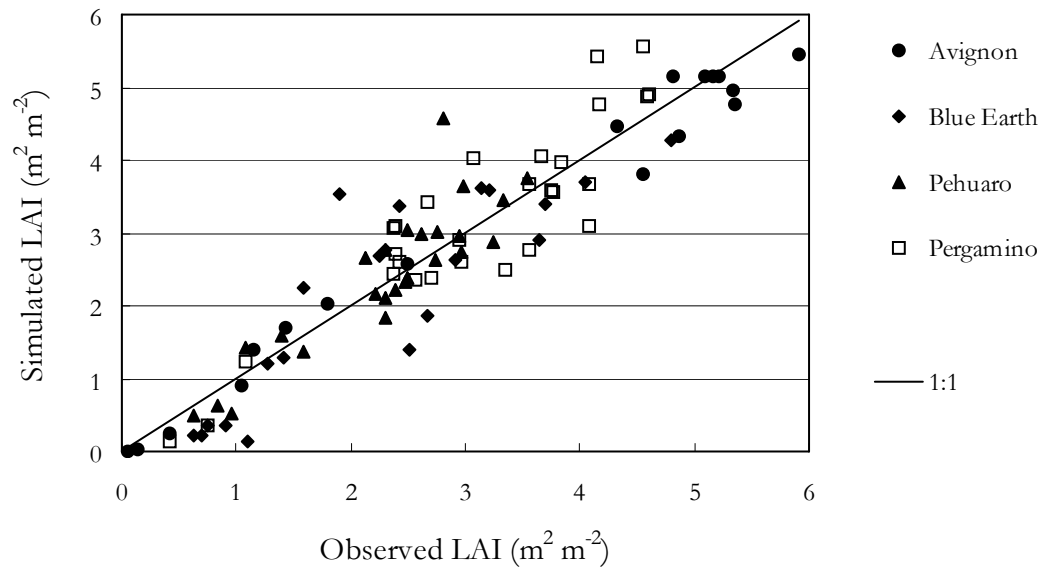


Figure 6.1 Model performance for leaf area index simulation (LAI; m² m⁻²) ($n = 128$; $r^2 = 0.96$; RMSE = 0.6 m² m⁻²).

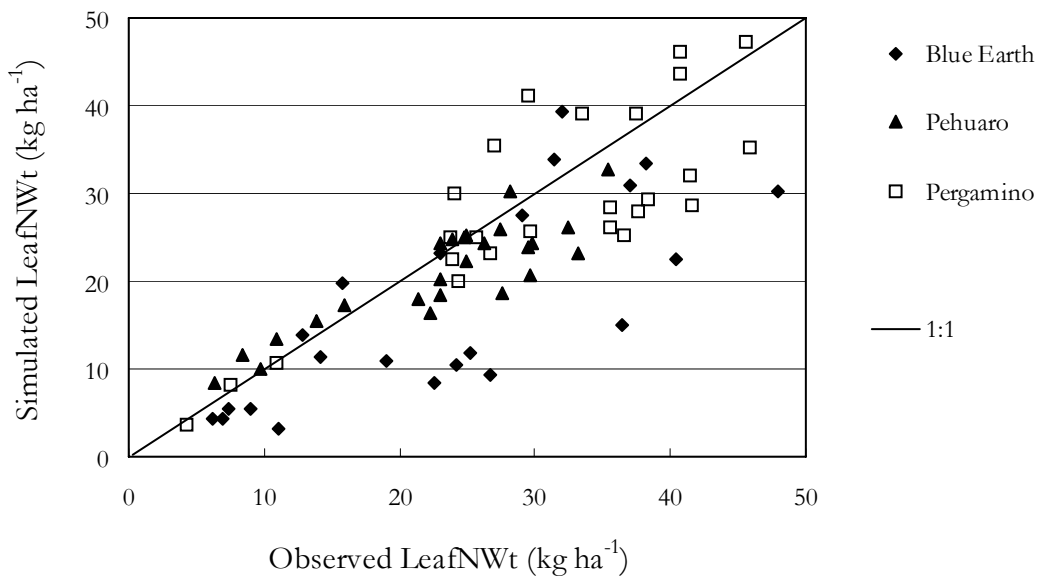


Figure 6.2 Model performance for leaf nitrogen content simulation (LeafNWt; kg ha⁻¹) ($n = 116$; $r^2 = 0.89$; RMSE = 9.6 kg ha⁻¹).

6.4.2 Scenario simulations

The *PlantSys* model was run for 32 remote sensing date combinations (frequencies), for 20 accuracy level combinations (ranging from -40 % to +40 %), for 3 calibration variables (LAI, LeafNWt and LAI + LeafNWt) and for 18 plots in Argentina and the USA, resulting in 34,560 simulation runs. The output variable FGY was used to calculate E_{FGY} (Equation 6.5).

6.4.3 Run-time calibration frequency

The frequency of remote sensing observations (1-5) of LAI and LeafNWt used in run-time calibration showed a distinct effect on E_{FGY} (Figure 6.3). The effects were averaged over the accuracy scenarios (0, 5, 10, 25 and 40 %) and for all possible combinations of a specific remote sensing frequency. LeafNWt calibrations showed a much stronger effect on E_{FGY} than LAI calibrations and standard deviations for E_{FGY} declined with increased remote sensing frequency.

Run-time calibration for both, LAI and LeafNWt were positively correlated with E_{FGY} . Calibration on LAI showed a linear decline in E_{FGY} with increasing remote sensing frequency, whereas calibration on LeafNWt showed an increase in E_{FGY} , but following the ‘law of diminishing returns’.

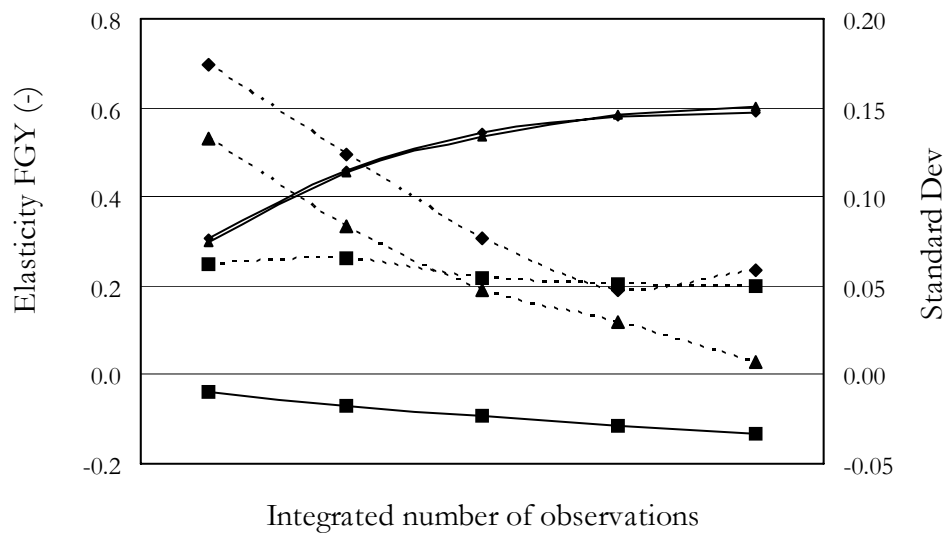


Figure 6.3 Elasticity (Equation 6.5; -) of Final Grain Yield (E_{FGY}) (solid lines) and standard deviation (dashed lines) of calibration variables LAI (■), LeafNWt (▲) and LAI + LeafNWt (◆) as function of the number of remote sensing dates integrated in the run-time calibration procedure (x-axis). Values are averages for all accuracy classes (5, 10, 25 and 40 %) and for all frequency distributions applied.

Increasing LeafNWt extends leaf life, which results in a prolonged period of light interception, especially in the last part (reproductive phase) of the maize growth cycle, and thus in higher grain yield. Higher LAI *persé*, not necessarily translates into higher production in the *PlantSys* model, as leaf nitrogen content and the vertical nitrogen distribution determine where in the canopy the incoming radiation is effectively intercepted.

In the majority of the simulated cases, a change in LAI did not affect the light interception significantly, but it did influence the average amount of crop biomass that had to be maintained by the crop. A reduction in leaf biomass with a small penalty on light interception may result in more carbohydrates that are available for grain yield formation as less carbohydrates are needed for crop maintenance respiration. Likewise, an increase in leaf biomass showed, on average, no significant change in light interception, but increased the amount of carbohydrates that were respired through maintenance respiration. As a result, less carbohydrates were available for grain yield formation, which is expressed in the negative effect of LAI increase on E_{FGY} . Calibrating both LAI and LeafNWt at the same time gave about the same results as a run-time calibration on LeafNWt alone. Between the variables, LeafNWt calibration has the largest effect on E_{FGY} and therefore, run-time calibration with LAI + LeafNWt is omitted from further analyses.

6.4.4 Run time calibration timing and accuracy

This study also investigated the timing of run-time calibration (or choice of calibration date in the growing season) with LAI and LeafNWt. Results showed different remote sensing acquisition moments for realizing maximum effect on E_{FGY} (Figure 6.4). Run-time calibration with LAI maximally affected E_{FGY} during the late vegetative stages and during tasseling/flowering, whereas run-time calibration with LeafNWt maximally affected E_{FGY} during tasseling/flowering and the early reproductive stages. This means that the accuracy of the remote sensing estimates for LAI should be high in crop stages V7-V9 and V9-VT if these are to be used for run-time calibration. The highest accuracy for LeafNWt estimations is required in crop stages R1-R2-R3 and R4-R5 if these are to be used for run-time calibration.

The E_{FGY} response curves of Figure 6.4 show an optimum (minimum or maximum, as run-time calibration takes place on driving variables that have a negative (LAI) or positive (LeafNWt) effect on simulated FGY) between the first and the last remote sensing image. The small effects in the early vegetative phase (V5-V7) are explained by the fact that they relate to small absolute values of crop variables. Furthermore, crop performance in the early growth phases has relatively little effect on grain yield. Run-time calibration effects increase as the calibration date is shifted forwards until adjustment takes place too late to appreciably affect grain yield and eventually E_{FGY} approaches 0.

LeafNWt calibrations showed the largest effect on E_{FGY} after tasseling/flowering (R1-R2-R3). Higher LeafNWt in this period increases light interception because of higher

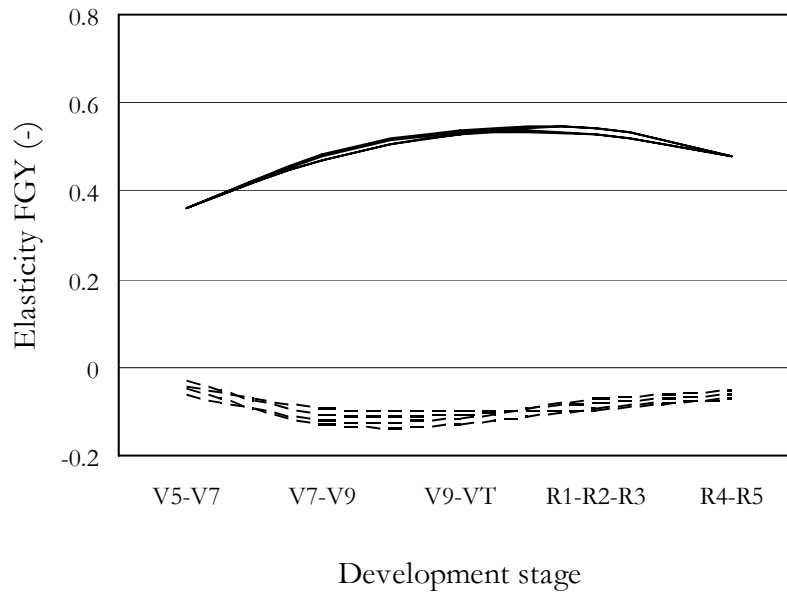


Figure 6.4 Elasticity (Equation 6.5; -) of Final Grain Yield (E_{FGY}) affected by run-time calibration date (x -axis; crop phenological stages; see Table 6.1) for LeafNWt (solid) and LAI (dashed). Line bundles result from accuracy scenarios (5, 10, 25 and 40 %).

leaf nitrogen contents. Moreover, higher LeafNWt delays leaf senescence, as during the grain filling period, when nitrogen is translocated from vegetative organs to the grain, higher LeafNWt allows more withdrawal from the leaves without affecting their performance. Nitrogen uptake during this period is limited, because of low soil nitrogen levels.

The accuracy of the LAI and LeafNWt estimates used in run-time calibration differentially affects simulated FGY when applied at different crop development stages. For LAI, overestimated values in the beginning of the growth period result in lower FGY, and if applied after tasseling/flowering (R1-R2-R3), to slightly higher FGY (Figure 6.5). Only severe underestimates of LAI (>25 %) affect FGY significantly, because of reduced maintenance respiration costs and limited effects on light interception.

Similar to the response of E_{FGY} , the relative effect of run-time calibration with LAI (Figure 6.5) is smaller than for run-time calibration with LeafNWt (Figure 6.6), for the same reasons. Underestimation of LeafNWt has a relatively stronger (negative) effect on simulated FGY than overestimation (positive). Surplus nitrogen may not be fully expressed in higher grain yield due to sink limitations. The crop can recover from nitrogen shortage, if it occurs in the early stages of crop development, but that is much more difficult, if it is imposed at later stages.

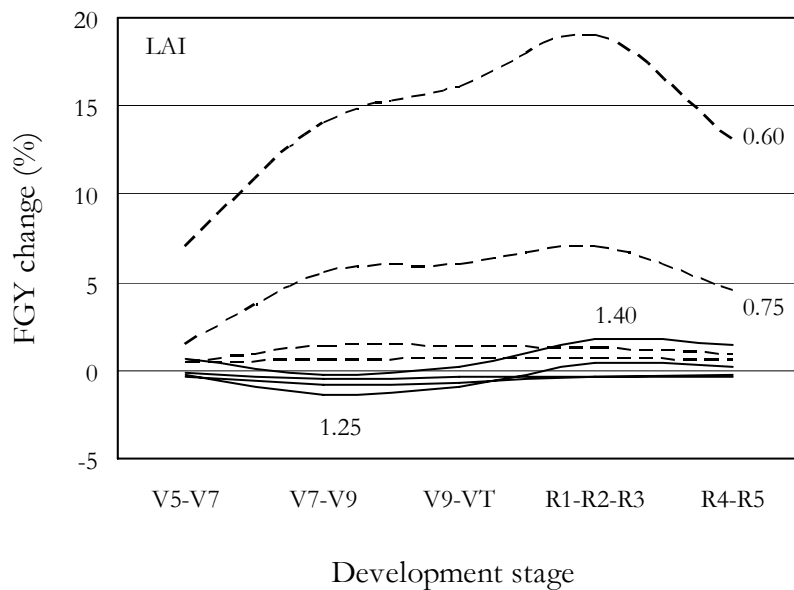


Figure 6.5 Relative effect of run-time calibration with LAI applied at different crop development stages (x-axis; crop phenological stages; see Table 6.1). Effects are presented for underestimations of LAI (dashed) and for overestimations of LAI (solid) and are relative to the situation where LAI is accurately estimated ($err=0$).

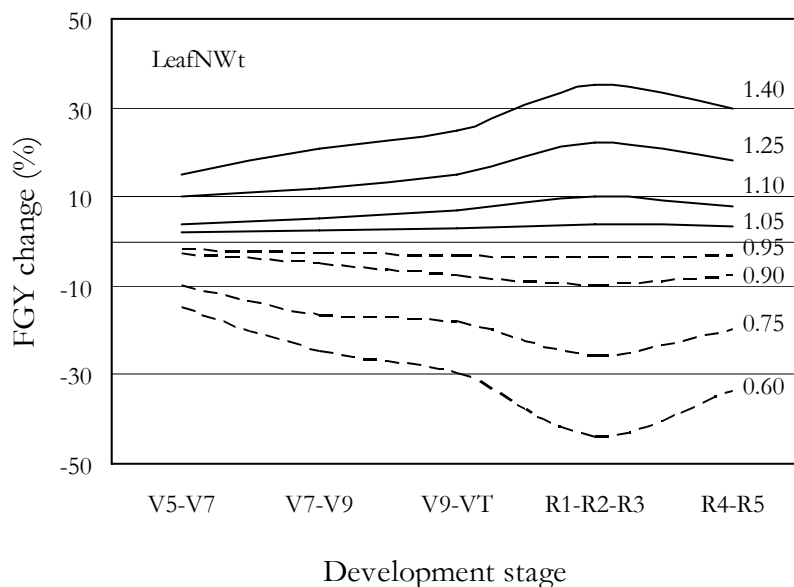


Figure 6.6 Relative effect of run-time calibration with LeafNWt applied at different crop development stages (x-axis; crop phenological stages; see Table 6.1). Effects are presented for underestimations (dashed) of LeafNWt and for overestimations (solid) of LeafNWt and are relative to the situation where LeafNWt is accurately estimated ($err=0$).

The results in Figure 6.5 and Figure 6.6 show that the variability in LAI and LeafNWt applied at different crop development stages results in differences in simulated FGY. For the *PlantSys* model, this might be significant for all LeafNWt observations and for LAI observations deviating more than 25 % of the mean. These results enable to spatially differentiate simulation runs for areas that are assumed to be homogeneous, such as a single crop on a single field with uniform management. However, within-field variability in crop performance may occur as a result of abiotic stress and/or biotic interference (such as pests and diseases). Biotic stresses often fall outside the model boundaries, whereas abiotic stresses at sub-plot level, for instance the (un-) availability of water and nutrients, are often disregarded for practical reasons, such as the costs and time requirements for soil sampling.

Accurate methods have been reported for the quantitative assessment of LAI and LeafNWt from remote sensing observations obtained from different platforms (Jago *et al.*, 1999; Broge and Leblanc, 2000; Thenkabail *et al.*, 2000; Broge and Mortensen, 2002; Jongschaap and Booij, 2004). At an appropriate spatial and spectral resolution, these methodologies can be used to observe in-field variability in LAI and LeafNWt, that might be the result of soil processes and stresses not incorporated in the model. By using these data for run-time calibration of a mechanistic simulation model, they allow spatially differentiating the model, which might result in more accurate predictions of FGY.

For such an application, remote sensing pixels that belong to a specific agricultural field should be classified in such a way that simulated FGY will give significantly different values. Classification should be done by quantitative assessment of LAI and LeafNWt. The results of our study indicate that pixels with an LAI deviating more than 25 % of the mean, and pixels with LeafNWt deviating more than 10 % from the mean, should be grouped and used for run-time calibration at sub-field level, especially at the early reproductive stages (R1-R2-R3).

6.5 Conclusions

The most important conclusions from our analysis of the effects of different run-time calibration scenarios of a mechanistic simulation model with LAI and LeafNWt, obtained from remote sensing observations, on simulated Final Grain Yield of maize, are:

- Depending on the major controlling variable for radiation interception in the model, LAI or LeafNWt should be used for run-time calibration. The effect of the two variables on simulated Final Grain Yield is different.
- A positive correlation was found between remote sensing frequency and the effect on simulated Final Grain Yield. Run-time calibration on LAI negatively affects FGY with a maximum elasticity of -0.15. The negative effect is the result of the change in maintenance respiration costs that is stronger than the change in radiation interception. For calibration on LeafNWt, the effect follows the 'law of diminishing returns', with a maximum elasticity of 0.60. Remote sensing frequency

has a negative correlation with the variability in simulated Final Grain Yield, i.e. higher observation frequency leads to more stable results.

- If a time-series of remote sensing images is not affordable for estimation of LAI and/or LeafNWt, preference should be given to acquiring images around the start of the reproductive phase, as run-time calibration during that time interval has the strongest influence on simulated Final Grain Yield.
- If the accuracy of LAI or LeafNWt estimates is interpreted as variability in the LAI or LeafNWt estimates that are used in run-time calibration, it results in different simulated Final Grain Yield. This result indicates that spatial assessment of a point-based simulation model is possible.

6.6 Acknowledgements

This study was part of the EU CROMA project (EVG1-2000-000027) and co-funded by the Research DG of the European Commission within the RTD activities of a generic nature of the Environment and Sustainable Development sub-programme (5th Framework Programme). The Dutch government has supported this research by funding through the Research program Precision Agriculture, executed by the DLO Research Institutes delegated by the Dutch Ministry of Agriculture, Nature Conservation and Fisheries. We are grateful to Prof. Dr. Steven M. de Jong and Prof. Dr. Herman van Keulen for useful comments on earlier versions of the manuscript.

6.7 References

- Bastiaanssen, W.G.M., D.J. Molden, I.W. Makin, 2000.
Remote sensing for irrigated agriculture: examples from research and possible applications. *Agric. Water Mngmt.* 46, 137-155.
- Blackmer, T.M., J.S. Schepers, G.E. Varvel, 1994.
Light reflectance compared with other nitrogen stress measurements in corn leaves. *Agron. J.* 86, 934-938.
- Boegh, E., M. Thorsen, M.B. Butts, S. Hansen, J.S. Christiansen, P. Abrahamsen, C.B. Hasager, N.O. Jensen, P. van der Keur, J.C. Refsgaard, K. Schelde, H. Soegaard, A. Thomsen, 2004.
Incorporating remote sensing data in physically based distributed agro-hydrological modelling. *J. Hydrol.* 287, 279-299.
- Boons-Prins, E.R., G.H.J. de Koning, C.A. van Diepen, F.W.T. Penning de Vries, 1993.
Crop specific simulation parameters for yield forecasting across the European Community. DLO Centre for Agrobiological Research (CABO-DLO), Joint Research Centre (JRC), Simulation Reports 32, Wageningen, the Netherlands.

- Broge, N.H., E. Leblanc, 2000.
Comparing prediction power and stability of broadband and hyperspectral vegetation indices for estimation of green leaf area index and canopy chlorophyll density. *Rem. Sens. Environ.* 76, 156-172.
- Broge, N.H., J.V. Mortensen, 2002.
Deriving green crop area index and canopy chlorophyll density of winter wheat from spectral reflectance data. *Rem. Sens. Environ.* 81, 45-57.
- Bouman, B.A.M., 1992.
Accuracy of estimating the leaf area index from vegetation indices derived from crop reflectance characteristics, a simulation study. *Int. J. Rem. Sens.* 13, 3096-3084.
- Clevers, J.G.P.W., 1989.
The application of a weighted infrared-red vegetation index for estimating leaf area index by correcting for soil moisture. *Rem. Sens. Environ.* 29, 25-37.
- Coelho, D.T., R.F. Dale, 1980.
An energy-crop growth variable and temperature function for predicting corn growth and development: planting to silking. *Agron. J.* 72, 503-510.
- Croma, 2002.
Crop Reflectance Operational Models for Agriculture. An EC research project (December 2000-May 2002). Final report EU-Croma (EVG1-2000-000027), Astrium, Toulouse, France.
- Ercoli, L., M. Mariotti, A. Masoni, F. Massantini, 1993.
Relationship between nitrogen and chlorophyll content and spectral properties in maize leaves. *Eur. J. Agron.* 2, 113-117.
- Farquhar, G.D., S. von Caemmerer, J.A. Berry, 1980.
A biochemical model of photosynthetic CO₂ assimilation of C₃ species. *Planta* 149, 78-90.
- Hillyer, C., J. Bolte, F. van Evert, A. Lamaker, 2003.
The *ModCom* modular simulation system. *Eur. J. Agron.* 18, 333-343.
- Jago, R.A., M.E.J. Cutler, P.J. Curran, 1999.
Estimating canopy chlorophyll concentration from field and airborne spectra. *Rem. Sens. Environ.* 68, 217-224.
- Jongschaap, R.E.E., 1996.
Rotask 1.0 - a simulation model for continuous cropping and tillage systems. Reference manual. DLO Institute for Agrobiological and Soil Fertility Research (AB-DLO), Report 70, Haren/Wageningen, the Netherlands, 40 pp. + annexes.
- Jongschaap, R.E.E., 2006.
Run-time calibration of simulation models by integrating remote sensing estimates of leaf area index and canopy nitrogen. *Eur. J. Agron.* 24, 328-336.
- Jongschaap, R.E.E., R. Booij, 2004.
Spectral measurements at different spatial scales in potato: relating leaf, plant and canopy nitrogen status. *Int. J. Appl. Earth Obs. Geoinform.* 5, 205-218.
- Jongschaap, R.E.E., P. Henstra, J. Verhagen, B. Rutgers, 2002.
Calibration, temporal and spatial application of the *PlantSys* 1.0 simulation model. Integrating forcing methods of remote sensing data. EU-Croma (EVG1-2000-

- 000027), Plant Research International, Delivery report D12 and D22, Wageningen, the Netherlands.
- Kraalingen, D.W.G. van, 1995.
The FSE system for crop simulation, version 2.1. DLO Institute for Agrobiolgy and Soil Fertility Research (AB-DLO), C.T. de Wit Graduate School for Production Ecology (PE), Quantitative Approaches in Systems Analysis 1, Wageningen, the Netherlands, 56 pp.
- Lemaire, G., D. Plénet, D. Grindlay, 1997.
Leaf N content as an indicator of crop N nutrition status. In: G. Lemaire (Ed.). Diagnosis on the nitrogen status in crops. Springer-Verlag, Heidelberg, Germany, pp. 189-199.
- Ma, B.L., B.L. Morrison, L.M. Dwyer, 1996.
Canopy light reflectance and field greenness to assess nitrogen fertilization and yield of maize. *Agron. J.* 88, 915-920.
- Markwell, J., J.C. Osterman, J.L. Mitchell, 1995.
Calibration of the Minolta SPAD-502 leaf chlorophyll meter. *Photos. Res.* 46, 467-472.
- McMaster, G.S., W.W. Wilhelm, 1997.
Growing degree-days: one equation, two interpretations. *Agric. Forest Meteorol.* 87, 291-300.
- Monteith, J.L., 1973.
Principles of environmental physics. Edward Arnold, London, UK, 241 pp.
- Ritchie, S.W., J.J. Hanway, G.O. Benson, 1993.
How a corn plant develops. Iowa State University of Science and Technology/ Cooperative Extension Service Ames, Special Report 48, Iowa, USA.
- Sibma, L., 1987.
Ontwikkeling en groei van maïs (*Zea mays* L.) onder Nederlandse omstandigheden. Pudoc, Wageningen, the Netherlands, 57 pp.
- Ta, C.T., R.T. Weiland, 1992a.
Allocation and retranslocation of ¹⁵N by maize (*Zea mays* L.) hybrids under field conditions of low and high N fertility. *Austr. J. Plant Physiol.* 19, 77-88.
- Ta, C.T., R.T. Weiland, 1992b.
Nitrogen partitioning in maize during ear development. *Crop Sci.* 32, 443-451.
- Thenkabail, P.S., R.B. Smith, E. de Pauw, 2000.
Hyperspectral vegetation indices and their relationship with agricultural crop characteristics. *Rem. Sens. Environ.* 71, 158-182.
- Turner, D.P., S.T. Gower, W.B. Cohen, M. Gregory, T.K. Maier, 2002.
Effects of spatial variability in light use efficiency on satellite based NPP monitoring. *Rem. Sens. Environ.* 80, 397-405.
- Vleeshouwers, L.M., R.E.E. Jongschaap, 2001.
Chlorophyll and nitrogen relations in maize with regards to spectral properties: Forcing methods of remote sensing data in crop growth simulation models. Deliverable D06 EU Croma (EVG1-2000-000027). Plant Research International, Report 38, Wageningen, the Netherlands, 44 pp. + annexes.

Yin, X., H. van Laar, 2005.

Crop Systems Dynamics. An ecophysiological simulation model for genotype-by-environment interactions. Wageningen Academic Publ., Wageningen, the Netherlands, 155 pp.

Yin, X., J. Verhagen, R. Jongschaap, A. Schapendonk, 2001.

A model to simulate responses of the crop-soil system in relation to environmental change. Plant Research International, Note 129, Wageningen, the Netherlands, 46 pp.

Yin, X., A. Schapendonk, M. Kropff, M. van Ooijen, P.S. Bindraban, 2000.

A generic equation for nitrogen-limited leaf area index and its application in crop growth models for predicting leaf senescence. Ann. Bot. 85, 579-585.

Chapter 7

General discussion and conclusions

The still growing population on our globe, the increasing standard of living, the continuing globalization, and the anticipated global (climate) change, increase the pressure on the scarce natural resources, which thus must be carefully managed to maintain their quality as a guarantee for their sustainable use. In that context, food security, food safety, environmentally-friendly production technologies and sustained use of renewable and non-renewable resources are important issues. In this study I investigated the scope and constraints for integrated use of crop growth simulation models and earth observation techniques as a basis for improved use of resources, aiming at providing a fair income to farmers, reducing production risks and preventing environmental degradation. In section 1.2, I presented the most important benefits and steps forward in further integration of crop growth simulation models and earth observation.

The following objectives presented the main challenges for integrating remote sensing and simulation modelling in this thesis:

- To derive values of important crop state variables from various remote sensing data and link these with field measurements
- To technically integrate important crop state variables derived from remote sensing time-series in dynamic simulation models in order to increase simulation accuracy
- To define the requirements for successful implementation and identify situations where this new integrated technique shows promising results, and to illustrate the effect of timing and accuracies of the remote sensing observations
- To apply point-based simulation models at a spatial scale, based on remote sensing observations
- Eventually improve resource use efficiency, avoid production risks and prevent environmental degradation by arable farming practices

7.1 Gained insights and pursuing the objectives

Dynamic and mechanistic crop growth simulation models can be successfully applied at field level if their limitations are taken into account and if data requirements are strictly met. While the use of such models generally leads to better yield predictions, improved management practices and reduced environmental impact, unavoidable random or unexpected events may cause the model to fail or simulation results to

differ from reality. Such events include pest and/or disease infestations or extreme weather conditions and/or flooding.

Application of such models with values for input parameters that cannot be accurately established may lead to unsatisfactory and unreliable simulation results. In general, the degree of success in applying such models is positively correlated with the insight in the functioning of the modelled system and the capability to translate that insight into the appropriate mathematical expressions and to accurately quantify the required model input parameters. By definition, quantification of parameters is more successful for a smaller area than for a larger area. A larger area implies a higher degree of variability in the system described by model parameters, such as soil characteristics and climate conditions. Use of average parameter values for a large region yields simulation results that do not reflect reality, because many non-linear relations are involved (Nonhebel, 1993). If conclusions at regional scale must be provided on the basis of results of point-based simulation models, point-based information must be used to derive from the simulation models representative values that are valid for specific (point) conditions, and sequentially these simulation results should be integrated over the larger area to draw conclusions valid for the regional scale.

The scope for application of this approach was demonstrated in Chapter 3, where wheat production at regional scale was predicted by integrating remote sensing data and a crop growth model. The combination of optical satellite data (for classification and area estimation) with radar satellite data (for tuning crop phenological phases) enabled application of a point-based dynamic simulation model for estimating regional wheat production. This appeared successful, as simulation results were in agreement with regional yield statistics. The methodology was used in combination with soil maps of the area, for derivation of the specific (soil) input parameters. The soil map was statistically applied and not overlaid with the wheat classification map, which would have been interesting and might have led to spatial specific and even better results if detailed soil parameters could have been derived from the soil map allowing differentiating soil characteristics between wheat fields. This was not feasible, as not all required model input parameters could be derived from the soil map, but this possibility warrants certainly attention in future studies.

As an alternative, crop performance in the course of the growing season (in which the soil characteristics are reflected) was monitored and crop status was compared to simulation results. Temporal crop status can be monitored through classical observation methods (destructive sampling) or through more sophisticated and less labour-intensive methods (such as remote or near sensing) that do not interfere with crop growth and yield formation. Comparison of simulation results with actual crop status may reveal possible deviant behaviour of the simulation model which allows identification of probable causes. Deviations of model results from the observations may be the result of erratic events, such as pest and/or disease infestations or extreme weather conditions, such as hail storms and flooding. Other sources of inaccuracies in model outcomes are inappropriate description of system processes, insufficient input parameter accuracy or high sensitivity to model input parameters that vary strongly over relatively small geographical distances. A factor of major importance in crop performance is the human factor, as crop management (such as sowing/planting dates,

field preparation, fertilizer regime, phytosanitary measures and irrigation regime) commonly affects crop status more strongly than variations in soil and weather conditions (Jongschaap and Zwart, 2004). Such management information is generally not readily available at regional, and certainly not at pixel level, but when known, these practices can easily be incorporated in the simulation. Most management practices are applied at whole fields and do not take into account within-field variation. If within-field variation can be observed, it must be at a specific scale that allows addressing this variability with appropriate equipment, either on the basis of prior knowledge or as a reaction to actual crop performance.

If point-based simulation models are to be applied for up-scaling to regional scale, simulation accuracy can be increased if actual crop status is used for 'run-time calibration'. This approach can be applied within fields or between fields. If within-field variability is monitored, differences in soil characteristics and other growth conditions (such as the occurrence of pests and diseases) are reflected in crop status which thus can be used to adjust model state variables. If important model variables are established and averaged for whole fields, differences among fields due to variations in field conditions and field treatments can be used to adjust model state variables.

Such a local approach requires that important model driving variables -that control crop growth and crop development-, can be successfully monitored and used for 'run-time calibration' of the simulation models. It is demonstrated that Leaf Area Index (LAI) and Canopy Nitrogen Status (CNS) for potato (Chapter 4) and maize (Chapter 6) can be derived successfully from near and remote sensing measurements and thus can be made available as calibration data at various moments in the course of the simulation period, as presented in Chapter 5. One of the objectives of this thesis is thereby achieved, i.e. show that it is possible to accurately derive important model state variables such as leaf area index (LAI) and canopy nitrogen status (CNS) from remote sensing data and link them to field measurements.

For the *PlantSys* simulation model these 2 variables, Leaf Area Index (LAI) and Canopy Nitrogen Status (CNS), determine the fraction of the incoming solar radiation that can be intercepted (by LAI) and the attainable Radiation Use Efficiency (controlled by CNS). It was demonstrated in Chapter 5, where I perform a run-time calibration of a simulation model by integrating estimates of leaf area index and canopy nitrogen status derived from remote sensing information, that the use of remote sensing observations for run-time adjustment of mechanistic and dynamic crop growth simulation models enhances simulation accuracy of state variables that are important in precision agriculture (e.g. soil inorganic nitrogen contents). Hence, the second objective of this thesis 'to technically integrate important crop state variables derived from remote sensing time-series with dynamic simulation models in order to increase simulation accuracy' also was attained.

The technical integration of the observed crop state variables creates an important scientific and model-technical dilemma: how to treat the associated crop state variables in the model? It is to be expected that when LAI is changed in the run-time calibration process, Leaf Weight and Leaf Nitrogen Weight need to be adjusted as well. Internal crop balances such as leaf/stem ratio, shoot/root ratio, harvest index and nutrient

concentrations will be modified if only one of the state variables is adapted. The key issue in solving this dilemma and making the right choice lies in the nature of the deviation between observed and simulated values of the state variables.

If the difference between observed and simulated values gradually develops, small inaccuracies in model process rate calculations are the most likely reason. In that situation, associated state variables should be adapted in such a way that internal balances are retained. An alternative option is to re-run the model and to re-initialize the input parameters in an iterative process, to attain closer agreement with the observed values. However, if this process has to be repeated at sequential observation dates, it could result in an endless iterative loop that will never be solved. This alternative option was not explored in this thesis but requires attention in further studies.

If the difference between observed and simulated values is changing abruptly, it is more likely associated with an erratic event, such as extreme weather or its consequences (i.e. a hail storm, a frost or a flood), or a pest or disease infestation, or an external intervention such as grazing, mowing or burning. In that situation, the observed state variables should be modified and internal balances should not be retained. Then, however, it is absolutely necessary to examine whether the model is capable of handling such situations. These findings contribute to realization of the overall objectives that aim at identification of ‘the requirements and situations where this new integrated technique shows promising results’.

Sensor characteristics of the earth observation devices, such as spectral domain, spectral resolution, pixel size, temporal resolution, and (geographical) coverage, (co-) determine their usefulness for generation of information underlying integration with dynamic crop growth simulation models. Spectral domain and spectral resolution of the remote sensing data determine the type of crop variables that can be derived and the attainable accuracy of the retrieved information. Pixel size determines the eventual application scale, but integration based on high resolution images allows using remote sensing information at larger scales. Finally, timing and frequency of the remote sensing information determine their additional value for run-time calibration. In Chapter 6, I investigate the effect of timing and accuracies of the remote sensing observations for determination of LAI and CNS in maize, on their use in run-time calibration of mechanistic and dynamic crop growth simulation models. Depending on the major controlling variable for radiation interception in the model, LAI or CNS should be used for run-time calibration. The effect of the two variables on simulated Final Grain Yield (FGY) is different. In general, an increase in remote sensing data integrated in the calibration process, leads to more stable simulation results (less variation). If the number of remote sensing observation is limited because of budget criteria, preference should be given to remote sensing observations around the start of the reproductive phase, as run-time calibration during that time interval has the strongest influence on FGY simulations. Remote sensing observations retrieved outside this optimal development window, have less impact on FGY simulation results. Different values for LAI and CNS can be obtained at different crop stages through optical remote sensing, leading to differences in simulation results as shown in Chapters 4 and 5. Within-field variability can also be observed within a single remote

sensing image. This opens the door to the spatial assessment of point-based simulation models, thereby expanding the use of these valuable research tools, as up-scaling is feasible.

All of the achievements illustrated above have provided building blocks for pursuing one of the last objectives and form the basis of a decision support system that allows taking advantage of both remote sensing techniques and crop growth simulation modelling. This contributes to the last objectives, to ‘increase resource efficiency, avoid production risks and prevent environmental degradation of arable farming practices’.

7.2 Validation of the hypotheses

In Chapter 1, this thesis started with formulation of a number of research objectives and hypotheses that were examined through a number of case studies at spatial scales ranging from single plants to canopies, from sub-fields to fields and from fields to a region. In the foregoing section, the degree of success in reaching the objectives of this thesis were presented. Now a scientific reasoning for accepting or rejecting these hypotheses is given.

In Chapter 5 it was demonstrated that sub-optimal growth conditions lead to slower leaf area development and to reduced leaf area index and lower canopy nitrogen status. Lower leaf area index and canopy nitrogen status could be estimated through near and remote sensing techniques as demonstrated in Chapters 4, 5 and 6. On the basis of an appropriate number of remote sensing observations, as discussed in Chapter 6, it was possible to reconstruct seasonal leaf area index and canopy nitrogen development curves. Such curves can be used for classical model calibrations, as shown before by other authors (e.g. Bouman, 1991). Integration of this information in crop growth simulation modelling revealed that sub-optimal production conditions were related to sub-optimal nitrogen fertilizer rates. On the basis of only remotely sensed information, the sub-optimal growth patterns could have been attributed to a range of sub-optimal growth conditions, such as soil moisture deficiency, nitrogen deficiency, or soil-borne diseases. For this situation, the simulation model was capable of estimating crop transpiration and soil evaporation, indicating adequate soil moisture conditions. If crop growth simulation modelling would have been used without run-time calibration by remote sensing estimates, the effect of sub-optimal fertilizer rates would have been simulated less accurately, as demonstrated in Chapter 5. The first hypothesis that ‘under sub-optimal production conditions, soil and crop processes that cause the production limitations can be identified through the integration of multi-sensor and multi-temporal measurements and simulation models’ could be validated.

In Chapter 5 it was demonstrated that integration of leaf area index and canopy nitrogen status obtained through remote sensing techniques in a simulation model improved simulation results not only for aboveground system state variables, but also for system state variables that cannot be derived directly from remote sensing information, such as inorganic soil nitrogen contents. The hypothesis that ‘using numerical, spatially and temporarily distributed values of selected variables obtained

through remote sensing techniques improves the dynamic simulation of the crop-soil system' can therefore be validated.

The second part of this hypothesis, i.e. 'the required complexity of the variable integration methods depends on the crop production level: simple for potential growth conditions to more complex for sub-optimal growth conditions' could also be validated. As demonstrated in Chapter 5, integration of state variables could be performed relatively straightforward in simulating potential growth situations. In potential growth situations, internal crop balances, such as root/shoot ratios and root/shoot nitrogen concentrations follow well-known patterns and can therefore easily be converted into explicit equations. Simulating sub-optimal growth conditions requires accurate simulation of the soil system to calculate soil moisture and nutrient availability. If in a real sub-optimal situation, remote sensing estimates of leaf area index and canopy nitrogen deviate from simulated values because of sub-optimal growth conditions, internal crop balances can be retained, but as a result, soil state variables have to be adjusted for calculated excess or shortage of crop nutrients and/or water that is forced on the model in the calibration process. A simple solution for this situation is not available, as was demonstrated in Chapter 5. A solution might be to use an iterative simulation approach, in which crop growth and crop senescence processes are adapted in such a way that the crop and soil system behave more in agreement with remotely sensed observations.

In the current study it was demonstrated that a decision support system based on an integration of crop growth simulation modelling and remotely sensed data is attainable and that nitrogen uptake and nitrogen distribution within the crop, as well inorganic nitrogen in the soil can be simulated more accurately with such a system. Based on this information, fertilizer regimes can be fine-tuned and improved. The last hypothesis, that 'multi-sensor and multi-temporal observations linked to dynamic modelling improve management decision support systems for environmentally sound agricultural production' could therefore be substantiated. The rate of success however, will depend on the factors discussed in this thesis, and on additional factors, such as the costs and time needed to obtain remote sensing data and crop growth simulation results.

7.3 Future research and developments

In this thesis, the scope for integration of remote sensing data with crop growth simulation models has been tested and this combination has been shown to be a valuable technique for classification and for run-time calibration of crop phenological stages, leaf area index (LAI) and canopy nitrogen status (CNS). These canopy characteristics are among the most important model driving variables strongly influencing simulation results and are the first to be calibrated in formalized model calibration. Other system variables may also be of interest, such as canopy temperatures, canopy colour and other relevant crop characteristics. These observations can be used for integration in crop growth simulation as indicated in this

thesis, either for run-time calibration or for supplying other data that result in more accurate simulations.

It may be attractive to derive additional crop state variables from remote sensing data and integrate those in crop growth simulation models, especially if the observation frequency is high. Increasing observation frequency would eventually provide a 'continuous' monitoring system, yielding information on most aboveground crop variables and interactions on a daily or hourly basis, at least during daylight hours. Simulation would then be necessary for following crop growth during night time and for simulating belowground interactions with the soil system.

Examples of such additional crop state variables that may be monitored continuously through remote sensing techniques are canopy temperatures (as indicators for crop water stress) by thermal infrared sensing and canopy colour (as indicator for nitrogen deficiency or alert for diseases) by optical remote sensing techniques. Future developments may include research on estimation of contents of more specific crop components from larger distance, such as chlorophyll, proteins or other valuable components by hyperspectral remote sensing techniques. These techniques are available for near sensing techniques (e.g. Schut, 2003), but up-scaling has been difficult to realize, so far.

Another opportunity that comes into sight for future research is the spatial analysis of specific spatial patterns that can be observed through remote sensing techniques. If whole fields can be isolated in remote sensing images, and if the spatial resolution of the remote sensing image allows analyzing and recognizing spatial patterns within these fields, these patterns may be related to specific diseases or special events, such as the outbreak of phytophthora in potato, or lodging in grain crops. Retrieval of such vegetation characteristics for crop monitoring is a feature that is practically applicable for research purposes and for decision support systems, such as fertilizer recommendation systems

In this thesis, it was demonstrated that it is possible to detect variation in crop growth and development at various stages in the growing season through remote sensing imagery. When these variations in crop status are used for run-time calibration, as they may reflect differences in soil characteristics leading to differences in resource use (water, nutrients), future approaches may include 2-D soil modelling and 2-D crop modelling. Coupled 2-D soil models with a combination of water and nutrient flows do exist, such as *FUSSIM* (Heinen and de Willigen, 1998), but so far, these have not been coupled with 2-D crop models.

As a start for this approach, point-based models may be applied at spatial scale by running them on a grid of pixels or for a set of polygons (identifying groups of pixels with more or less the same value) resulting from image analysis and classification procedures. These pixels or polygons may contain information from a specific sensor or from multiple sensors and may provide quantitative information for a range of crop characteristics, such as LAI, CNS, canopy colour and canopy temperatures.

7.4 References

- Bouman, B.A.M., 1991.
Linking X-band radar backscattering and optical reflectance with crop growth models. Ph. D. Thesis, Wageningen Agricultural University, Wageningen, the Netherlands, 167 pp.
- Heinen, M., P. de Willigen, 1998.
FUSSIM2. A two-dimensional simulation model for water flow, solute transport, and root uptake of water and nutrients in partly unsaturated porous media. Production Ecology (PE), DLO Institute for Agrobiological and Soil Fertility Research (AB-DLO), Quantitative approaches in systems analysis 20, 140 pp.
- Jongschaap, R.E.E., K.B. Zwart, 2004.
Simulation of De la Lande Cremer experiments. In: J. Verhagen, J. P. Kuikman (Eds). Separation of direct and indirect effects on carbon sequestration and C stocks: an inventory of methodologies. Plant Research International, Report 88, Wageningen, the Netherlands, 38 pp. + annexes.
- Nonhebel, S., 1993.
The importance of weather data in crop growth simulation models and assessment of climatic change effects. Ph. D. Thesis, Wageningen Agricultural University, Wageningen, the Netherlands, 144 pp.
- Schut, A.G.T., 2003.
Imaging spectroscopy for characterisation of grass swards. Ph. D. Thesis, Wageningen University, Wageningen, the Netherlands, 264 pp.

Acronyms and symbols

Acronym	Meaning	Unit
2-D	2 Dimensional	
3-D	3 Dimensional	
AB-DLO	DLO Institute for Agrobiology and Soil Fertility Research	
AVIRIS	Airborne Visible Infrared Imaging Spectrometer	
ATSAVI	Adjusted Transformed Soil Adjusted Vegetation Index	
AVHRR	Advanced Very High Resolution Radiometer	
BACROS	BASic CROp growth Simulator (model)	
BLE	Blue Earth (experimental test site)	
BPR	Biologically Plausible Range	
BuNaSols	BUreau NAional des SOLS (Burkina Faso)	
CABO-DLO	DLO Centre for Agrobiological Research	
CACI	Chlorophyll Absorption Continuum Index	
CARI	Chlorophyll Absorption Reflection Index	
CFCs	Chlorofluorocarbons	
CGM	Crop Growth Monitoring	
CGMS	Crop Growth Monitoring System	
CIP	Centro Internacional de la Papa (Perú)	
CIR	Colour Infrared Photography	
CNS	Canopy Nitrogen Status	
CPRO-DLO	DLO Centre for Plant Breeding and Reproduction Research	
CrOMA	Crop Operational Models in Agriculture (project)	
CV	Coefficient of Variance	
DAIS	Digital Airborne Imaging Spectrometer	
DBMS	Data Base Management System	
DG	Director General	
DME	Desarrollo Metodológica Eco-regional (project)	
DN	Digital Number	
DoE	Date of Experiment	
DoY	Date of Year	
DSS	Decision Support System	
DVI	Difference Vegetation Index	
E_{FGY}	Elasticity of Final Grain Yield	(-)
ELCROS	ELementary CROp Simulator (model)	
EM	Electro Magnetic	
ERS	European Remote Sensing satellite	
ERTS	Earth Resources Technology Satellite	
ESA	European Space Agency	
EVI	Enhanced Vegetation Index	
EWS	Early Warning System	

Acronym	Meaning	Unit
F ₇₃₅ /F ₇₀₀	Chlorophyll Fluorescence Ratio	
FAO	Food and Agriculture Organization of the United Nations	
FGY	Final Grain Yield	(g m ⁻²)
FOV	Field Of View	
FWBI	Floating Water Band Index	
GEMI	Global Environment Monitoring Index	
GESAVI	GEneralized Soil Adjusted Vegetation Index	
GMAP-filter	Gamma Maximum A Posteriori filter	
GNDVI	Green Normalized Difference Vegetation Index	
GPP	Gross Primary Production	(g m ⁻²)
GPS	Global Positioning System	
GrainWt	Grain Weight	(g m ⁻²)
HRV	High Resolution Visible	
IB-DLO	DLO Institute for Soil Fertility Research	
IPO-DLO	DLO Institute for Plant Protection	
IS	Imaging Spectroscopy	
JERS	Japanese Earth Resources Satellite	
KAS	Calcium ammonium nitrate (fertilizer)	
κ_L	Light extinction coefficient	(m ⁻¹)
κ_N	Nitrogen extinction coefficient	(m ² soil g ⁻¹ N)
LAI	Leaf Area Index	(m ² m ⁻²)
LeafN	Leaf Nitrogen	(g m ⁻²)
LeafN _{Log}	Leaf organic Nitrogen per unit Leaf area	(g m ⁻²)
LeafN _{Sorg}	Leaf organic Nitrogen per unit Soil area	(g m ⁻²)
LeafN _{Stot}	Leaf Total Nitrogen per unit soil area	(g m ⁻²)
LeafNWt	Leaf Nitrogen Weight	(g m ⁻²)
MARS	Monitoring of Agriculture with Remote Sensing (project)	
MCARI	Modified Chlorophyll Absorption in Reflection Index	
MDG	Millenium Development Goal	
MDS	Management Decision Support	
MIR	Middle Infrared	
MP	<i>Midi-Pyrénées</i> (French department)	
MSAVI	Modified Soil Adjusted Vegetation Index	
MSAVI2	Modified Soil Adjusted Vegetation Index, No. 2	
NASA	National Aeronautics and Space Administration	
NDVI	Normalized Difference Vegetation Index	
NIR	Near Infrared	
NOAA	National Oceanic and Atmospheric Administration	
NPP	Net Primary Production	(g m ⁻²)
OBS	Openbare Basis School	
OSAVI	Optimized Soil Adjusted Vegetation Index	
PA	Precision Agriculture	
PAC	<i>Provence-Alpes-Côte d'Azur</i> (French department)	

Acronym	Meaning	Unit
PAR	Photosynthetically Active Radiation	(MJ m ⁻²)
PG	Pergamino (experimental test site in Argentina)	
PH	Pehuaró (experimental test site in Argentina)	
<i>PlantSys</i>	Plant System (model)	
PRI	Photochemical Reflectance Index	
PSSRa	Pigment Specific Simple Ratio (Chl a)	
PSSRb	Pigment Specific Simple Ratio (Chl b)	
PSSRc	Pigment Specific Simple Ratio (Carotenoids)	
PVI	Perpendicular Vegetation Index	
r ²	Correlation coefficient	
RADAR	RAdio Detection And Ranging	
RARSa	Ratio Analysis of Reflection Spectra (Chlorofyll a)	
RARSb	Ratio Analysis of Reflection Spectra (Chlorofyll b)	
RARSc	Ratio Analysis of Reflection Spectra (Carotenoids)	
RDBMS	Relational Data Base Management System	
RDVI	Renormalized Difference Vegetation Index	
REP	Red Edge Position	
ReSeDA	Remote Sensing Data Assimilation (project)	
RGI	Relative Greenness Index	
RMSE	Root Mean Square Error	
<i>Rotask</i>	Rotation model Agrosystems Innovations (model)	
RS	Remote Sensing	
RUE	Radiation Use Efficiency	(g MJ ⁻¹)
RVI	Ratio Vegetation Index	
SAR	Synthetic Aperture Radar	
SAVI	Soil Adjusted Vegetation Index	
SAVI2	Soil Adjusted Vegetation Index, No.2	
ShootWt	Shoot Weight	(g m ⁻²)
SIPI	Structure Independent Pigment Index	
SLAR	Side Looking Airborne Radar	
SR	Simple Ratio	
StemWt	Stem Weight	(g m ⁻²)
<i>SUCROS</i>	Simple and Universal CROp Simulator (model)	
SVAT	Soil Vegetation Atmospheric Transfer	
T	Transmittance fraction	(-)
TIR	Thermal Infrared	
TIROS	Television Infrared Observation Satellite	
TM	Thematic Mapper	
TNUpt	Total Nitrogen Uptake	(g m ⁻²)
TSAVI	Transformed Soil Adjusted Vegetation Index	
TSP	Triple Super Phosphate	
TVI	Triangular Vegetation Index	
UV	Ultra Violet	

Acronym	Meaning	Unit
VI	Vegetation Index	
VIS	Visible	
VWO	Voortgezet Wetenschappelijk Onderwijs	
WAU	Wageningen Agricultural University	
WBI	Water Band Index	
WDVI	Weighted Difference Vegetation Index	
WUR	Wageningen University and Research centre	
XS	Multi spectral	

Symbol	Meaning	Unit
λ	Wavelength	(nm)
λ_{rep}	Red edge position wavelength	(nm)
R_{λ}	Reflectance at wavelength λ	(%)

Samenvatting

In dit proefschrift is onderzocht wat de mogelijkheden en de voorwaarden zijn om hoogwaardige gewasgroeimodellen en aardobservatietechnieken zodanige te integreren dat ze als geheel een bijdrage kunnen leveren aan het efficiënter gebruik van hulpbronnen in de landbouw, risico's kunnen verminderen die een rol spelen bij gewasproductie, de achteruitgang van het milieu kunnen beperken en kunnen bijdragen aan de toename van het inkomen van het boerenbedrijf.

In het verleden hebben zowel gewasgroeimodellen als aardobservatietechnieken op individuele basis laten zien dat ze een waardevolle bijdrage kunnen leveren aan toepassingen in de landbouw. Voor gewasgroeimodellering bestaan deze waardevolle bijdragen o.a. uit betrouwbare oogstvoorspellingen, de prototypering van gewascultivars, het genereren van kengetallen voor verbeterde productietechnieken en de teeltbegeleiding op veldniveau. Ook aardobservatietechnieken hebben succesvolle bijgedragen geleverd, bv. aan de classificatie van gewassen en bij het kwantificeren van vegetatiekarakteristieken op ruimtelijke en temporele schaal van verschillende grootte. Het uitgangspunt van deze studie was de hypothese dat de integratie van beide technieken zoveel synergie oplevert, dat het mogelijk is om een teeltbegeleidingsysteem te ontwerpen op basis van nauwkeuriger simulaties van het bodemgewassysteem en zo een belangrijke bijdrage levert aan verantwoord gebruik van (natuurlijke) hulpbronnen in de landbouw.

In het verleden zijn pogingen om gewasgroeimodellering en aardobservatietechnieken van elkaar te laten profiteren beperkt gebleven tot het klassificeren van gewassen (om het juiste model te kiezen) en het kwantificeren van gewasgroe- en ontwikkelingscurves, bv. door het schatten van bladoppervlakte uit een tijdserie van aardobservaties, voor de calibratie van een gewasgroeimodel voor (vaak) gunstige groeiomstandigheden. In een beperkt aantal studies zijn de mogelijkheden onderzocht om aardobservaties te gebruiken om simulatiemodellen voor de groei en ontwikkeling van een specifiek gewas te initialiseren. In dit proefschrift zijn deze mogelijkheden uitgebreid naar een meer dynamische en doorlopende aanpak, waarin aardobservaties niet alleen gebruikt worden voor het initialiseren van het model, maar om ook tijdens de simulatieperiode op gezette tijden (bij beschikbaarheid van informatie uit aardobservaties), het model dynamisch te calibreren ('dynamische calibratie'). Tijdens zo'n procedure worden gesimuleerde waarden van bv. het bladoppervlak (LAI) en de gewasstikstofstatus (CNS) vervangen door geschatte waarden die verkregen zijn uit aardobservaties in de loop van het groeiseizoen. LAI en CNS zijn belangrijke variabelen die de groei bepalen van (landbouw-) gewassen, zoals aardappelen, tarwe en maïs. In dit proefschrift is deze dynamische calibratie uitgevoerd in een aantal deelstudies, met simulaties van een volledig groeiseizoen onder zowel gunstige als ongunstige groeiomstandigheden. Door het toepassen van dynamische calibratie kan ruimtelijk onderscheid gemaakt worden in de gewasgroeisimulatie, omdat de variabiliteit in de gewasstatus die het gevolg is van lokale verschillen in groeiomstandigheden leidt tot verschillen in de signalen die ruimtelijk waargenomen kunnen worden door aardobservatietechnieken.

In dit proefschrift zijn de relaties onderzocht tussen aardobservaties op blad-, plant- en gewasniveau. Bovendien is het effect op uiteindelijke simulatieresultaten (bv.

gewasopbrengst) geanalyseerd van onnauwkeurigheden in de schatting van LAI en CNS uit aardobservaties, die vervolgens gebruikt zijn voor de dynamische calibratie. Aardappelproeven in Nederland hebben aangetoond dat het mogelijk is om stikstofwaarnemingen op bladniveau op te schalen naar plant- en gewasniveau, door rekening te houden met de verticale stikstofverdeling in het gewas. Door het toepassen van een stikstof-extinctiecoëfficiënt ($k_N=0.41$) nam de nauwkeurigheid toe van de relatie ($r^2=0.91$) tussen SPAD-metingen (een aardobservatietechniek op bladniveau) en de stikstofconcentratie in het gewas, uitgedrukt per eenheid bladoppervlakte. Aardobservatietechnieken op gewasniveau hoeven geen rekening te houden met de verticale verdeling van stikstof in het gewas als de hoeveelheid stikstof wordt uitgedrukt per eenheid bodemoppervlakte, omdat daarmee de hoeveelheid stikstof over de gewasdiepte wordt geïntegreerd. De positie van de 'red edge' (een index die uit aardobservaties bepaald kan worden) gaf een nauwkeurige relatie ($r^2=0.82$) met de hoeveelheid stikstof van het gewas (g N m^{-2} grond). Voor het gebruik in dynamische calibratie, kon het bladoppervlak van aardappel (in Nederland) en maïs (in Argentinië, Frankrijk en de VS) ook nauwkeurig afgeleid worden uit aardobservaties in het veld, uit het vliegtuig en vanuit de ruimte. Het gebruik van LAI waarden die dmv. aardobservaties verkregen werden en vervolgens gebruikt zijn voor dynamische calibratie waarbij de gesimuleerde stikstofconcentratie in het blad gehandhaafd werd, gaf ook nauwkeuriger simulatieresultaten voor de stikstofhoeveelheid in het gewas en in de bodem.

In een deelstudie in het zuidoosten van Frankrijk bleek het mogelijk om in velden met wintertarwe, verschillende ontwikkelingsstadia (opkomst, bloei) en teelthandelingen (oogst) met succes te identificeren uit informatie van optische en radar aardobservaties. Het vaststellen van het moment van deze ontwikkelingsstadia en teelthandelingen is belangrijk voor het calibreren van modellen omdat ze de lengte van de groeiperiode bepalen, en m.n. de lengte van de korrelvullingsperiode aangeven die medebepalend is voor de uiteindelijke korrelopbrengst. Tijdens de bloei is de hoeveelheid verse biomassa op het veld maximaal en wordt het radarsignaal van de bodem maximaal gemaskeerd door het vocht in het bovengrondse deel van het gewas. Dit kenmerk is met succes gebruikt om een regionale schatting van het bloeimoment te maken en dit samen met statistische informatie uit bodemkaarten toe te passen voor de simulatie van graanproductie op regionale schaal. De voorspelde waarde voor de regionale tarweproductie kwam goed overeen met regionale landbouwstatistieken. Deze integratie geeft meerwaarde aan het gebruik van bewezen waardevolle (punt-) simulatiemodellen, doordat het mogelijk wordt ze ruimtelijk toe te passen en op deze manier op te schalen.

Als de uit aardobservatie verkregen schattingen van bladoppervlakte of stikstofstatus worden gebruikt voor dynamische calibratie van gewasgroeimodellen (aardappel en maïs), dan neemt de nauwkeurigheid van simulatieresultaten toe voor zowel bovengrondse gewasdelen als voor variabelen die niet direct waargenomen kunnen worden door aardobservatietechnieken, zoals bv. minerale stikstof in de bodem. De mate van succes en de robuustheid van deze geïntegreerde aanpak hangt af van het moment, de nauwkeurigheid en het aantal aardobservaties dat beschikbaar is voor dynamische calibratie van het model gedurende de simulatieperiode. De

nauwkeurigheid van de simulatie met dynamische calibratie was positief gecorreleerd met het aantal aardobservaties dat gebruikt werd. Het integreren van informatie uit aardobservaties die plaatsvinden rond de bloei hadden het grootste effect op de berekende korrelopbrengst, veel groter dan waarnemingen voor of na deze periode.

Deze studie heeft aangetoond dat een teeltbegeleidingssysteem ontwikkeld kan worden, gebaseerd op een dynamische integratie van gewasgroeisimulatiemodellen en aardobservatietechnieken. In zo'n systeem worden stikstofopname, de verticale verdeling van stikstof in het gewas en de minerale stikstof in de bodem nauwkeurig gesimuleerd en deze informatie kan gebruikt worden voor het aanpassen van bemestingsstrategieën, waardoor een belangrijke bijdrage geleverd wordt aan duurzame agrarische productiemethoden en een beter milieu.

Uit dit onderzoek is gebleken dat de nauwkeurigheid van voorspellingen van mechanistische gewasgroeisimulatiemodellen significant toeneemt als informatie uit aardobservaties op dynamische wijze wordt geïntegreerd. Dit resulteert niet alleen in nauwkeurigere schattingen van biofysische variabelen, zoals het bladoppervlak en de stikstofstatus van het gewas, maar draagt ook bij aan verbeterde schattingen op regionaal niveau. Zulke modellen die betrouwbare voorspellingen van het gewas geven op veldniveau, zijn dus effectieve middelen voor het ontwikkelen en evalueren van milieuvriendelijke productiemethoden en voor het optimaliseren van het gebruik van onze natuurlijke hulpbronnen.

Vervolgonderzoek zou zich moeten richten op de mogelijkheden om additionele gewaskarakteristieken te schatten door middel van aardobservatietechnieken en deze op gelijksoortige wijze te integreren in gewasgroeimodellen. Mogelijk kunnen teelt-handelingen geïnitieerd worden op basis van waarnemingen van additionele gewaskarakteristieken, zoals: 1) gewastemperatuur, geschat uit thermische aardobservatietechnieken als indicator voor vochtgebrek, 2) gewasverkleuring, geschat uit optische aardobservatietechnieken als indicator voor nutriëntengebrek en 3) gewasstructuur, geschat uit radar observatietechnieken als indicator voor de vocht- en nutriëntenuishouding van het gewas. Aardobservatietechnieken zijn ook bij uitstek geschikt om ruimtelijke patronen te herkennen die het gevolg zijn van de lokale groeiomstandigheden van het gewas. Patroonherkenning zou gerelateerd kunnen worden aan speciale ziektes of speciale gebeurtenissen, zoals de uitbraak van aardappel-moeheid bij aardappel, of het legeren van granen.

De verschillende gewassen en de verscheidenheid aan groeiomstandigheden, de verschillen in bodemvruchtbaarheid en de verschillen in teelt-handelingen die in de verschillende deelstudies van dit proefschrift zijn onderzocht, laten zien dat een geïntegreerde toepassing van mechanistische simulatiemodellen en aardobservatietechnieken een brede toepasbaarheid heeft. Er is voldoende om deze geïntegreerde techniek aan te passen of uit te breiden voor specifieke toepassingen in het landbouwkundig onderzoek, teeltbegeleidingssystemen en voor het genereren van regionale statistieken.

Curriculum vitae

Raymond Elmar Etienne Jongschaap was born on June 24, 1968 in Deventer, the Netherlands. From 1968 to 1987 he lived in Groningen in the north of the Netherlands. After the *Jenaplanschool OBS Midwolde*, he started the *Praedinius gymnasium* in Groningen in 1981, but finished his VWO at the *Nienoordcollege* in Leek in 1987. After high school, he went to *Wageningen Agricultural University* (WAU) in 1987 to major in Tropical Crop Science, Soil Science and Geology and in Extension Science. He spent 10 months in Costa Rica and 6 months in Chile for his Masters degree. In Guápiles in the Atlantic zone of Costa Rica he studied Palmheart (*Bactris gasipaes* H.B.K.) and at *Agraria* in Coelemu, in the VIIIa region in Chile, he studied farmers' organizations and extension services. In 1993 he finished his studies at *Wageningen Agricultural University*. Conscientious objections to the military service led to 12 months alternative civil service followed by short term contracts at the *Institute for Soil Fertility Research* (IB-DLO) in Haren, Groningen. During that period he was associated with *Bureau National des Sols* (BuNaSols) in Ouagadougou, Burkina Faso, where he worked on the development of a dynamic crop growth simulation model for soil tillage and crop management of millet, sorghum and maize. After IB-DLO merged with the *Centre for Agrobiological Research* (CABO-DLO) in 1999 to become the *Institute for Agrobiology and Soil Fertility Research* (AB-DLO), he acquired tenure in Wageningen. In the following years, he worked on various projects in the Netherlands (modelling crop-rotations and soil organic matter dynamics, precision agriculture and remote sensing), in Europe (France: ReSeDA, CrOMA), in South-America (Perú/Bolivia), in Africa (Mali) and Asia (China), in which he studied the use of remote sensing data for agricultural and environmental applications. These projects served as a learning experience and provided the basis and data for the research presented in this thesis. He expanded his fields of interest considerably following the merge of AB-DLO with other institutes in 2000 into *Plant Research International* and its integration into *Wageningen University and Research centre* (WUR) in 2001. His work includes the dynamic simulation of natural vegetation (Common Reed; *Phragmites australis* (Cav.) Trin. ex Steud), arable crops (Potato; *Solanum tuberosum* L.; Wheat; *Triticum aestivum* L., Maize; *Zea mays* L.) and greenhouse cropping systems, such as vegetables: Cucumber (*Cucumis sativus* L.), Sweet pepper (*Capsicum annuum* L.), Tomato (*Lycopersicon esculentum* L.) and flowers: Rose (*Rosa* spp.). Recently he has also become involved in biofuel research, with emphasis on the potentials of Physic nut (*Jatropha curcas* L.) oilseed production in developing countries as an option for rural and local energy production for the poor.

Selected publications

2006

- Hemming, S., N. van der Braak, Th. A. Dueck, R.E.E. Jongschaap, N. Marissen, 2006.
Filtering natural light by the greenhouse covering using model simulations - More production and better plant quality by diffuse light? *Acta Hort.* (*in press*).
- Jongschaap, R.E.E., 2006a.
Run-time calibration of simulation models by integrating remote sensing estimates of leaf area index and canopy nitrogen. *Eur. J. Agron.* 24, 328-336.
- Jongschaap, R.E.E., 2006b.
The effect of LAI and N parameter variability used in run-time calibration of mechanistic and dynamic crop growth simulation models. *Ecol. Mod.* (*submitted*).
- Jongschaap, R.E.E., Th. A. Dueck, N. Marissen, S. Hemming, L.F.M. Marcelis, 2006.
Simulating seasonal patterns of increased greenhouse crop production by conversion of direct radiation into diffuse radiation. *Acta Hort.* (*in press*).
- Paganini, M., P.S. Bindraban, R.E.E. Jongschaap, H. van Keulen, 2006.
Resource endowment and resource use efficiency in sub-Saharan Africa: a model analysis. *Field Crops Res.* (*submitted*).

2005

- Jongschaap, R.E.E., L.S.M. Schouten, 2005.
Predicting wheat production at regional scale by integration of remote sensing data with a simulation model. *Agron. Sust. Dev.* 25, 481-489.

2004

- Jongschaap, R.E.E., R. Booij, 2004.
Spectral measurements at different spatial scales in potato: relating leaf, plant and canopy nitrogen status. *Int. J. Appl. Earth Obs. Geoinf.* 5, 205-218.
- Jongschaap, R.E.E., K.B. Zwart, 2004.
Simulation of De la Lande Cremer experiments. In: J. Verhagen, P. Kuikman (Eds). Separation of direct and indirect effects on carbon sequestration and C stocks: an inventory of methodologies. *Plant Research International, Report 88*, Wageningen, the Netherlands, 38 pp. + annexes.

2002

- Clevers, J.G.P.W., O.W. Vonder, R.E.E. Jongschaap, J.F. Desprats, C. King, L. Prévot, N. Bruguier, 2002.
Using SPOT data for calibrating a wheat growth model under Mediterranean conditions. *Agronomie* 22, 687-694.

2001

- Clevers, J.G.P.W., R.E.E. Jongschaap, 2001a.
Regional mapping of carbon fixation by terrestrial ecosystems using the red-edge index derived from MERIS. In: *Proc. 8th International Symposium Physical*

Measurements and Signatures in Remote Sensing. 8-12 January 2001, Aussois, France, pp. 521-526.

Clevers, J.G.P.W., R.E.E. Jongschaap, 2001b.

Imaging spectrometry for agricultural applications. In: F.D. van der Meer, S.M. de Jong (Eds.). Imaging spectrometry: basic principles and prospective applications. Book series Remote sensing and digital image processing 4, Chapter 6, pp. 157-199, Kluwer Academic Publ., Dordrecht, the Netherlands, 425 pp.

Vleeshouwers, L.M., R.E.E. Jongschaap, 2001.

Chlorophyll and nitrogen relations in maize with regards to spectral properties. Plant Research International, Report 38, Wageningen, the Netherlands, 44 pp.

Yin, X., J. Verhagen, R.E.E. Jongschaap, A.H.C.M. Schapendonk, 2001.

A model to simulate responses of the crop-soil system in relation to environmental change. Plant Research International, Note 129, Wageningen, the Netherlands, 46 pp.

2000

Clevers, J.G.P.W., O.W. Vonder, R.E.E. Jongschaap, J.F. Desprats, C. King, L. Prévot, N. Bruguier, 2000a.

A semi-empirical approach for estimating plant parameters within the ReSeDa project. In: Proceedings XIXth Congress of the International Society for Photogrammetry and Remote Sensing (ISPRS): ISPRS, Amsterdam. - (International Archives of Photogrammetry and Remote Sensing; XXXIII (B7)), pp. 272-279.

Clevers, J.G.P.W., O.W. Vonder, R.E.E. Jongschaap, J.F. Desprats, C. King, L. Prévot, N. Bruguier, 2000b.

Monitoring wheat growth by calibrating a crop growth model using optical satellite data. Geophysical Research Abstracts, Hydrol. Earth Syst. Sci. 2, p. 424.

1999

Jongschaap, R.E.E., 1999.

Linking remote sensing, GIS and crop growth simulation modeling to evaluate regional production scenarios. Second Annual and progress report, reporting period: 01-11-1997 to 30-04-99. DLO Institute for Agrobiolgy and Soil Fertility Research (AB-DLO), Note 182, Wageningen, the Netherlands, 28 pp. + annexes.

Smit, A.L., R.E.E. Jongschaap, G.J. Molema, P. van Velde, 1999.

Potentiële monitoring systemen op het gebied van teeltmaatregelen, ziekten en plagen. DLO Institute for Agrobiolgy and Soil Fertility Research (AB-DLO), Note 188, Wageningen, the Netherlands.

1998

Prévot, L., F. Baret, A. Olioso, B.A.M. Bouman, J.G.P.W. Clevers, R.E.E. Jongschaap, H.J.C. van Leeuwen, L.S.M. Schouten, O.W. Vonder (*et al.*), 1998.

Assimilation of multi-temporal remote sensing data to monitor vegetation and soil: the Alpilles-ReSeDA project. In: Proc. IGARSS '98 Symposium, Vol. 5. 6-10 July 1998, Seattle, WA, USA, pp. 2399-2401.

1997

Jongschaap, R.E.E., 1997a.

Linking remote sensing, GIS and crop growth simulation modelling to evaluate regional production scenarios. Workplan and 6-months progress report, reporting period: 01-11-1996 to 30-04-97. Project 10705.50 (DME-Sur): (Integrating remote sensing, GIS and modelling for land-use monitoring in the arid/semi-arid Andes) 1996-1999. DLO Institute for Agrobiolgy and Soil Fertility Research (AB-DLO), Note 57, Wageningen, the Netherlands, 11 pp. + annexes.

Jongschaap, R.E.E., 1997b.

Linking remote sensing, GIS and crop growth simulation modelling to evaluate regional production scenarios. Annual and 6-months progress report, reporting period: 01-05-1997 to 31-10-97. Project 10705.50 (DME-Sur): (Integrating remote sensing, GIS and modelling for land-use monitoring in the arid/semi-arid Andes) 1996-1999. DLO Institute for Agrobiolgy and Soil Fertility Research (AB-DLO), Note 85, Wageningen, the Netherlands, 26 pp. + annexes.

1996

Jongschaap, R.E.E., 1996.

Rotaské 1.0 - A dynamic simulation model for continuous cropping systems. Reference manual. DLO Institute for Agrobiolgy and Soil Fertility Research (AB-DLO), Report 70, Haren/Wageningen, the Netherlands, 40 p. + annexes.

1995

Bazi, H., A. Sanou, E. Verberne, R. Jongschaap, G. Dijksterhuis, M. Bonzi, 1995.

Manuel du logiciel interactif (*CP-BKF3*): sorgho, mil et mais. DLO Institute for Agrobiolgy and Soil Fertility Research (AB-DLO), Note 20, Haren/Wageningen, the Netherlands, 29 pp.

Jongschaap, R., 1995a.

BAOBAB - La Base des données des Analyses Chimiques et des OBservations Agro-pédologiques du Bunasols. Version Française. DLO Institute for Agrobiolgy and Soil Fertility Research (AB-DLO), Note 28, Haren/Wageningen, the Netherlands, 28 pp.

Jongschaap, R., 1995b.

BAOBAB - La Base des données des Analyses Chimiques et des OBservations Agro-pédologiques du Bunasols. Version Anglaise. DLO Institute for Agrobiolgy and Soil Fertility Research (AB-DLO), Note 19, Haren/Wageningen, the Netherlands, 27 pp.

Sanou, A., R.E.E. Jongschaap, 1995.

Traitement informatique des données de sol. In: Interprétation agronomiques des données de sol: un outil pour la gestion des sols et le développement agricole. DLO Institute for Agrobiolgy and Soil Fertility Research (AB-DLO), Thema's 2, Haren/Wageningen, the Netherlands, pp. 37-43.

Verberne, E., G. Dijksterhuis, R. Jongschaap, H. Bazi, A. Sanou, M. Bonzi, 1995.

Simulation des cultures pluviales au Burkina Faso (*CP-BKF3*): sorgho, mil et mais. DLO Institute for Agrobiolgy and Soil Fertility Research (AB-DLO), Note 18, Haren/Wageningen, the Netherlands, 71 pp.